



Ocular drug delivery with topical administration

Laura Lorenzo Soler

Thesis for the degree of Philosophiae Doctor

November 2022

School of Health Sciences

FACULTY OF MEDICINE

UNIVERSITY OF ICELAND

Ocular drug delivery with topical administration

Laura Lorenzo Soler

Thesis for the degree of Philosophiae Doctor

Supervisor(s)

Prof. Einar Stefánsson MD PhD
Assistant Prof. Ólöf Birna Ólafsdóttir PhD

Doctoral committee

Prof. Þorsteinn Loftsson PhD
Associate Prof. Gauti Jóhannesson MD PhD
Prof. Gerhard Garhöfer MD PhD

November 2022

School of Health Sciences

FACULTY OF MEDICINE

UNIVERSITY OF ICELAND

Flutningur lyfja með augndropum inn í auga

Laura Lorenzo Soler

Ritgerð til doktorsgráðu

Leiðbeinandi/leiðbeinendur

Próf. Einar Stefánsson MD PhD
Lektor Ólöf Birna Ólafsdóttir PhD

Doktorsnefnd

Próf. Þorsteinn Loftsson PhD
Dósent Gauti Jóhannesson MD PhD
Próf. Gerhard Garhöfer MD PhD

Nóvember 2022

Heilbrigðisvísindasvið

LÆKNADEILD

HÁSKÓLI ÍSLANDS

Thesis for a doctoral degree at the University of Iceland. All right reserved. The document is confidential. No part of this publication may be reproduced in any form without the prior permission of the copyright holder.

© Laura Lorenzo Soler 2022

ORCID 0000-0002-2514-1323

ISBN 978-9935-9699-1-0

Printing by Háskólaprent.

Reykjavik, Iceland 2022

Ágrip

Tilgangur:

Fyrir marga lyfjaflokka þykir staðbundin lyfjagjöf í augndropaformi ákjósanlegasta leiðin vegna einfaldleika við lyfjagjöf. Eru augndropar algengasta aðferðin til að meðhöndla augnsjúkdóma í fremri hluta augans. Staðbundin lyfjagjöf í augndropaformi yfir hornhimnu er hinsvegar óhagkvæm þegar meðhöndla þarf aftari hluta augans. Hefðbundin lyfjameðferð fyrir aftari hluta augans felur í sér að lyfinu er dælt í glerhlaup augans en með tilheyrandi áhættu á fylgikvillum ásamt tilheyrandi óþægindum fyrir sjúklinga.

Sýnt hefur verið fram á að leiðin í gegnum augnslímhúð og augnhvítu hefur hlutfallslega hærra gegndræpi fyrir rísasameindir, stærra aðgengilegt yfirborð og meiri nálægð við sjónhimnu samanborið við hornhimnu. Fyrir vikið hafa verið kenningar um að augnslímhúð og augnhvíta sé mögulega leið lyfja í augndropaformi yfir í aftari hluta augans.

Meginmarkmið þessarar ritgerðar eru (1) að kanna hversu vel ákveðin lyf í sýklódextrín augndropaformi flytjast yfir í fremri og aftari hluta augans, (2) að ákvarða lyfjafræðileg áhrif angíótensínviðtaka-hamlara á augnþrýsting eftir augndropagjöf, (3) að meta og bera saman *in vitro* gegndræpi í gegnum hornhimnu og í gegnum augnslímhúð og augnhvítu fyrir staðbundna augndropalyfjagjöf í aftari hluta augans og (4) að bera kennsl á helstu eðlisefnafræðilega eiginleika sem hafa áhrif á gegndræpi lyfja yfir hornhimnu í fullri þykkt og leiðina frá augnslímhúð, í gegnum augnhvítu og æðahimnu að sjónhimnu (augnslímhúð-augnhvítu-æðahimnu-sjónhimnu leið).

Aðferðir

1. Framkvæmdar voru tvær *in vivo* rannsóknir á kanínum þar sem mældur var lyfjastyrkur í augnvefjum eftir stakan skammt af augnlyfjum í sýklódextrín nanóögnum. Í fyrri rannsókninni voru tveir mismunandi angíótensínviðtakahamlarar, 1.5% irbesartan og 0.15% candesartan, gefnir 49 kanínum. Styrkur lyfjanna var mældur í hornhimnu og augnvökva eftir 1, 2, 3, 6 og 12 klukkustundir frá lyfjagjöf. Í seinni rannsókninni var ný γ -sýklódextrín öragna augnlyfjaferja með cediranib maleate (öflugur VEGF hamlari) prófuð á 26 kanínum. Styrkur cediranib maleate var mældur í vefjum fremri og aftari hluta augans eftir 1, 3, og klukkustundir frá lyfjagjöf.
2. Augnþrýstingslækkandi áhrif irbesartan og candesartan voru mæld í 10 kanínum. Algengt glákuaugndropalyf, 0.5% timolol, var síðan notað til

samanburðar. Augnþrýstingur var mældur með sérstökum augnþrýstingsmæli á tíma 0, 2 og 4 klukkustundum eftir stakan lyfjaskammt.

3. Framkvæmd var *in vitro* rannsókn á augnvef úr svínum með Franz-sveimklefa til að bera saman gegndræpi 27 mismunandi efnasambanda yfir hornhimnu og augnslímhúð – augnhvítu – æðahimnu og sjónhimnu. Reiknað var út flæði lyfja og gegndræpisstuðlar fyrir hvert efnasamband og vef. Lýsing á 39 sameindum fyrir efnasamböndin sem voru notuð, voru fengin frá ákveðnum gagnagrunnum á alnetinu og notuð til að reikna út fylgni við gegndræpisstuðul með Spearman's rho fylgnistuðul.

Niðurstöður

1. Styrkur irbesartan í augnvökva meðferðarauga fór upp í 282 ± 159 ng/g (meðaltal \pm SD, $n = 26$) og fyrir candesartan 70 ± 73 ng/g. Hæsti styrkur í hornhimnu var $3662,6 \pm 987,7$ ng/g fyrir irbesartan og $3503,9 \pm 801,5$ ng/g fyrir candesartan. Cediranib maleate mældist í sjónhimnu í styrkleika 1070 ± 1404 nM og í glerhlaupi 19 ± 9 nM ($n = 6$).
2. Candesartan hafði mest lækkandi áhrif á augnþrýsting, með breytingu upp á 5,6 mmHg fjórum klukkustundum eftir lyfjagjöf samanborið við 4,0 mmHg fyrir irbesartan og 4,6 mmHg fyrir timolol.
3. 22 af 27 efnasamböndum (81%) sýndu hærra gegndræpi í gegnum augnslímhúð-augnhvítu-æðahimnu-sjónhimnu leiðina, samanborið við hornhimnu. Meðalgegndræpi fyrir augnslímhúð-augnhvítu-æðahimnu-sjónhimnu vefina var 2,9 sinnum hærra en gegndræpi hornhimnunnar. Fylgni var á milli aukins vatnsleysnis og meira gegndræpis yfir bæði hornhimnu í fullri þykkt og augnslímhúð-augnhvítu-æðahimnu-sjónhimnu-leiðina, á meðan hærri fitusækni, mólmassi og fjöldi hringa leiddi til lægri gegndræpisstuðla.

Umræða

Irbesartan, candesartan og cediranib mældust í styrk af tilætluðum lyfjafræðilegum áhrifum í fremri og aftari hluta augans eftir lyfjagjöf með sýklódextrin augnlyfjaferjum. Niðurstöðurnar gefa til kynna staðbundna dreifingu lyfjanna sem gæti komið í veg fyrir þörf á inngripsmiklum lyfjagjöfum.

Irbesartan og candesartan í augndropaformi lækkuðu augnþrýsting hjá kanínum með góðum árangri, sem gæti bent til nýs flokks glákulyfja.

In vitro gögn okkar benda til þess að fyrir mörg efnasambönd gæti augnslímhúð-augnhvítu leiðin verið áhrifameiri og mögulega eina leiðin til að skila lyfjum í vefi í aftari hluta augans með staðbundinni augndropalyfjagjöf.

Lykilorð: augnlyfjagjöf, staðbundin gjöf, sýklódextrín, gegndræpi, hornhimnu leið, augnslímhúð-augnhvítu leið

Abstract

Purpose: Topical ocular administration is the preferred route for many classes of drugs because of its ease of administration. It is the most common way of treating eye diseases in the anterior segment. Topical administration through the cornea, however, is inefficient for drug delivery to the back of the eye. Intravitreal injections are the standard drug treatment for posterior segment disorders but are associated with the risk of complications and patient discomfort.

The conjunctiva-sclera route has shown a relatively higher permeability to macromolecules, a larger surface of exposed tissue and a closer location to the retina when compared to the cornea. Consequently, it has been suggested as an alternative route for topical drug delivery to the posterior segment.

The main goals of this thesis are (1) to test the efficacy of cyclodextrin-based eye drop formulations in delivering certain drugs to the anterior and posterior segments of the eye, (2) to determine the pharmacological effect of angiotensin receptor blockers on intraocular pressure after topical administration, (3) to evaluate and compare the *in vitro* permeabilities of the corneal and noncorneal routes for topical drug delivery to the posterior segment and (4) to identify the main physicochemical properties affecting the permeation of drugs across full-thickness cornea and conjunctiva-sclera-choroid-retina.

Methods:

1. Two separate *in vivo* studies were performed in rabbits to measure the drug concentration in the intraocular tissues after a single dose administration of cyclodextrin-based nanosuspension eye drops. In the first study, two different angiotensin receptor blockers, 1.5% irbesartan and 0.15% candesartan, were administered to 49 rabbits and the drug concentrations in the cornea and aqueous humour were quantified at 1, 2, 3, 6 and 12 hours after administration. In the second study, a novel γ -cyclodextrin nanoparticle eye drops formulation containing cediranib maleate, was applied to 26 rabbits. The concentration of cediranib maleate in the tissues of both anterior and posterior segments was quantified at 1, 3 and 6 hours after administration.
2. The potential lowering effect of irbesartan and candesartan on intraocular pressure was investigated in 10 rabbits. The IOP was measured at 0, 2 and 4 hours after a single-dose administration using a rebound tonometer and compared with a commercial 0.5% timolol solution.
3. *In vitro* studies were performed using porcine ocular tissues mounted on Franz-diffusion cells to compare the permeability of 27 different compounds across

full-thickness cornea and conjunctiva-sclera-choroid-retina. The drug fluxes and permeability coefficients were calculated for each compound and tissue. 39 molecular descriptors were obtained for our compounds from different online databases and correlated with their permeability coefficient using Spearman's rho.

Results:

1. Irbesartan and candesartan reached maximum concentrations in the aqueous humour of the treated eyes three hours after administration. Cediranib maleate was found in all studied tissues, and the highest concentrations in the retina and vitreous were found 1 hour after the administration.
2. Irbesartan and candesartan showed an IOP lowering effect that was equivalent to that of timolol four hours after the administration.
3. Regarding the *in vitro* permeability data, 22 out of 27 compounds (81%) showed a higher permeability across conjunctiva-sclera-choroid-retina compared with the full-thickness cornea. The mean permeability of the noncorneal route was 2.9 times higher than the cornea. The correlation analysis showed that charge, mass and size, lipophilicity, and the ability to form hydrogen bonds were the most relevant properties for corneal permeability, while lipophilicity and the number of rings and rotatable bonds were more important for the noncorneal route.

Discussion: The drugs were found at pharmacologically relevant concentrations in both anterior and posterior segments of the eye after topical administration of cyclodextrin-based formulations. These results indicate a local delivery that could contribute to minimizing systemic drug absorption while replacing the need for invasive drug delivery techniques.

Irbesartan and candesartan successfully lowered the IOP in rabbits when topically administered, suggesting the potential for a new class of glaucoma drugs.

Our *in vitro* data suggest that, for many compounds, the noncorneal route could represent a more effective, and possibly the only way of drug delivery to the posterior segment following topical administration.

Keywords: Ocular drug delivery, topical administration, cyclodextrins, permeability, corneal route, conjunctiva-sclera route.

Acknowledgements

This thesis was carried out between 2018 and 2022 at the Faculty of Medicine, University of Iceland. The project received funding from *transMed*, a European Union's Horizon 2020 research and innovation programme under the Marie Skłodowska-Curie grant agreement No 765441, PREVIN, a Eurostar European Union's programme under the project No E11008, and Oculis ehf. (Reykjavík, Iceland).

After months of dedication to this project, I would like to thank all those people whose support and guidance made this Ph.D. possible, turning it into an outstanding experience for me, both personally and professionally.

First, I want to thank my thesis advisors, Einar and Ólöf, whose invaluable experience and advice have helped me become, I believe, a more confident, independent, creative and critical researcher. I highly appreciate their constant support, as well as the autonomy I was always given during this project. I was also lucky to count on the crucial help of my co-advisor, Thorsteinn Loftsson, in answering any question I had, especially in the initial stages of the project, and the team at Oculis ehf., for their instructions in setting up experiments and new techniques. I would also like to thank Dr Pitsiree Praphanwittaya for her help during the studies described in Paper II, including the development and analysis of the drug formulation, as well as her valuable participation in writing and revising the manuscript.

To my parents, for their unconditional encouragement; dad, thanks for always reminding me that the only way is forward; mom, thanks for helping me keep my feet on the ground and to both of you for always trusting I can overcome any obstacle. To my sister, Berta, for helping me see things clearer. To the rest of my family, you make everything better by just being.

To Aurelija, one of the best things Iceland has given me, it would take pages to thank you for everything you do. To you I owe you every bit of strength in the middle of every crisis during this Ph.D. Thank you for believing in me every time I don't.

To all my friends, who made these years a greatly enjoyable experience. Fatih, to you especially, for welcoming me to Iceland and learning together how Mediterraneans can cope with the cold and dark months. And to Ingvi, for your patience, help and involvement in making sense of all numbers, formulas and calculations.

To the other members of my doctoral committee, Dr Gauti Jóhannesson and Dr Gerhard Garhöfer, for their collaboration in this thesis and their helpful advice.

Finally, to the *transMed* network, I am truly grateful for the precious opportunity to be part of this programme. I want to thank you for all the guidance, the resources, the meetings, the lectures, and the trips, which made this experience an even more unforgettable one. To my co-advisor within the *transMed* project, Heiko von der Leyen, for his interest in my project and his insightful help.

Contents

Ágrip	iii
Abstract	v
Acknowledgements	vii
Contents	ix
List of abbreviations	xii
Table of figures	xiv
List of tables	xvi
List of original papers	xvii
Declaration of contribution	xviii
1 General introduction	1
1.1 Ocular drug delivery	2
1.1.1 Topical ocular drug delivery.....	3
1.1.2 Delivery routes	4
1.2 Tissue layers and permeability	6
1.2.1 Anterior segment.....	6
1.2.2 Posterior segment.....	10
1.3 Ocular diseases	14
1.3.1 Intraocular pressure	15
1.3.2 Neovascularization	19
1.4 Ocular delivery systems.....	20
1.4.1 Cyclodextrins	21
1.4.2 Lipidic nanocapsules.....	22
1.5 Ocular pharmacokinetics.....	23
1.5.1 Pharmacokinetic models	23
1.5.2 <i>In vitro</i> and <i>ex vivo</i> models.....	24
1.5.3 Diffusion in permeation studies	25
1.5.4 Prediction of permeability in drug development	32
2 Aims	33
2.1 Paper I: Angiotensin Receptor Blockers in cyclodextrin nanoparticle eye drops: Ocular pharmacokinetics and pharmacologic effect on intraocular pressure.....	33

2.2	Paper II: Topical Noninvasive Retinal Drug Delivery of a Tyrosine Kinase Inhibitor: 3% Cediranib Maleate Cyclodextrin Nanoparticle Eye Drops in the Rabbit Eye.	33
2.3	Paper III: Drug permeability across full-thickness cornea and conjunctiva-sclera-choroid-retina: <i>in vitro</i> studies.	33
3	Materials and Methods	35
3.1	Paper I	35
3.1.1	Ethical statement	35
3.1.2	Animals.....	35
3.1.3	Test compounds	35
3.1.4	Intraocular pressure	36
3.1.5	Pharmacokinetic study.....	36
3.2	Paper II.....	38
3.2.1	Ethical statement	38
3.2.2	<i>In vivo</i> studies	38
3.2.3	Test compounds	38
3.2.4	Sample preparation	39
3.2.5	Quantitative determinations.....	39
3.2.6	Statistical analysis	40
3.3	Paper III.....	40
3.3.1	Compounds and sample preparation	40
3.3.2	Tissue preparation	41
3.3.3	Permeation experiments	41
3.3.4	Analytical Methods	42
3.3.5	Calculations of corneal and conjunctiva-sclera-choroid-retina permeability	42
3.3.6	Testing of new compounds and formulations	43
3.3.7	Correlation between permeability and physicochemical properties	44
3.3.8	Data analysis and statistics	44
4	Results	45
4.1	Effect of angiotensin receptor blockers on the intraocular pressure after topical administration	45

4.2	Ocular pharmacokinetics of angiotensin receptor blockers in the anterior segment	46
4.3	Ocular pharmacokinetics of cediranib maleate in γ -cyclodextrin eye drop nanoparticles	49
4.4	Comparison between fresh and frozen tissues for the permeation experiments	53
4.4.1	Full-thickness cornea	53
4.4.2	Conjunctiva-sclera-choroid-retina.....	54
4.5	Determination of steady-state flux and permeability coefficient	55
4.5.1	Sink conditions.....	55
4.5.2	Non-sink conditions	56
4.5.3	Atypical permeation profiles	57
4.6	Corneal and conjunctiva-sclera-choroid-retina permeability	58
4.7	cGMP and lipidic nanocapsules	60
4.8	Correlation between permeability and molecular properties	61
4.8.1	Full-thickness cornea	61
4.8.2	Conjunctiva-sclera-choroid-retina.....	62
5	Discussion	65
5.1	<i>In vivo</i> pharmacokinetics	66
5.1.1	Angiotensin receptor blockers.....	66
5.1.2	Cediranib maleate	68
5.2	Comparative permeability of corneal and conjunctiva-scleral delivery routes	69
5.2.1	<i>Ex vivo</i> testing of new compounds	71
5.2.2	Ocular permeability and physicochemical properties	72
6	Conclusions	77
	References.....	79
	Paper I	99
	Paper II	109
	Paper III	121
	Appendix I.....	165

List of abbreviations

ACE	Angiotensin-converting enzyme
AMD	Age-related macular degeneration
ARB	Angiotensin receptor blocker
ARVO	The Association for Research in Vision and Ophthalmology
AT	Angiotensin
CAD	Charged aerosol detector
CD	Cyclodextrin
ESI	Electrospray ionization
HLB	Hydrophilic-Lipophilic-Balanced
HPLC	High-performance liquid chromatography
IC50	Half-maximal inhibitory concentration
IOP	Intraocular pressure
IVI	Intravitreal injection
KDR	Kinase domain receptor
LC-MS	Liquid chromatography-mass spectrometry
LC-MS/MS	Liquid chromatography with tandem mass spectrometry
LNC	Lipid nanocapsule
MAST	Matvælastofnun (Icelandic Food and Veterinary Authority)
MRM	Multiple reacting monitoring
PBS	Phosphate-buffered saline

PK	Pharmacokinetics
QSAR	Quantitative structure-activity relationship
RAAS	Renin-angiotensin-aldosterone system
RAS	Renin-angiotensin system
RPE	Retinal pigment epithelium
SD	Standard deviation
TKI	Tyrosine kinase inhibitor
TKR	Tyrosine kinase receptor
UV-Vis	Ultraviolet-visible
VEGF	Vascular-endothelial growth factor
VEGFR	Vascular-endothelial growth factor receptor
cGMP	cyclic guanosine- 3' ,5' - monophosphate

Table of figures

Figure 1. Primary layers of the eye..	1
Figure 2. Sites and methods for ocular drug delivery to the eye.....	2
Figure 3. Intravitreal injection.	3
Figure 4. Main layers of the cornea: epithelium, stroma and endothelium.	4
Figure 5. Main layers of the posterior segment	5
Figure 6. Schematic drawing of the eye.....	6
Figure 7. Layers of the cornea..	7
Figure 8. Layers and tissues in the anterior segment of the eye.....	8
Figure 9. Posterior segment of the eye..	10
Figure 10. Layers of the sclera.....	11
Figure 11. Inner layers of the retina	13
Figure 12. Aqueous humour flow through the conventional pathway (trabecular outflow, yellow) and the non-conventional pathway (uveoscleral outflow, red).	16
Figure 13. Renin-angiotensin system.....	17
Figure 14. Cyclodextrin-drug inclusion complex formation.	21
Figure 15. Schematic diagram comparing dimensions between rabbit and human eye.	25
Figure 16. Example of permeation profile plot (cumulative permeated amount versus time).....	27
Figure 17. Schematic representation of different permeation profiles.	29
Figure 18. Dissected tissues after eye enucleation. Top row, left: aqueous humour; middle and right: cornea. Middle row, left to right: iris, lens and vitreous. Bottom row, left: sclera and retina; right: sclera without retina.....	39
Figure 19. Franz-type diffusion cell.	42
Figure 20. Mean (mmHg, mean \pm SD) and individual values for IOP change for each of the different drug and control groups four hours after eye drop application.	45
Figure 21. IOP change (mmHg, mean \pm SD, n=10) at different timepoints after eye drop administration for each drug.	46

Figure 22. Top: irbesartan concentration (n = 26, mean ± SD; ng/g) in the cornea. Bottom: irbesartan concentration in the aqueous humour. Charts show drug concentration at timepoints (hours) after administration. Study eyes are shown in blue and untreated fellow eyes are shown in grey.	48
Figure 23. Top: candesartan concentration (n = 23, mean ± SD; ng/g and nmol) in the cornea. Bottom: candesartan concentration in the aqueous humour. Charts show drug concentration at timepoints (hours) after administration. Study eyes are shown in orange and untreated fellow eyes are shown in grey.	49
Figure 24. 3% cediranib maleate concentration (mean ± SD; ng/g, n = 6) in the different eye tissues for the study eye (solid line), the untreated fellow eye (dotted line) and blood samples at different timepoints after administration.	52
Figure 25. Cumulative permeated amount per area ($\mu\text{g}/\text{cm}^2$, mean ± SD, n = 3) of 2.4% Irbesartan through fresh (dashed line) and frozen-thawed full-thickness cornea (solid line).	54
Figure 26. Cumulative permeated amount per area ($\mu\text{g}/\text{cm}^2$, mean ± SD, n = 3) of 2.4% Irbesartan through fresh (dashed line) and frozen-thawed conjunctiva-sclera-choroid-retina (solid line).	54
Figure 27. Cumulative amount permeated per area ($\mu\text{g}/\text{cm}^2$, mean ± SD, n = 3) of atenolol through full-thickness cornea.	55
Figure 30. Cumulative amount permeated per area ($\mu\text{g}/\text{cm}^2$, mean ± SD, n = 3) of dexamethasone through full-thickness cornea.	56
Figure 29. Cumulative amount permeated per area ($\mu\text{g}/\text{cm}^2$, mean ± SD, n = 3) of propranolol hydrochloride through conjunctiva-sclera-choroid-retina.	57
Figure 31. Individual permeability coefficient values (cm/s, mean ± SD, n = 3) for full-thickness cornea (gray) and conjunctiva-sclera-choroid-retina (black) for each compound tested.	58
Figure 32. Mean permeability coefficient values ($\times 10^{-6}$ cm/s, mean ± SD, n = 27) for full thickness cornea (gray) and conjunctiva-sclera-choroid-retina (black) for all compounds tested.	58
Figure 33. Cumulative amount permeated per area ($\mu\text{g}/\text{cm}^2$, mean ± SD, n = 3) of DF003 as a naked compound (dashed line) and in a formulation with lipidic nanocapsules (solid line) through full-thickness cornea (top) and conjunctiva-sclera-choroid-retina (bottom).	60
Figure 35. Scatter plots for the correlations between physicochemical properties and the permeability of compounds across full-thickness cornea.	62
Figure 36. Scatter plots for the correlations between physicochemical properties and the permeability of compounds across conjunctiva-sclera-choroid-retina.	64

List of tables

Table 1. Comparison of eyeball dimensions between rabbit, pig and human.	24
Table 2. Concentration of irbesartan (ng/g, mean \pm SD, n = 26) in the corneal tissue and aqueous humour at different timepoints after eye drop administration.	46
Table 3. Concentration of candesartan (ng/g, mean \pm SD, n = 23) in the corneal tissue and aqueous humour at different timepoints after eye drop administration.	47
Table 4. Highest concentration of cediranib maleate (nM, mean \pm SD; n = 6) in each tissue for the study eye (left) and corresponding concentration in the fellow eye (right). p-value indicates the difference (p < 0.05) in concentration levels of cediranib maleate between the study eye and the untreated fellow eye.	53
Table 5. Permeability coefficient values (10^{-6} cm/s, mean \pm SD, n = 3) for full-thickness cornea and conjunctiva-sclera-retina-choroid for all compounds tested.	59

List of original papers

This thesis is based on the following original publications, which are referred to in the text by their Roman numerals (I-V [as needed]):

- I. Lorenzo-Soler L, Olafsdottir OB, Garhöfer G, Jansook P, Kristinsdottir IM, Tan A, Loftsson T, Stefansson E. Angiotensin Receptor Blockers in cyclodextrin nanoparticle eye drops: Ocular pharmacokinetics and pharmacologic effect on intraocular pressure. *Acta Ophthalmol.* 2021 Jun;99(4):376-382.
- II. Lorenzo-Soler L, Praphanwittaya P, Olafsdottir OB, Kristinsdottir IM, Asgrimsdottir GM, Loftsson T, Stefansson E. Topical noninvasive retinal drug delivery of a tyrosine kinase inhibitor: 3% cediranib maleate cyclodextrin nanoparticle eye drops in the rabbit eye. *Acta Ophthalmol.* 2022 Jan 26.
- III. Lorenzo-Soler, L., Olafsdottir, O. B. & Stefansson, E. Corneal and conjunctival-scleral routes for topical ocular drug delivery. "Submitted".

Declaration of contribution

The doctoral student, Laura Lorenzo Soler, and her supervisors Einar Stefánsson and Ólöf Birna Ólafsdóttir, worked together in planning the general research and studies described in this thesis. The doctoral student designed and performed the *in vivo* experiments described in Paper I (intraocular pressure measurements) and Paper II, including scheduling of the animal studies, eye drops administration, intraocular measurements and collection and analysis of the data. She also designed and performed the *in vitro* studies using Franz-diffusion cells, including picking up the pig eyes, the dissection of tissues employed in the experiments, the experimental setup, the collection of samples, the drug concentration measurements and calculation of permeability coefficients.

The cyclodextrin-based formulations with angiotensin receptor blockers candesartan and irbesartan were developed by Dr Phatsawee Jansook as described in his paper (Jansook et al., 2015).

The *in vivo* pharmacokinetic studies with angiotensin receptor blockers described in Paper I were performed at the Medical University of Vienna, under the supervision of Dr Gerhard Garhöfer. The student attended and assisted the study during the eye drop administration and enucleation and dissection of the eyes. The samples were sent to Aimin Tan from Nucro-Technics (Ontario, Canada), where they were analyzed by HPLC. Aimin Tan designed and performed the drug measurements in the ocular tissues for candesartan and irbesartan, and kindly provided a detailed description of the methodology used.

The cyclodextrin-based formulation used in the *in vivo* experiments of Paper II, which contained the tyrosine kinase inhibitor cediranib maleate, was developed by Dr Pitsiree Praphanwittaya at the Faculty of Pharmacy, University of Iceland. She participated in the writing and revision of the manuscript of Paper II, kindly providing detailed information about the development and analysis of the drug formulation.

During the *in vivo* studies described in Paper II, professional assistance by a veterinarian at the Institute for Experimental Pathology from the University of Iceland was provided when carrying out euthanasia of the rabbits with pentobarbital. After euthanasia, the student, assisted by her supervisor, enucleated the eyes, and dissected and collected the tissues, which were sent to Charles River Laboratories (Hertogenbosch, Netherlands) for drug quantification by LC-MS/MS.

Once the quantification results were obtained from Charles River, the student analyzed the data, drafted the manuscript and wrote the thesis, guided and assisted by her supervisors.

Guðrún Marta Ásgrímsdóttir and Íris Mýrdal Kristinsdóttir, employees of Oculis ehf., provided the protocol and assisted in scheduling the *in vivo* experiments, where the pharmacokinetics of candesartan and irbesartan (Paper I) and cediranib maleate (Paper II) were tested. As co-authors of both Papers I and II, they reviewed the final drafts before submission.

1 General introduction

The eye is a sensitive organ protected from foreign materials by its architecture, compartmental organization, impermeable epithelium, tear secretion and ocular drainage pathways (Agrahari et al., 2016). The human eyeball consists of three primary layers: the outermost supporting layer of the eye, consisting of clear cornea, opaque sclera and the border between them, designated as the limbus; the middle uveal layer of the eye, which encompasses the iris, ciliary body, and choroid; and the interior layer of the eye, the retina (Kels et al., 2015).

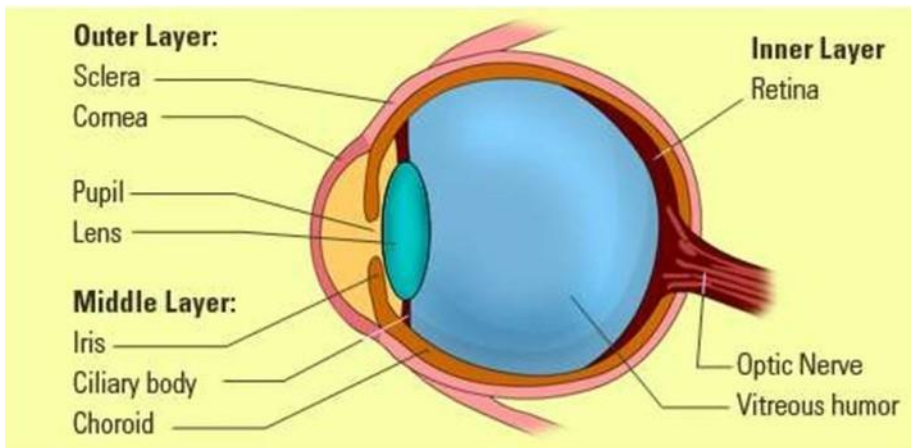


Figure 1. Primary layers of the eye. From Ophthalmology for healthcare assistant's. (<https://ophthalmologyforhealthcareassistants.wordpress.com/2017/04/06/basic-parts-and-functions-of-the-eye/>).

The eye is compartmentalized as the anterior and posterior segments. The anterior mainly consists of light focusing elements, such as cornea, iris, lens, aqueous humour and conjunctiva, while the posterior contains the posterior sclera, vitreous humour, choroid, retina and optic nerve (H. Chen, 2015).

1.1 Ocular drug delivery

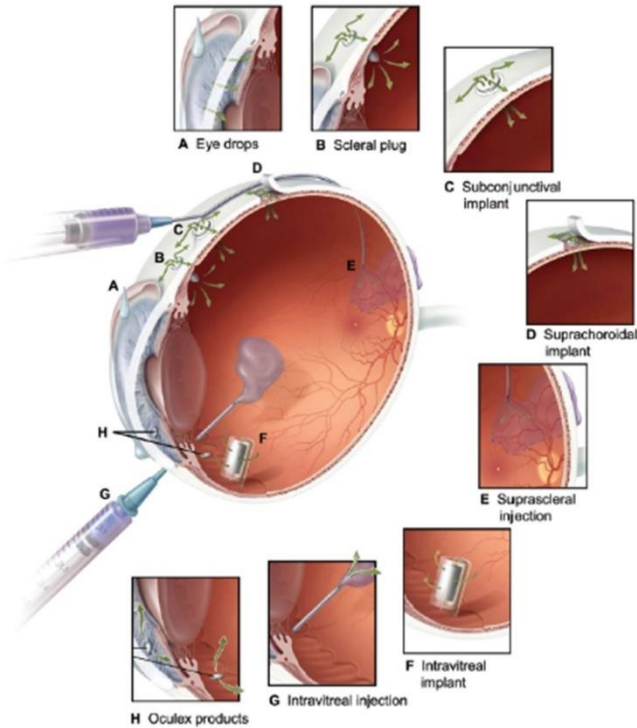


Figure 2. Sites and methods for ocular drug delivery to the eye (Short, 2008).

Ophthalmic drug delivery is one of the most interesting and challenging endeavours in the field of pharmaceutical sciences. The anatomy, physiology, and biochemistry of the eye render this organ highly inaccessible to foreign substances. Therefore, achieving an optimal concentration of a drug at the active site is one of the main issues when designing a therapeutic system (Shastri et al., 2010).

Diseases in the posterior segment of the eye are leading causes of visual impairment and irreversible blindness (Thrimawithana et al., 2011). In clinical practice, the standard procedures in treating these disorders are the intravitreal (IVI) administration of drugs or systemic drug administration.

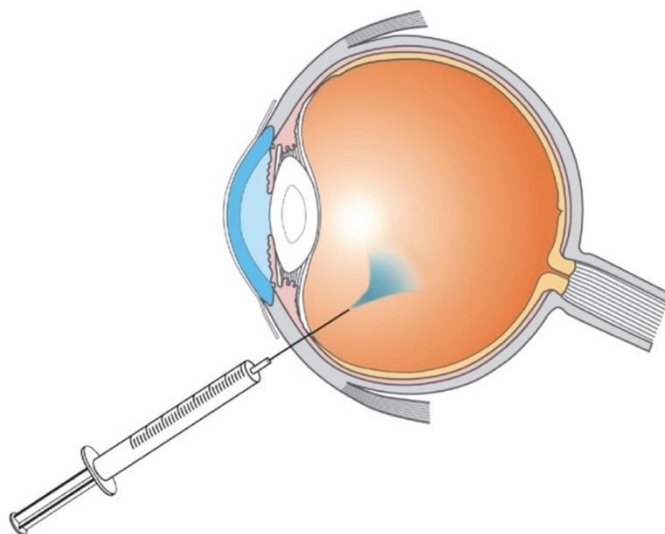


Figure 3. Intravitreal injection (Honda et al., 2013).

The advantage of the IVI technique is the ability to maximize intraocular levels of medications (Moisseiev & Loewenstein, 2017a; Peyman et al., 2009). The procedure is short and simple, has a good local and systemic safety profile, and enables restoration and preservation of visual acuity in a large number of patients (Moisseiev & Loewenstein, 2019). These injections, however, are associated with the risk of complications, mostly due to the repeated injections and long-term treatments that are commonly needed (Falavarjani & Nguyen, 2013). These complications may include raised intraocular pressure, floaters, vitreous haemorrhage, transient blurry vision, retinal haemorrhage, retinal tears, retinal detachment, endophthalmitis, and cataracts (Edelhauser et al., 2010).

1.1.1 Topical ocular drug delivery

The topical administration of drugs remains the preferred route for the treatment of ocular diseases due to its non-invasiveness, ease of application and patient convenience. It is especially commonly used in the treatment of anterior segment disorders such as elevated intraocular pressure, infections, and inflammations (Boddu et al., 2014; Fuchs & Igney, 2017; Souza et al., 2014). Conventional ocular drug delivery systems constitute a wide range of ophthalmic products available in the market, including topical solution eye drops, emulsions, suspensions and ointments (A. Patel et al., 2013).

To be effective, topically administered drugs must penetrate across the eyewall (e.g., cornea, sclera, and conjunctiva) to reach therapeutic targets within the globe (Prausnitz, 1998). The bioavailability of ocular drugs is, therefore, greatly limited by the many physical and biochemical barriers that form the eye (Awwad et al., 2017).

For the anterior segment of the eye, precorneal factors such as dosage spill-over, nasolacrimal drainage, blinking, tear film and tear mucin contribute to the low absorption and distribution of topically applied drugs (H. Chen, 2015). It is generally assumed that only 5% or less of the instilled dose can effectively be delivered through the corneal route (Djebli et al., 2017). Moreover, the delivery of drugs to the back of the eye following administration to the cornea is highly inefficient due to the distance drugs need to overcome before reaching the target sites (e.g. vitreous and retina). Consequently, few therapeutic agents have been shown to successfully reach the posterior segment at therapeutic concentrations (Ako-Adounvo & Karla, 2018; Edelhauser et al., 2010).

1.1.2 Delivery routes

After topical administration, drugs can penetrate the intraocular tissues in three different ways: 1) corneal route, 2) systemic circulation or 3) direct penetration pathway (Ranta & Urtti, 2006a).

The corneal route is generally seen as the main absorption path for most ophthalmic therapeutics and has traditionally been the mechanism by which topically applied drugs are believed to gain access to the internal ocular structures (Barar et al., 2008). However, corneal absorption is also considered to be a rate-limited process due to the presence of the corneal epithelium, a lipoidal layer that creates resistance to the permeation of topically administered hydrophilic compounds. In contrast, the corneal stroma, which is the corneal layer located between the epithelium and the endothelium comprising 90% of the corneal thickness, is composed of a highly hydrated extracellular matrix that limits the permeation of lipophilic substances (Gaudana et al., 2010).

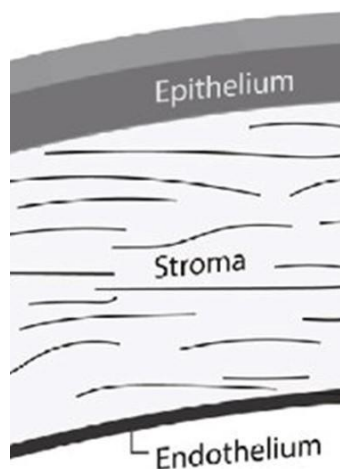


Figure 4. Main layers of the cornea: epithelium, stroma and endothelium (Matthyssen et al., 2018).

Although the anatomy and physiology of the eye seem to pose almost insurmountable barriers for topical drug delivery to the posterior segment tissues, topically administered drugs have also been shown to reach the back of the eye (Edelhauser et al., 2010).

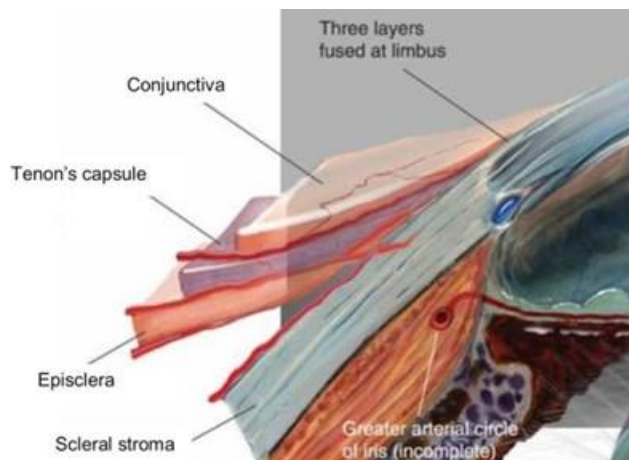


Figure 5. Main layers of the posterior segment (Boote et al., 2020).

An alternative noncorneal route, based on the direct penetration of drugs through conjunctiva and sclera, has been increasingly on the scope in the field of drug delivery, due to its relatively high permeability to macromolecules compared with the cornea (Ranta & Urtili, 2006a). Based on several studies that investigate the importance of different routes to intravitreal drug delivery, the penetration of drugs through the conjunctiva-scleral pathway is the most important delivery route for compounds that have widely differing physicochemical properties (Ambati et al., 2000; Cruysberg et al., 2005; Hämäläinen et al., 1997; Olsen et al., 1995). Thus, in terms of topical ophthalmic drug delivery, the noncorneal absorption route may be important for drugs that are poorly absorbed across the cornea due to their physicochemical properties (Pescina et al., 2015; Ranta & Urtili, 2006a).

In addition, the conjunctiva-sclera presents a mean total surface area of 16-17 cm², which is relatively large compared with a corneal surface area of approximately 1 cm² (Olsen et al., 1995). No measurements of the area of exposed sclera are found in the literature, however, several studies have reported an index of the size of visible sclera, measured as the ratio between the width of the exposed eyeball and the diameter of the iris in humans. Based on their results, the amount of exposed sclera is twice that of the iris and, consequently, the cornea, which provides a significantly larger avenue for drug diffusion to the inside of the eye (Caspar et al., 2021; Danel et al., 2018; Kobayashi & Kohshima, 1997, 2001).

1.2 Tissue layers and permeability

From a physiological point of view, the eye can be divided into two segments, an anterior segment consisting of the cornea, the conjunctiva, the ciliary body, the iris, aqueous humour, lens, and lacrimal system, and a posterior segment composed of the retina, the vitreous humour, the choroid and the sclera (Agrahari et al., 2016; A. Patel et al., 2013). Each layer presents different properties, most of them affecting the permeation of drugs to the intraocular tissues.

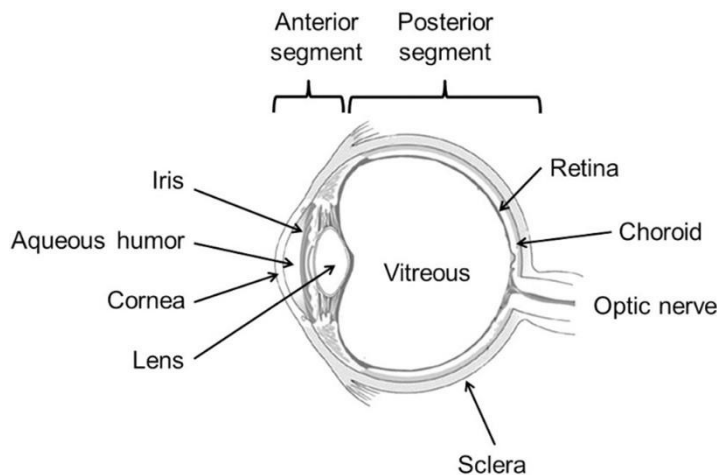


Figure 6. Schematic drawing of the eye (Loftsson & Stefánsson, 2017).

1.2.1 Anterior segment

1.2.1.1 Cornea

The cornea is normally clear, avascular and in a state of relative dehydration. Being negatively charged at physiological pH (~7.4), the cornea is more permeable to cations than anions. Moreover, the presence of tight junctions between the corneal epithelial cells retards paracellular drug permeation, thus limiting corneal permeability to hydrophilic and ionized molecules (Achouri et al., 2013; Gaudana et al., 2010).

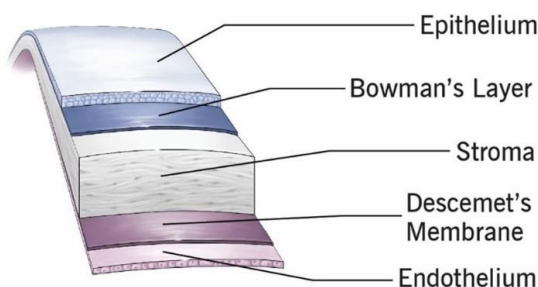


Figure 7. Layers of the cornea (Cornea transplant. 2020. Eye anatomy and layers of the cornea. Cleveland Clinic. <https://my.clevelandclinic.org/health/treatments/17714-cornea-transplant>).

The cornea comprises five layers, starting from the outermost epithelium, Bowman's membrane, stroma, Descemet's membrane, and endothelium.

The permeation of compounds through the cornea is restricted by the epithelium, the permeability of which resembles the permeability of the full-thickness cornea, suggesting that the epithelium is the rate-limiting step for these compounds. Drug penetration is also influenced by the molecular size, with the epithelium being almost impermeable to macromolecules (Agrahari et al., 2016).

Immediately underneath the epithelium is the Bowman's membrane, a thin homogeneous layer forming a transition toward the stroma. The Bowman's membrane, however, similar to Descemet's membrane does not provide significant resistance to drug penetration (Ghate & Edelhauser, 2006).

The stroma lies between the epithelium and endothelium and it forms the main section of the cornea, at around 90% of the total thickness. It is predominantly composed of hydrated collagen fibrils, creating a diffusion barrier to the penetration of lipophilic drugs (P. Agarwal & Rupenthal, 2016).

Descemet's membrane is a tough, homogeneous band supporting the endothelium, a single layer of cells important in keeping the stroma constantly hydrated (Morrison et al., 2013).

The endothelium is a monolayer of cells located at the internal base of the cornea. Solutes can diffuse across the endothelium by the paracellular route, which is a water-filled pathway with gap and tight junctions favoured by hydrophilic molecules and ions, or the transcellular route, where hydrophobic molecules partition into and diffuse within the cell membranes (Edwards & Prausnitz, 2001).

1.2.1.2 Iris

The iris, located between the cornea and the lens, is composed of two different layers: the iris pigment epithelium, a highly vascularized connective tissue, and an anterior cellular border layer. The iris responds to light, controlling the amount that enters the eye (Borrás, 2014).

The accumulation of drugs in pigmented tissues, such as the iris pigment epithelium, is an important factor due to their binding to melanin, and it can influence ocular pharmacokinetics after both local and systemic drug administration. Comparative studies have demonstrated that many drugs reach higher levels of 1-2 orders of magnitude in the pigmented tissues when compared to respective albino tissues (Rimpelä, Reinisalo, et al., 2018).

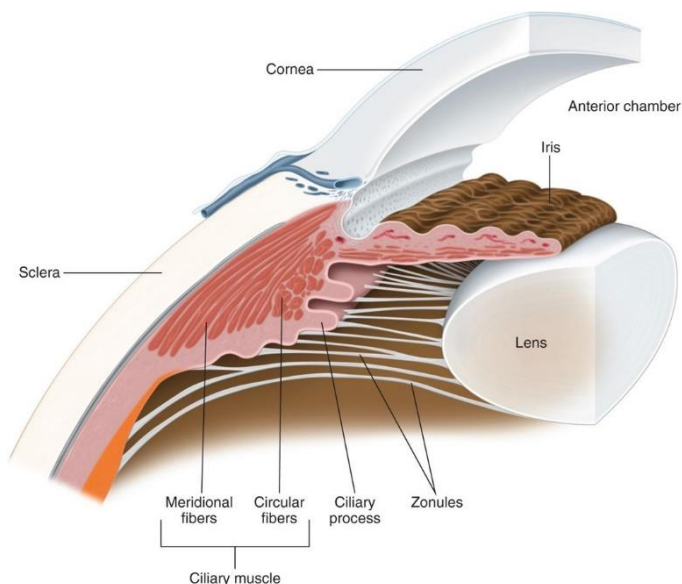


Figure 8. Layers and tissues in the anterior segment of the eye. (Lens anatomy. 2020. *Lens zonules*. The cataract course. <http://cataractcourse.com/lens-anatomy-and-development/lens-anatomy/>).

1.2.1.3 Ciliary body

The ciliary body is a ring of tissue positioned just behind the posterior surface of the iris that separates the aqueous compartment into a posterior and anterior chamber. The surface of the ciliary body shows a series of ridges named ciliary processes that increase the surface area available for the secretion of the aqueous humour (Bill & Helsing, 1965; Borges- Giampani & Giampani, 2013; Delamere, 2005; Grant, 1963).

The entire surface of the ciliary body is covered with a specialized bilayer made of two different cell types, pigmented and non-pigmented ciliary epithelial cells. The tightness of these cell layers effectively isolates the anterior of the eyeball from the blood circulation, avoiding blood and associated molecules to interfere with our vision, and leaving easy access only for highly diffusible and very small molecules (Delamere, 2005; Borges- Giampani & Giampani, 2013; Sarmiento, 2015).

1.2.1.4 Lens

The basic function of the eye lens, which is attached to the ciliary body by fine

ligaments, is to transmit and focus light onto the retina. The contraction of the ciliary muscle causes accommodation, making the lens assume a more rounded shape that causes a shift in our vision focus (Hejtmancik & Shiels, 2015).

The lens is surrounded by a collagenous capsule, which acts as a barrier to diffusion and helps to shape the lens in the accommodation process. The anterior epithelial cells of the lens are connected by gap junctions, allowing an exchange of low-molecular-weight metabolites and ions (Augusteyn, 2007; Delamere, 2005; Gorthy et al., 1971).

1.2.1.5 Aqueous humour

The aqueous humour is a transparent liquid, analogous to a blood surrogate, that provides nutrition, stabilizes the ocular structures, removes excretory products from metabolism and contributes to the regulation of the homeostasis of the ocular tissues while allowing the light transmission to the cornea and lens (Cholkar et al., 2013; Goel, 2010). The aqueous humour is formed by the ciliary epithelium of the ciliary processes from the ciliary body (To et al., 2002). Circulating aqueous humour flows around the lens and through the pupil into the anterior chamber (Heys & Barocas, 2002).

The aqueous humour leaves the eye by passive flow via two pathways at the anterior chamber angle, anatomically located at the limbus (Goel et al., 2010). The conventional pathway consists of aqueous humour passing through the trabecular meshwork, across the inner wall of Schlemm's canal, into its lumen, and into draining collector channels, aqueous veins and episcleral veins (Ascher, 1954; Goldmann, 1950). The non-conventional route is composed of the uveal meshwork and the anterior face of the ciliary muscle. The aqueous humour enters the connective tissue between the muscle bundles, through the suprachoroidal space, and out through the sclera (Bill & Hellsing, 1965; Johnson & Erickson, 2000).

The aqueous humour also plays a key role in maintaining the intraocular pressure, which depends on the balance between its production and drainage through the trabecular meshwork (Nesterova et al., 2020). There is also strong evidence that a fraction of aqueous humour flows through the vitreous and across the retina in the healthy eye as vitreous outflow. Krishnamoorthy et al. studied the elimination of drugs with different physicochemical properties after intravitreal injection or controlled-release implant. They observed that drug elimination followed two main pathways: the aqueous outflow pathway and the vitreous outflow pathway (through the retina) and that a high value of aqueous to vitreous drug concentrations at the beginning of the elimination phase indicates that the drug is preferentially eliminated through the anterior chamber. They suggested that knowing the mode of clearance (Schlemm's canal or retina) would provide information about how much drug would clear through the aqueous chamber and how much would reach the target site in the posterior segment. This would be very useful in estimating the therapeutic range for administering the drugs (Araie & Maurice, 1991; Krishnamoorthy et al., 2008).

1.2.1.6 Conjunctiva

The conjunctiva is a thin, transparent membrane that produces mucus that lines and lubricates the surface of the eye. Like the cornea, the conjunctiva is composed of an epithelial layer covering an underlying stroma. The conjunctival epithelium, however, shows larger paracellular pores (4.0 ± 2.1 nm) than the corneal epithelium (2.0 ± 0.2 nm), offering substantially less resistance to molecules (Ahmed & Patton, 1985; Hämäläinen et al., 1997).

However, a significant proportion of active ingredients is eliminated from the eye to the systemic circulation, caused by the high degree of vascularization of the conjunctiva. Systemic absorption is a component of conjunctival absorption since drugs picked up by the blood are no longer able to diffuse into the underlying tissues. In this context, the importance of bulbar conjunctival absorption to intraocular drug penetration is likely to depend on the relative permeability of the conjunctival epithelium and the blood capillaries, which in turn would depend on drug properties, including lipophilicity. This systemic absorption represents an obstacle to posterior segment applications since the intraocular drug levels achieved are often below effective concentrations (Prausnitz, 1998; Urtili & Salminen, 1993).

1.2.2 Posterior segment

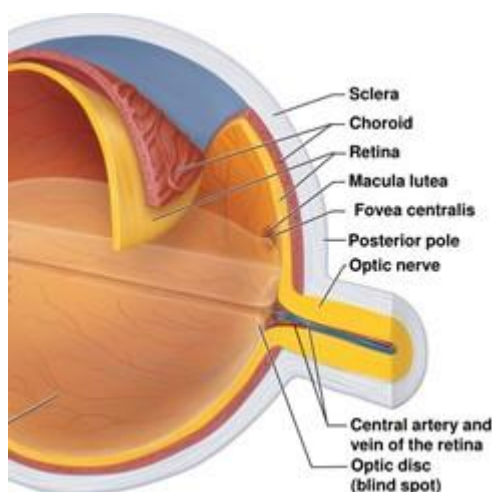


Figure 9. Posterior segment of the eye. (<https://healthengine.com.au/info/the-eye-and-vision>).

1.2.2.1 Sclera

The sclera is the opaque, fibrous, protective, outer layer tissue of the eye. It forms around 85% of the outer tunic of the eyeball, being part of both anterior and posterior segments (Boote et al., 2020). The sclera is composed primarily of collagen, mucopolysaccharides and some elastic fibre. On its anterior surface adjacent to the

cornea, the sclera is covered by the conjunctiva. From the outer to the innermost, the four layers forming the sclera are episclera, stroma, endothelium and lamina fusca. Internally, it is lined by the choroid, which contains blood vessels, and the retina (H. Chen, 2015).

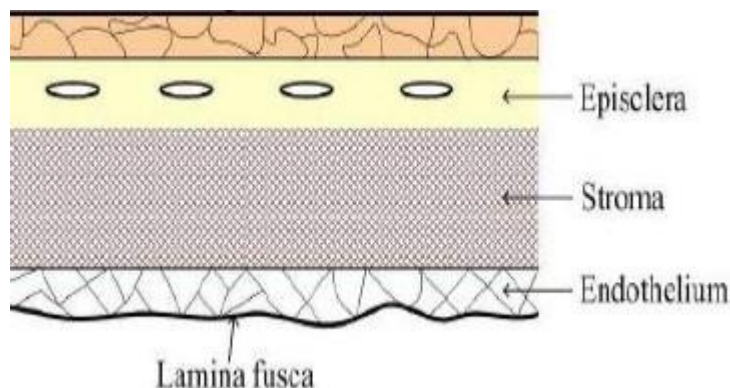


Figure 10. Layers of the sclera (The eyeball membrane. The structure of the sclera. The deformation of the human eyeball when undergoing scleral buckling. Universiti Teknologi Malaysia).

Drugs may diffuse across the sclera by three possible pathways: (1) through perivascular spaces; (2) through the aqueous media of gel-like mucopolysaccharides; or (3) across the scleral substance composed of a matrix of collagen fibrils. It has been reported that the sclera generally offers less resistance to diffusion than the cornea. The primary mechanism for drug permeation in the sclera is likely to be diffusion across the intercellular aqueous media as in the case of the structurally similar corneal stroma (Ahmed & Gokhale, 1972).

Early experiments did suggest that the transscleral route was indeed quite permeable to a range of solutes and that it might be possible to exploit the scleral absorption route to promote site-specific delivery of drugs to intraocular tissues in the back of the eye (Ahmed & Patton, 1985; Prausnitz, 1998). While some studies have demonstrated a clear inverse relationship between permeability and molecular weight, with an abrupt decline in permeability at the larger molecular weights (Ambati et al., 2000; Maurice & Polgar, 1977; Olsen et al., 1995), other permeability studies have shown the sclera to be permeable to a wide range of solutes and that permeability is best correlated with molecular radius (Ambati & Adamis, 2002).

The average surface area of the human sclera (16-17 cm²), with 2.5 cm² of exposed tissue compared to 1 cm² of the exposed cornea, provides a significantly larger surface for drug diffusion to the inside of the eye compared to the surface of the cornea (Olsen et al., 1995; Sridhar, 2018). Moreover, drug delivery through the sclera is dependent upon the thickness of the tissue that the solute must traverse, as well as the surface area available to the compound for diffusion. Geroski and Edelhauser suggested that if

transscleral drug delivery could be directed near the equator, the flux of the applied solute could be maximized (Ambati et al., 2000; Ambati & Adamis, 2002; Edwards & Prausnitz, 1998; Geroski & Edelhauser, 2001; Moisseiev & Loewenstein, 2017b; Nicoli et al., 2009; Watson & Young, 2004).

Besides having a larger area of exposed tissue when compared with the cornea, the conjunctiva-sclera shows a higher permeability to macromolecules, and it is located closer to the tissues of the back of the eye. This suggests that the conjunctiva sclera route could represent a more effective way of delivering drugs to the posterior segment.

1.2.2.2 Choroid

The choroid of the eye is a vascular structure supplying the outer retina. It consists mostly of blood vessels, non-vascular smooth muscle cells, secretory cells and intrinsic choroidal neurons (Nickla & Wallman, 2010). The choroid is part of the blood-retinal barrier and its function depends on tight junctions that restrict the intercellular movement of all water-soluble molecules preventing them from entering the retinal tissue. The fenestrated capillaries in the choroid are very permeable to low molecular weight substances, which results in high concentrations and rapid turnover of nutrients in the extra-vascular compartment of the choroid. However, free diffusion is restricted by the retinal pigment epithelium barrier (Törnquist et al., 1990).

1.2.2.3 Retinal pigment epithelium

The retinal pigment epithelium (RPE) forms a tight-junction epithelium that constitutes a simple layer of cuboidal cells situated behind the photoreceptor cells. The RPE cells exhibit a hexagonal shape, with microvilli that surround the outer segments of both rod and cone photoreceptors. These microvilli expands the surface area of the RPE up to 30-fold, facilitating the functional relationship with the photoreceptor cells. RPE cells carry out many functions including the conversion and storage of retinoid, the phagocytosis of shed photoreceptors outer segment membrane, the absorption of scattered light and ion and fluid transport (Anderson & Fisher, 1979; la Cour & Tezel, 2005; R. Sparrow et al., 2010).

The tight junctions in the RPE form a physical barrier that prevents the passage of molecules and ions through the paracellular space, making the RPE cells the guardians of the outer blood-retinal barrier. The tight junctions of the RPE, however, exhibit some selective leakiness, allowing the presence of some transport mechanisms and creating a selectively permeable barrier to diffusion (Rizzolo, 2007; Shin et al., 2006).

Permeability studies for the RPE are not as extensive as those for, for example, the sclera. The RPE, however, can be easily removed and its permeability characteristics understood by comparing tissue permeability values with and without RPE removal. Pitkänen et al. studied the effect of molecular weight and lipophilicity on the

permeability of the RPE, concluding that it is a major barrier and might be the rate-limiting factor in the retinal delivery of hydrophilic drugs and macromolecules through the transscleral route. The permeability of the RPE also affects the permeation of drugs from the choroidal circulation to the neural retina after systemic administration and the elimination of drugs from the vitreous after intravitreal injection. Permeation rates and transport mechanisms of only sparse and individual drug-like molecules in the RPE are known. However, systematic data on the permeation properties of molecules as a function of size and lipophilicity is needed to predict the permeabilities of new compounds in the RPE and to compare its barrier properties with other ocular membranes (Araie & Kimura, 1997; S. H. Kim et al., 2007; Pitkänen et al., 2005).

1.2.2.4 Retina

The retina is a layered structure with a large diversity of component cells. These cells form morphologically and functionally distinct circuits that work in parallel, and in combination, to produce a complex visual output. The retinal tissue is divided into two segments: the neural retina and the aforementioned retinal pigment epithelium (Hoon et al., 2014; Kolb, 1995).

In the neural retina we find the photoreceptor layer with rod and cone cells. These photoreceptors are specialized neurons that function in the initial step of vision. They are responsible for the process known as phototransduction, which consists of the capture of light and its conversion into electrical signals (Molday & Moritz, 2015; Schwartz et al., 2013).

Located approximately in the centre of the retina is the optic nerve. The optic nerve contains the ganglion cell axons running to the brain and, from the centre of the optic nerve radiate the major blood vessels of the retina which open into the tissue to vascularize the retinal layers and neurons (Kolb, 1995).

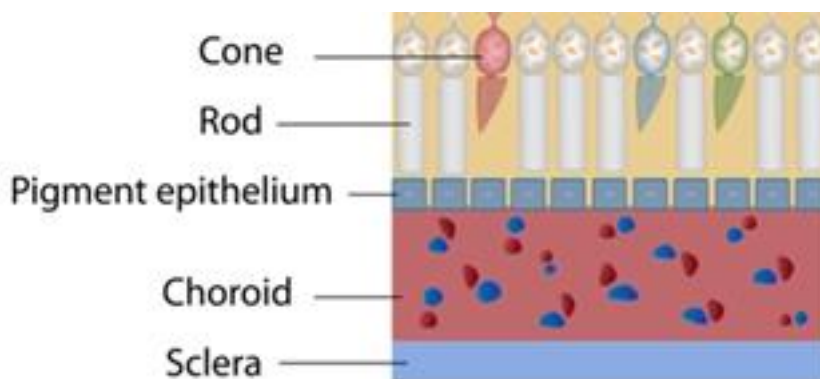


Figure 11. Inner layers of the retina (Layers of the retina. 2020. *Structure of the retina*. The discovery eye foundation. <https://discoveryeye.org/layers-of-the-retina/>).

Jackson et al. carried out a study to determine the maximum size of a molecule capable of freely diffusing across the human retina, concluding that the inner and outer layers are sites of high resistance to the diffusion of large molecules, limiting the free diffusion of molecules larger than 76.5 kDa (Jackson et al., 2003).

Despite the potential importance of trans-retinal macromolecular diffusion in experimental and clinical science, there is a lack of knowledge of the complete permeability of the retina and the principal intraretinal barriers to diffusion have not been fully characterized (Krishnamoorthy et al., 2008).

1.2.2.5 Vitreous humour

The vitreous is a highly hydrated gelatinous mass, consisting mainly of water, collagen and hyaluronic acid, that fills the space between the lens and the retina. The major function of the vitreous is to allow light to reach the retina and to maintain the shape of the eyeball. Moreover, it also modulates the diffusion of all molecules, such as drugs, oxygen and growth factors. (Gisladottir et al., 2009; Murthy et al., 2014).

The water content of the vitreous is about 99%. Its viscosity, however, is two to four times greater than water, due to the viscosity of collagen fibrils and hyaluronic acid, which give the vitreous humour its gelatinous consistency.

Being large, relatively stagnant, and with easy access to the retina, the vitreous is an attractive site for bolus or controlled-release delivery of therapeutic drugs. However, depending on the size and surface properties of molecules, their diffusion can be strongly hindered (J. Xu et al., 2000). Another factor that might influence the pharmacokinetics of small molecules in the eye is protein binding, which is expected to slow down the elimination of drugs, however, little data is available regarding protein binding in the vitreous (Fuchs & Igney, 2017; Käs Dorf et al., 2015; J. Xu et al., 2000).

Intravitreal delivery is currently the method of choice for retinal drug delivery. New delivery systems are needed to prolong the injection intervals in the new retinal drug treatments, but the development of intravitreal drug delivery systems is difficult particularly due to tolerability issues (Shikamura et al., 2016).

1.3 Ocular diseases

Based on recent reports from the World Health Organization (WHO), 253 million people are affected by ocular disorders and visual impairment, globally. Of those, an estimated 85.8% are blind, while the rest suffer from moderate to severe vision impairment (Ako-Adounvo & Karla, 2018).

Ocular disorders are divided into diseases affecting the anterior or posterior segments of the eye. Anterior segment diseases are leading causes of ocular morbidity, usually presenting a continuous progression of symptoms that leads to different degrees of

visual loss (Romero et al., 2014). On the other side, disorders affecting the posterior segment are major causes of visual impairment, accounting for 55% of all ocular diseases leading to irreversible blindness (Ako-Adounvo & Karla, 2018; Ranta & Urtili, 2006b).

In this thesis, we studied the *in vivo* pharmacokinetics of different therapeutics targeting two anterior and posterior segments disorders:

(1) elevated intraocular pressure, a symptom of glaucoma that can lead to optic nerve damage and eventual vision loss, and

(2) retinal neovascularization, associated with age-related macular degeneration (AMD) and diabetic retinopathy (DR), both leading causes of blindness in elderly and working-age people.

1.3.1 Intraocular pressure

The tissue pressure of the intraocular contents is called the intraocular pressure (IOP). The normal range for IOP is 11–21 mm Hg and is maintained at this level throughout life regardless the sex, under some diurnal and seasonal variations. Under normal conditions, the homeostatic balance of formation and outflow of aqueous humour, which occurs in or near the ciliary body and the iris, regulates the pressure inside the eye (Murgatroyd & Bembridge, 2008). Elevated IOP is a well-recognized risk factor associated with glaucoma and is, currently, the only pharmacological target for therapeutic intervention in the management of the disease. In the chronic setting, raised IOP may cause nerve damage at the head of the optic nerve leading to visual field loss (van der Spek et al., 2013).

The intraocular pressure is regulated by the balance between continuous secretion and reabsorption of the aqueous humour (Civan & Macknight, 2004). As mentioned earlier, the aqueous humour is secreted from the epithelial layers of the ciliary body into the posterior chamber and exits the eye via the conventional or trabecular outflow pathway, or the unconventional or uveoscleral outflow pathway (Tamm, 2009b, 2009a).

Under physiological conditions, only the trabecular outflow pathways are relevant for the generation and maintenance of IOP. In the normal eye, the volume in the outflow of aqueous humour through the trabecular pathways equals its secretion from the ciliary body, driven by a pressure gradient (Tamm et al., 2015). However, when an imbalance occurs between secretion and reabsorption, alterations in the IOP arise (Sunderland & Sapra, 2022). In patients with primary open-angle glaucoma, the juxtacanalicular tissue (JCT), the deepest area of the trabecular meshwork, undergoes a series of structural changes that have been linked to an increase in the resistance against the outflow of the aqueous humour, leading to an increase in the IOP (Keller & Acott, 2013).

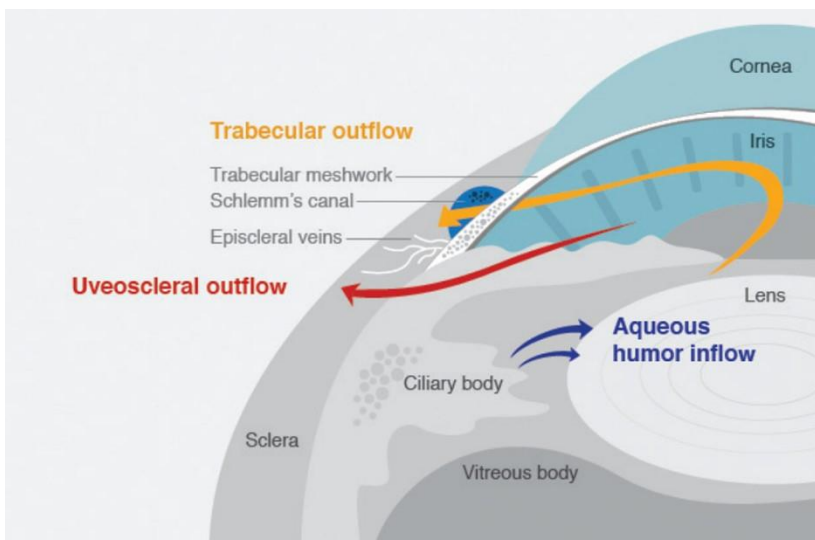


Figure 12. Aqueous humour flow through the conventional pathway (trabecular outflow, yellow) and the non-conventional pathway (uveoscleral outflow, red). (<https://crstoday.com/articles/2018-mar/newly-approved-glaucoma-therapy-increases-options-for-patients-and-providers/>)

1.3.1.1 The renin-angiotensin system

The renin-angiotensin system (RAS) is one of the oldest and most extensively studied human peptide cascades and it is well-known for its role in regulating blood pressure (Holappa et al., 2020a).

Angiotensin II is a multifunctional hormone derived from angiotensinogen in 2 proteolytic steps. In the first step, renin, an enzyme produced by the juxtaglomerular cells of the kidneys, cleaves angiotensin I from angiotensinogen. In the second step, angiotensin I is transformed into angiotensin II by the angiotensin-converting enzyme (ACE) (Touyz & Berry, 2002).

The interaction of angiotensin II with the AT1 and AT2 receptors, located on the plasma membrane of the tissues responsive to the hormone, amplifies volume-retaining and vasoconstrictive effects on the peripheral vascular system, regulating the blood pressure homeostasis. When aldosterone is included, the renin-angiotensin-aldosterone system (RAAS) is involved also in fluid and electrolyte homeostasis (Holappa et al., 2015, 2020a).

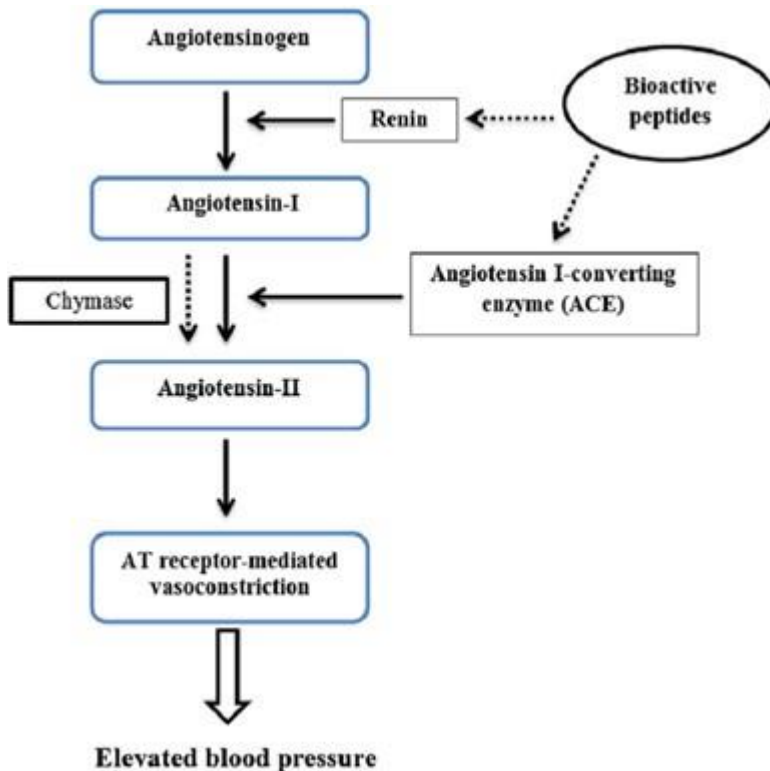


Figure 13. Renin-angiotensin system (Mohammadian et al., 2017).

The renin-angiotensin system can be differentiated into “circulating” and “local” RAS. The circulating RAS comprises kidney-derived renin acting on liver-derived angiotensinogen. Local RAS refers to tissue-based mechanisms of angiotensin peptide formation that operate separately from the circulating RAS (Campbell, 2014).

The evidence for the presence of RAS components necessary for the generation of angiotensin II in the eye is suggestive of a local ocular RAS, which might be involved in the regulation of IOP. However, the precise function and significance of local RAS in the eye have not yet been established (Vaajanen, 2009). Many RAS components have been found in tissues responsible for aqueous humour formation, such as non-pigmented epithelium cells, and in tissues relevant to glaucoma, such as the ciliary body, neural retina and optic nerve, suggesting that local RAS may have a significant

role in the formation and/or drainage of aqueous humour (Cullinane et al., 2002; Downie et al., 2009; Lin et al., 1990; Senanayake et al., 2007).

Continuous remodelling of the extracellular matrix (ECM) in the juxtacanalicular tissue is critical in preserving aqueous outflow channels in an open state by releasing trapped debris and associated ECM fragments from the outflow pathways (Keller & Acott, 2013). Studies have shown that in primary open-angle eyes, there is a significant reduction in the number of trabecular meshwork cells and a significant increase in the ECM deposition in JCT (Acott & Kelley, 2008).

The interplay between RAAS, growth factors and regulatory proteins in the ECM has been described. Activation of angiotensin receptor I has shown to stimulate transforming growth factors, such as TGF- β , which reduces matrix metalloproteinase expression via the stimulation of plasminogen activator inhibitor 1 (Holappa et al., 2020b). Matrix metalloproteinases (MMPs) have been described as important modulators for the continuous remodelling of ECM (P. Agarwal & Agarwal, 2018; De Groef et al., 2013).

Disturbances in the extracellular matrix of the trabecular meshwork, caused by excessive ECM deposition and reduced proteolysis for ECM breakdown, are one of the main factors that contribute to increasing the resistance of aqueous humour outflow and, consequently, an increase in the IOP (Johnson, 2006; Overby et al., 2009).

1.3.1.2 IOP treatment

The mechanisms by which elevated IOP can be reduced are two: decreasing the volume of aqueous that is being produced or increasing its outflow (Jayanetti et al., 2020).

Beta-blockers and carbonic anhydrase inhibitors are commonly used as suppressants of the aqueous humour production, while prostaglandin analogues, cholinergic agonists, and Rho Kinase Inhibitors lower the IOP by facilitating the aqueous outflow. Some drugs, like alpha-2 agonists, act by simultaneously reducing aqueous production and increasing aqueous outflow (Cantor, 2006; Reitsamer et al., 2006).

The use of these therapies is often mainly limited by either localized or systemic side effects caused by their administration. Alpha-2 agonists, for example, show adverse effects ranging from ocular erythema and irritation in adults, to central nervous system depression, fatigue, and fainting episodes in children (Bowman et al., 2004; Cantor, 2000; Scahill, 2009). Beta-blockers, such as Timolol, when administered topically, can present with systemic absorption and it is generally avoided for patients with a history of asthma, chronic airflow limitation, or cardiac disease (Zimmerman, 1993).

Besides potential adverse effects, patient convenience is also an important factor in the selection of an appropriate ocular hypotensive drug (Noecker, 2006). Single

medication and once-a-day dosing regimens are preferred in order to increase patient compliance and minimize potential side effects (Coons et al., 1994; S. C. Patel & Spaeth, 1995).

1.3.1.3 Angiotensin receptor blockers

Current literature suggests a role of RAS in increasing the aqueous outflow by modulating the secretion of matrix metalloproteases, which can lead to remodelling and restoring the extracellular matrix of the trabecular meshwork and, eventually, reestablishing the ECM homeostasis (Cabral-Pacheco et al., 2020; De Groef et al., 2013).

Angiotensin receptor blockers (ARBs) represent a class of antihypertensive drugs that selectively hinder the binding of angiotensin II to the receptor (Ram, 2008). In their study, Agarwal et al. observed that losartan, an angiotensin receptor blocker, increased aqueous humour levels of matrix metalloproteinases after topical administration. An increase in MMPs is responsible for increased TM cellularity and reduced ECM deposition, which alters tissue composition and results in lower IOP. Additionally, they suggest that inhibition of angiotensin II, which has a role in stimulating the secretion of the aqueous humour from the ciliary body via angiotensin II type I receptors, may contribute to the IOP lowering effect by reducing the rate of aqueous humour secretion (P. Agarwal & Agarwal, 2018).

Similarly to ARBs, angiotensin-converting enzyme inhibitors (ACE-Is) have been shown to lower intraocular pressure by inhibiting the formation of angiotensin II and, thereby, reducing the stimulation of angiotensin type I receptors (Agarwal et al., 2014). Although both classes of drugs, ACE inhibitors and ARBs, can lower the IOP by blocking the renin-angiotensin system, the production of angiotensin II can occur through non-ACE pathways, which remain unaffected by ACE inhibition. Moreover, ARBs show some advantages over ACE-I including once-daily dosing, an absence of significant adverse reactions, a well-tolerated side effect profile and cost-effectiveness (Al Sabbah et al., 2013).

1.3.2 Neovascularization

Angiogenesis is the formation and maintenance of blood vessel structures and is essential for the physiological functions of tissues and the progression of diseases, such as cancer and inflammation (Shibuya & Claesson-Welsh, 2006).

Vascular endothelial growth factors (VEGF) and their receptors are key regulators in the signal transduction systems involved in angiogenesis and are produced by various cell types, including tumor cells, and activated macrophages.

VEGFs bind to their specific transmembrane receptors, Flt-1 (VEGFR-1) and KDR (VEGFR-2), found on endothelial cells. VEGFRs are typical tyrosine kinase receptors

(TKRs) carrying an extracellular domain for ligand binding, a transmembrane domain and a cytoplasmic domain, including a tyrosine kinase domain (Shibuya & Claesson-Welsh, 2006). The binding of VEGFs to their receptors causes a conformational change that stimulates intrinsic kinase activity, a major stimulator of angiogenesis and vascular permeability (Wedge et al., 2005). The VEGF-VEGFR system is unique in that it consists of a very limited number of molecules that play a central role in angiogenesis. The evidence underlining the clinical importance of VEGF is supported by the fact that most tumours produce VEGF, and that inhibition of VEGF-induced angiogenesis significantly inhibits tumour growth *in vivo* (Hennequin et al., 1999).

Neovascular age-related macular degeneration (AMD) and diabetic retinopathy (DR) are the leading causes of blindness in elderly and working-age people, respectively, and are associated with neovascularization in the posterior segment of the eye. Both neovascular AMD and DR are characterized by endothelial cell proliferation and migration, increase in vascular permeability and inflammation, all processes in which Vascular Endothelial Growth Factor-A (VEGF-A) plays a role (Amadio et al., 2016).

1.3.2.1 Anti-VEGF therapies

Current protein-based anti-VEGF therapies, such as ranibizumab, bevacizumab and aflibercept, bind circulating VEGF, thereby inhibiting the binding of VEGF to its receptors (Beljanski, 2007). Because of their large molecular size, these drugs are administered by repeated intraocular injections, with discomfort and risk of injury and infection to patients (Falavarjani & Nguyen, 2013; Moisseiev & Loewenstein, 2017a).

1.4 Ocular delivery systems

Due to the sensitivity of the ocular tissues and the presence of the barriers described in a previous section, the development of therapeutics for the treatment of eye diseases is a challenging issue for drug formulators (Yellepeddi & Palakurthi, 2016).

Nonetheless, ocular drug administration has witnessed great improvement with the development of new delivery systems. Several technologies have tried to overcome the barriers of topical drug delivery using emulsions, contact lenses, microneedles and nanoparticles (A. Patel et al., 2013). These formulations can enhance the permeation of drugs through the aqueous tear film to the lipophilic epithelium, which represents the ocular barrier to topical drug delivery, increasing the drug's bioavailability at the membrane surface (Göktürk et al., 2012; Radu et al., 2016).

Currently, aqueous solutions and nanosuspensions form the majority of the commercially available ophthalmic formulations (Yellepeddi & Palakurthi, 2016). In this thesis, we focused on the pharmacokinetics of two promising platforms for topical drug delivery to the eye: (1) cyclodextrins and (2) lipid nanocapsules.

1.4.1 Cyclodextrins

A promising approach to addressing problems in drug solubility is the complexation with cyclodextrins (CDs) to form inclusion complexes. Cyclodextrins are oligosaccharides derived from starch containing six (α CD), seven (β CD), eight (γ CD) or more (α -1,4)-glucopyranoside units and are used as a solubilizing excipient in the pharmaceutical field. The solubility of poorly soluble drugs can be increased up to 1000-fold by cyclodextrin complexation, increasing their drug concentration gradient over the mucus layer and enhancing their delivery across the tear fluid (Jansook et al., 2010; Johannsdottir et al., 2018a). Once included in the cyclodextrin cavity, the drug molecules may be dissociated from the cyclodextrin molecules through complex dilution in the aqueous tear fluid. If the guest-host complex is located in close approximation to a lipophilic biological membrane (such as the eye cornea), the drug may be transferred to the matrix, for which it has the highest affinity. Importantly, since no covalent bonds are formed or broken during the drug-CD complex formation, the complexes are in dynamic equilibrium with free drug and cyclodextrin molecules (Loftsson & Stefánsson, 2002).

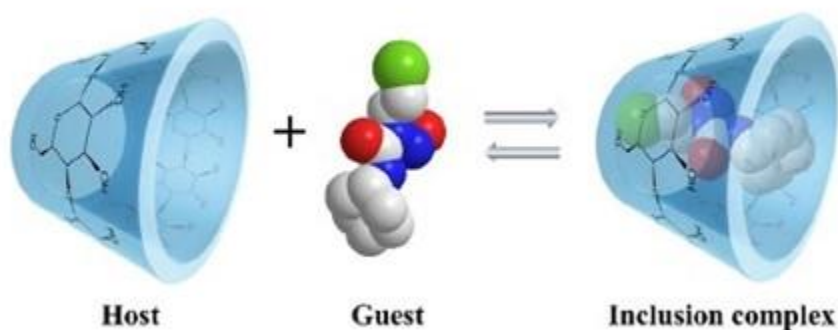


Figure 14. Cyclodextrin-drug inclusion complex formation (Tian et al., 2020).

In vivo studies in rabbits have shown that the nanoparticulated eye drop delivers the drug to both the anterior and posterior segments of the eye much more efficiently than conventional eye drops. Clinical studies in humans have confirmed their ability to topically deliver drugs to the posterior segment of the eye (Jansook et al., 2015).

In this thesis, we analysed the pharmacokinetics of different cyclodextrin-based formulations, including two different angiotensin receptor blockers (ARBs) and a tyrosine kinase inhibitor (TKI).

ARBs are commonly delivered orally, which is commonly associated with systemic side effects, involving the cardiovascular system. Topical administration of both ARBs and ACEs for the treatment of elevated intraocular pressure could decrease the potential systemic side effects due to oral administration. However, the physicochemical

properties of ARBs and ACE-Is, such as poor aqueous solubility and instability in aqueous solutions, can hamper their formulation as clinically effective eye drops (R. Agarwal et al., 2014; Chiang et al., 1996; Muankaew et al., 2014). Jansook et al. used γ -cyclodextrin nanoparticles to formulate eye drops containing on one hand 1.5% Irbesartan and, on the other, 0.15% Candesartan. The formulation has been described in detail in a previous publication (Jansook et al., 2015). This formulation provides high concentration and sustained release in the tear film and may, therefore, be ideal to deliver ARBs into the eye through topical delivery, becoming a new class of glaucoma drugs.

Tyrosine kinase inhibitors (TKIs) are a group of small molecules that bind to the receptors' tyrosine kinase pocket, disabling their function and blocking various signalling molecules in downstream pathways (Busse et al., 2001; Shi et al., 2019). Since TKIs are small lipophilic molecules, they present a potential for topical delivery to the retina by eye drops. However, most small-molecule protein kinase inhibitors are neutral or weakly basic lipophilic compounds with very poor solubility in aqueous media, which decreases their ability to permeate biological membranes (Praphanwittaya et al., 2020). Many studies, however, have shown that cyclodextrins can be used to enhance water solubility of kinase inhibitors such as erlotinib, lapatinib and gefitinib (Phillip Lee et al. 2009; Tóth Gerg Jánoska et al 2017; Tóth Gerg Jánoska et al 2016).

1.4.2 Lipidic nanocapsules

Lipid-based nanocarriers have recently emerged as novel delivery systems with promising outcomes in relation to the actual challenges of ocular drug delivery. These formulations have been used in both preclinical and clinical practice, with favourable results that show an increase in bioavailability, solubility, residence time and permeation, while reducing metabolic degradation, potential adverse effects and dosing frequency (Navarro-Partida, Castro-Castaneda, et al., 2021). *Ex vivo* studies with porcine eye tissues and lipid nanocarriers for the anterior segment showed that the formulations provided a longer residence time and improved corneal permeation (Abdelkader et al., 2016; Singh et al., 2019).

In this thesis, we analyzed the pharmacokinetic properties of lipidic nanocapsules *ex vivo* using a porcine model. The tested lipid nanocapsules-based formulation included DFO03, a newly synthesized molecule, part of a novel class of cGMP (cyclic guanosine-3',5'-monophosphate) analogues that have shown to be potentially effective in the treatment of retinal degenerations (Ekström et al., 2019; Vighi et al., 2018). The compound in its naked form, as well as the lipid nanocapsule-based formulation, were kindly provided by RISE (Research Institutes of Sweden, Södertälje, Sweden) and BIOLOG (Biolog Life Science Institute, Bremen, Germany). The formulation has been described in detail in a previous publication (Urimi et al., 2021).

1.5 Ocular pharmacokinetics

Pharmacokinetics is the assessment of drug absorption and distribution, concerning time and dosage, of administered drugs and is essential to providing a complete understanding of the interaction between physiology and molecular properties (Agrahari et al., 2016; Durairaj, 2017; Loch et al., 2012). Pharmacodynamics, on the other hand, studies the molecular, biochemical and physiological effects of drugs. These effects result from the interaction of drugs with other biological structures or targets, such as the binding with receptors, and produce subsequent effects that can be measured by biochemical or clinical means (Marino et al., 2022).

A successful drug candidate requires not only potency and selectivity but also a suitable pharmacokinetic profile (Van de Waterbeemd et al., 2001). Important tools to help develop and assess potential drug candidates are pharmacokinetic/pharmacodynamic models. The primary objective of such models is to enhance the accuracy of estimates of the dynamic state of drug behavior in an actual clinical situation (Robinson, 1997).

1.5.1 Pharmacokinetic models

Absorption, distribution, metabolism and excretion characteristics of drug compounds are crucial for the successful therapeutic activity of pharmaceuticals. It is reported that approximately 40% of the failures in clinical phases of drug development are caused by problems in pharmacokinetics and drug delivery (Mälkiä et al., 2004).

An accurate description of *in vivo* pharmacokinetics is vital to obtain appropriate information regarding drug behaviour and anticipate or prevent important failures in later stages of the development process. Preclinical *in vivo* studies are important components of the drug development process, designed to investigate the pharmacokinetics of drug candidates, and play a key role in other parts of drug discovery, such as the amount and frequency of doses.

During drug development, human pharmacokinetics is generally assessed after oral or intravenous administration by sampling plasma at different time points. However, for drugs administered by topical ocular route, the target tissues located in the eye can generally not be sampled. This is one of the main reasons why, when studying drug distribution in ocular tissues, animal models are more commonly used (Khier et al., 2016).

Although *in vivo* studies in animals provide a good overview of pharmacokinetics, they are resource-intensive and ethically questionable. The European Union has addressed the issue by declaring that animal experiments should not be performed if an alternative method exists (Deng et al., 2016; Sellick, 2011).

1.5.2 *In vitro* and *ex vivo* models

In vitro models are characterized by good control of experimental conditions and are relatively cheap. Rabbit is commonly considered the reference animal model for both *in vivo* and *in vitro* ocular experiments, especially due to the ease of handling. However, when compared to the human eye, the rabbit eye is smaller and has a bigger cornea in relationship to the whole globe, representing a large absorption area for drugs. This, and the lack of the Bowman’s membrane in the rabbit eyes, might explain why they usually result in higher permeabilities. The sclera of the rabbit is also different in size and thickness from the human eye, being only 1/10 in thickness of the human sclera (Loch et al., 2012; Pescina et al., 2015). Bovine and porcine ocular tissues are considered a good alternative to rabbit for *in vitro* studies. Particularly, the pig eye is considered a suitable model of the human eye concerning size, vascular anatomy, histology, physiology and mechanical properties. Furthermore, pigs being intended for human consumption, porcine ocular bulbs are easy to get from slaughterhouses as byproducts (Nicoli et al., 2009).

Table 1. Comparison of eyeball dimensions between rabbit, pig and human.

	Rabbit	Pig	Human	Reference
Eye globe \varnothing (mm)	18-20	24	24	(E. P. Y. Choy et al., 2004; Loch et al., 2012; McMenamin & Steptoe, 1991)
Cornea total surface area (cm ²)	7.06	1.15	1.07	(E. P. Y. Choy et al., 2004; Loch et al., 2012; Olsen et al., 2002)
Corneal thickness (mm)	0.3-0.4	0.5-0.7	0.5-0.7	(E. P. Y. Choy et al., 2004; Loch et al., 2012)
Sclera total surface area (cm ²)	8.61	11.9	16	(Barathi et al., 2002; Olsen et al., 1995)
Scleral thickness (mm)	0.2	0.4	0.4	(Olsen et al., 2002)
Bowman’s membrane	Absent	Absent	Present	(Wilson, 2020)

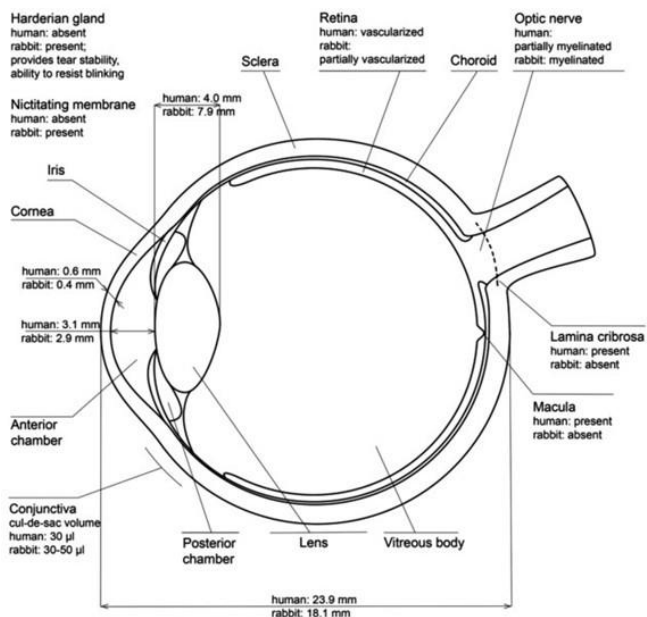


Figure 15. Schematic diagram comparing dimensions between rabbit and human eye (Y. Zernii et al., 2016).

The primary goal of *in vitro* permeation studies is to predict the *in vivo* permeation of drugs. The use of diffusion cells in permeation studies was first described by T.J. Franz in 1975. In his report, he described a method to compare the *in vitro* skin permeation of compounds that had been previously tested by others *in vivo*. His results demonstrated a qualitative agreement between the two methods, showing that *in vitro* absorption studies accurately reflect the living state (Franz, 1975; Friend, 1992). Franz cells are currently a widely used methodology, performed at the beginning of most studies involving percutaneous absorption. Although these methods are not able to replace important aspects of *in vivo* pharmacokinetics, such as metabolism, excretion and toxicology assessment, they can be used as a screening tool for the absorption and permeation of drugs (del Amo, 2015; Deng et al., 2016; Moiseev et al., 2019; Salamanca et al., 2018; Sellick, 2011).

1.5.3 Diffusion in permeation studies

Diffusion is the driving force behind passive transport, therefore, physicochemical information on the diffusion of drug compounds is useful for analyzing drug delivery systems and drug pharmacokinetics (Miyamoto et al., 2018).

The diffusion process can be described using Fick's first law:

Equation 1:

$$J = -D \frac{dC}{dx}$$

which describes the flux (J) as a function of the concentration gradient (dC/dx) for a solute with a diffusion coefficient D . The negative sign of the equation signifies that diffusion occurs in a direction opposite to that of increasing concentration (Mattiasson, 2020).

The diffusion coefficient, D , of a molecule with radius r can be calculated by the Stokes-Einstein equation:

Equation 2:

$$D = \frac{k_B \cdot T}{6\pi r \eta_0}$$

where k_B is the Boltzmann constant, η_0 is the solvent viscosity, and T is the absolute temperature. Therefore, the diffusion coefficient of a molecule is inversely dependent on its molecular size (Miyamoto & Shimonon, 2020).

The flux can be defined as the number of molecules crossing a barrier during a given period of time and, in permeation studies using Franz cells, Equation 1 can be simplified to:

Equation 3:

$$J = \frac{Q}{t \cdot A}$$

where flux (J) equals the amount of substance (Q) that has crossed the membrane (A) during a period of time (t).

In permeation experiments, the meaningful data obtained is usually the permeation profile, based on the amount of diffusant permeated to the receptor side (Shah, 1993). The permeation profile can be represented by plotting the cumulative amount permeated in the receiver ($\mu\text{g}/\text{cm}^2$) against time (Niedorf et al., 2008).

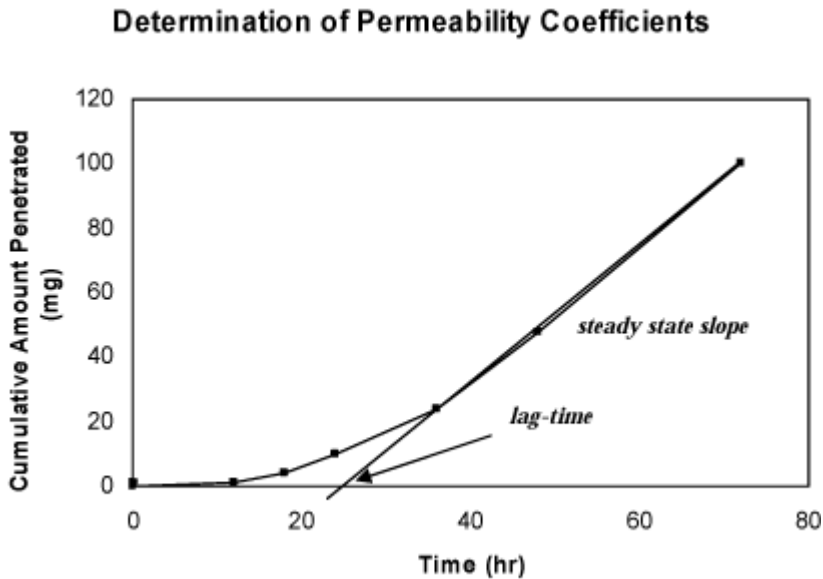


Figure 16. Example of permeation profile plot (cumulative permeated amount versus time). (https://www2.mst.dk/udgiv/publications/2009/978-87-7052-980-8/html/kap05_eng.htm)

Usually, the drug permeation profile in diffusion studies can be divided into different steps:

- (1) Lag-time: this is a time interval with non-detectable flux where, before reaching the acceptor compartment, the drug needs to partition and diffuse through the membrane (Niedorf et al., 2008). The lag-time is dependent on the diffusion coefficient of each molecule, which is assumed to be constant throughout the entire membrane and independent of diffusant concentration (Frisch, 1957).
- (2) Steady-state: a time interval where the flux increases and becomes constant.

Graphical representation of the permeation profile can be used to obtain the lag time (T_{lag}) and the steady-state flux (J_{ss}), where J_{ss} is obtained from the slope of the curve at steady state from typical mean cumulative concentration-time plots. T_{lag} and J_{ss} can also be calculated using the following equations, given that the thickness of the used membrane is known:

Equation 4:

$$T_{lag} = \frac{h^2}{6D}$$

Equation 5:

$$J_{ss} = \frac{D * Km * Cs}{h}$$

Where h is the thickness of the membrane (cm), D is the diffusion coefficient (cm^2/h), Km is the membrane-donor phase partition coefficient and Cs is the saturation solubility of diffusant in the donor phase (mmol/ml) (Miyamoto & Shimono, 2020; Shah, 1993). Once the steady-state flux has been obtained, the permeability value for the permeant can be calculated.

1.5.3.1 Sink conditions

Permeability values are commonly estimated under the assumption of sink conditions, where the drug concentration in the acceptor is negligible compared to that in the donor. A generally accepted limit for sink conditions is that the concentration in the receiver must always be <10% of the concentration in the donor. In such cases, a simple version of Fick's law can be used to relate fluxes and permeabilities:

Equation 6:

$$P = \frac{J_{ss}}{C_0 * A}$$

Where J_{ss} is the flux during the steady-state period and C_0 is the initial concentration in the donor compartment (Brodin et al., 2010).

Tavelin et al., however, suggested that in most permeation experiments, the concentrations in the donor (C_d) and receiver (C_r), and, therefore, the amount in the receiver (M_r), will change with time. To emphasize this time dependence, and avoid the limitations of the classical equation for sink conditions, Equation 6 can be rewritten as a differential equation for the variables M_r , C_d and C_r (Mangas-Sanjuan et al., 2014; Tavelin et al., 2002a):

Equation 7:

$$\frac{dM_r(t)}{dt} = P * A * [C_d(t) - C_r(t)]$$

1.5.3.2 Atypical permeation profiles

Tavelin et al. also highlighted that atypical permeation profiles that deviate from the linearity of those obtained in experiments under sink conditions can sometimes be observed (Mangas-Sanjuan et al., 2014; Tavelin et al., 2002b).

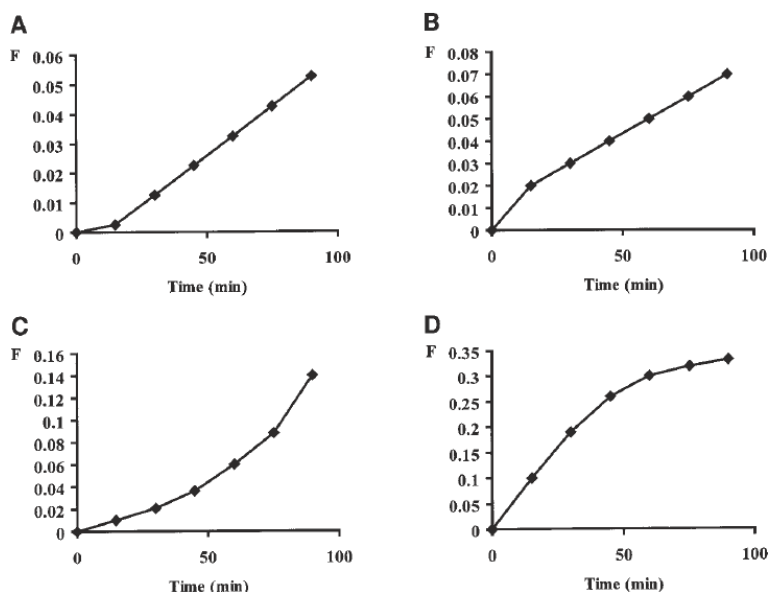


Figure 17. Schematic representation of different permeation profiles (Tavelin et al., 2002b).

Figure 17 shows different situations in which drug transport across a membrane is non-linear. The following reasons for each one of the profiles are suggested by Tavelin et al.:

Profile A describes a situation in which less drug is transported during the first sampling interval. Reasons for this phenomenon include poor temperature control at the beginning of the experiment, or the partition of the drug into the tissue being the rate-limiting step.

In profile B, in contrast to A, more drug is transported during the first sampling interval. This is sometimes observed when the transport of radiolabeled drugs is studied, caused by radiolabeled low molecular weight impurities that are transported at a higher rate than the drug. Another possible explanation is that the membrane is affected by a too harsh application of the drug solution.

In profile C, the transport rate increases with time, which might indicate a decreased integrity of the membrane over time, either by degradation during too long experiments or by toxicity from the drug. Poor temperature control during the experiment is another possible explanation.

Profile D, which shows a transport rate that decreases with time, can be attributed to the fact that sink conditions are significantly exceeded. This profile is especially common in experiments with highly permeable compounds, where the transport of a drug candidate from the donor compartment to the receiver can cause a first-order decrease of the concentration in the donor chamber, accompanied by an increase in its concentration in the receiver. In these situations, the concentration gradient cannot be considered constant, and the permeability cannot be calculated directly from the previous equations where sink conditions existed (Brodin et al., 2010; Mangas-Sanjuan et al., 2014; Tavelin et al., 2002b).

1.5.3.3 Non-sink conditions

As the sink conditions may not be maintained with high permeability compounds, models to estimate the permeability coefficient under non-sink conditions have been proposed (Heikkinen et al., 2010). In these cases, Equation 7: can be solved to consider the continuous change in donor and receiver concentrations. To do this, the equation must be expressed in a single variable for the amount of drug in the receiver ($M_r(t)$), the concentration in the receiver ($C_r(t)$) and the concentration in the donor ($C_d(t)$).

The amount of drug on the donor side is calculated by the difference between the total amount of drug in the system (M_{tot}) and the amount of drug in the receiver (C_r). The concentration in the donor can then be calculated by dividing the amount of drug in the donor (C_d) by the donor solution volume (V_d):

Equation 8:

$$C_d(t) = \frac{M_{tot} - C_r(t) * V_r}{V_d}$$

The change in the amount of drug in the receiver then becomes:

Equation 9:

$$\frac{dM_r(t)}{dt} = \frac{dC_r(t)}{dt} * V_r$$

Equation 7, Equation 8 and Equation 9 then give:

Equation 10:

$$\frac{dC_r(t)}{dt} = \frac{P * A}{V_r} * \left(\frac{M_{tot}}{V_d} - C_r(t) * \frac{V_r + V_d}{V_d} \right)$$

Which has the solution:

Equation 11:

$$Cr(t) = \left(\frac{M_{tot}}{V_d + V_r} \right) + \left(Cr(t-1) - \frac{M_{tot}}{V_d + V_r} \right) * e^{-P_{app} * A \left(\frac{1}{V_r} + \frac{1}{V_d} \right) * t}$$

where $Cr(t)$ is the drug concentration in the receiver chamber at time t , M_{tot} is the total amount of drug in both chambers, V_r and V_d are the volumes of each chamber, $Cr(t-1)$ is the drug concentration in the receiver chamber at the previous time, A is the surface area of the membrane, t is the time interval and P_{app} is the intermediate permeability coefficient calculated as sink conditions (Hubatsch et al., 2007; Kratz et al., 2011; Mangas-Sanjuan et al., 2014; Teixeira et al., 2020).

Equation 11 describes the concentration development with time in the receiver chamber and it is valid in either sink or non-sink conditions (Mangas-Sanjuan et al., 2014). However, in permeation experiments with Franz cells, the substance is removed from the receiver and new diluent is added, causing the concentration in the receiver to be instantaneously diluted at every sampling timepoint (Tavelin et al., 2002b).

To account for this, the initial concentration in the receiver at each time interval needs to be calculated as:

Equation 12:

$$Cr(i) = Cr(i-1) * f = Cr(i-1) * (V_r - V_s) / V_r$$

where $Cr(i)$ is the initial receiver concentration at time interval i , $Cr(i-1)$ is the concentration in the receiver at the previous interval and f is the dilution factor.

The amount of drug in the system is calculated at each time interval as:

Equation 13:

$$M_{tot}(i) = M_{tot}(i-1) - M_{sampl}(i-1) = M_{tot}(i-1) - Cr(i-1) * V_s$$

where $M_{tot}(i)$ is the amount of drug in the system at time interval i , $M_{tot}(i-1)$ is the amount of drug in the system at the previous interval and $M_{sampl}(i-1)$ is the amount of drug in the sample at the previous interval.

The theoretical concentration in the receiver at each timepoint can be calculated using Equation 11 and then fitted as a non-linear curve to the experimental receiver concentrations values, using the initial value of permeability coefficient (P).

By using a solver software to minimize the sum of squared residuals (SEE, Equation 14) of each one of the time intervals, an adjusted permeability coefficient (P), that allows the best fit of the theoretical values to the experimental values, can be calculated.

Equation 14:

$$SSE = \sum [Cr(i, obs) - Cr(i)]$$

Where $Cr(i, obs)$ is the experimentally determined concentration in the receiver, and $Cr(i)$ the theoretical concentration in the receiver calculated as Equation 11.

1.5.4 Prediction of permeability in drug development

Understanding drug permeability across cellular membranes is key during drug design and development. The ability of a molecule to reach and bind an intracellular target depends on its bioavailability, which results from its ability to permeate across the membranes (Bennion et al., 2017; Ramsay et al., 2018a).

Poor biopharmaceutical properties contribute to a high failure rate during drug development, both at the early and late stages of the process (Teixeira et al., 2020). In addition to experimental measurements, statistical methods such as multivariate analysis, have been widely used to study the quantitative structure-activity relationship (QSAR) in pharmaceutical sciences (G. Chen et al., 2020). QSAR techniques are extensively applied in drug design, where the chemical structure of compounds is correlated and used to, hopefully, predict biological activities, such as membrane permeation (Collantes et al., 1996).

2 Aims

2.1 Paper I: Angiotensin Receptor Blockers in cyclodextrin nanoparticle eye drops: Ocular pharmacokinetics and pharmacologic effect on intraocular pressure.

The aims of this study are (1) to examine the pharmacokinetics of irbesartan and candesartan in γ -cyclodextrin nanoparticle eye drops in the anterior segment of the rabbit eye and (2) test the hypothesis that irbesartan and candesartan eye drops lower intraocular pressure in rabbits.

2.2 Paper II: Topical Noninvasive Retinal Drug Delivery of a Tyrosine Kinase Inhibitor: 3% Cediranib Maleate Cyclodextrin Nanoparticle Eye Drops in the Rabbit Eye.

In this study, we investigate the retinal delivery and overall ocular pharmacokinetics of a novel γ -cyclodextrin-based eye drops formulation with cediranib maleate, a potent small-molecule tyrosine kinase inhibitor of all three VEGF receptors (VEGFR-1, -2 and -3), after a single-dose topical application.

2.3 Paper III: Drug permeability across full-thickness cornea and conjunctiva-sclera-choroid-retina: *in vitro* studies.

In this study, we tested the hypothesis that the conjunctiva-sclera could represent a more efficient pathway of topical drug delivery to the posterior segment than the corneal route. For this purpose, we used *ex vivo* full-thickness cornea and conjunctiva-sclera-choroid-retina to:

- (1) investigate and compare the permeability of drugs with different physicochemical properties across both tissues,
- (2) to perform a screening permeability study, comparing two different formulations for a newly developed compound,
- (3) to highlight the main physicochemical properties affecting the permeability of molecular compounds across both tissues.

To conduct these experiments, we selected porcine full-thickness cornea and conjunctiva-sclera-choroid-retina for their anatomical and physiological resemblance to the human eye.

3 Materials and Methods

3.1 Paper I

3.1.1 Ethical statement

This research followed the ARVO Statement for the Use of Animals in Ophthalmic and Vision Research. For the IOP study, professional assistance by veterinarians at the Institute for Experimental Pathology from the University of Iceland was provided and approved by the Icelandic Food and Veterinary Authority (MAST). The pharmacokinetics study was approved by the local animal welfare committee (GZ BMWFW-66.009/0163-V/3b/2018) (Lorenzo-Soler et al., 2021).

3.1.2 Animals

59 New Zealand rabbits (*Oryctolagus cuniculus*; weight, 3.0 to 6 kg) were used in the studies. 10 rabbits were used in the IOP study and 49 rabbits (26 for irbesartan and 23 for candesartan) were used in the pharmacokinetic study. They were housed in groups of two in cages with raised areas, kept under controlled, standardized conditions (artificial L/D cycle 12:12, room temperature $22\pm 2^{\circ}\text{C}$, humidity $55\pm 10\%$) and had *ad libitum* access to complete feed for rabbits. They were acclimatized for a minimum of seven days. The rabbits were not anaesthetized during the procedures and no topical agent was used before the eye drops administration (Lorenzo-Soler et al., 2021).

3.1.3 Test compounds

1.5% irbesartan, 0.15% candesartan and vehicle eye drops in γ -cyclodextrin nanoparticle suspensions were tested. The difference in concentration for the two ARBs is due to solubility and stability issues during the formulation of the drugs. The formulations have been described previously (Jansook et al., 2015; Lorenzo-Soler et al., 2021).

The eye drops were placed into a sonicator at 40°C for 30 minutes and shaken thoroughly, until homogeneously suspended, immediately before eye drops administration to the rabbits (Muankaew et al., 2014). After use, they were stored at controlled room temperature ($\sim 25^{\circ}\text{C}$) and protected from light. For the IOP study, a commercial 0.5% timolol solution (Optimol, Oftan, Japan) was also tested, administering the eye drops directly from the vial (Lorenzo-Soler et al., 2021).

3.1.4 Intraocular pressure

3.1.4.1 Eye drops administration

Ten rabbits were tested repeatedly with five different drugs or controls in eye drop applications with one application per day (treatment 1: 0.15% candesartan, treatment 2: 1.5% irbesartan, treatment 3: 0.5% timolol, treatment 4: blank, treatment 5: vehicle). 50 µl of each suspension was topically administered to the left eye of each rabbit using a pipette. Timolol solution was administered as one drop directly from the vial. The blank group received no treatment. A minimum of a two-day wash-out period was observed between study days (Lorenzo-Soler et al., 2021).

3.1.4.2 Intraocular pressure measurements

Four measurement timepoints were established for each treatment group: baseline (right before eye drop administration), one minute, two hours and four hours after administration. Baseline and one minute after administration measurements were averaged due to the closeness of values and timepoints. IOP was measured only on the left eye (treated eye) using a rebound tonometer (® TonoVet Plus, iCare, Finland) and IOP measurements were taken at the same time of the day for all groups to minimize fluctuations due to circadian rhythm. All ten rabbits were tested with all study drugs and controls at different times (Lorenzo-Soler et al., 2021).

3.1.4.3 Statistical analysis

For the statistical analysis regarding IOP measurements data, GraphPad Prism 8.0 for Windows (GraphPad, California, USA) was used and a t-test analysis was applied to compare the groups, the significance level was set at $p < 0.05$ (Lorenzo-Soler et al., 2021).

3.1.5 Pharmacokinetic study

3.1.5.1 Eye drops administration

A total of 49 animals were used, 26 rabbits for irbesartan and 23 for candesartan, and 35 µL of the ophthalmic solution was administered into the conjunctival sac of the (left) study eye of each rabbit with no drug application to the fellow eye. Rabbits were euthanized in anaesthesia (ketamine 60 mg/kg, xylazine 16 mg/kg, s.c.) by an overdose of pentobarbitone sodium at five predefined time points (0.5h, 1.5h, 3h, 6h, 12h) after drug administration. Immediately after euthanasia, both eyes were enucleated from each animal. The study eye demonstrates the combination of topical and systemic absorption, whereas the fellow eye shows systemic absorption alone (Lorenzo-Soler et al., 2021).

Enucleated eyes were frozen immediately and stored at -80°C until further processing. For separation of the different ocular tissues, the eyeball was removed from storage and dissected into different parts: cornea, aqueous humour, vitreous body and the retina/choroid, each of which was stored separately in different tubes. All tissues were collected and separately weighted upon collection. Tissue samples including aqueous humour, cornea, retina and vitreous were sent to Nucro-Technics (Scarborough, Ontario, Canada) for assessment of the study drug concentrations (Lorenzo-Soler et al., 2021).

3.1.5.2 Drug concentration measurements

Weighed rabbit eye tissue samples were homogenized in H_2O -diluted rabbit plasma (rabbit plasma/water, 1/14, v/v) in a ratio of 1 to 19 (i.e., 1 g or 1 mL of rabbit eye tissue in 19 mL of diluted rabbit plasma). A 200 μl aliquot of rabbit tissue homogenate supernatants was mixed sequentially with 100 μl of internal standards (8 ng/ml of candesartan- d_4 and 20 ng/ml of irbesartan- d_4 in methanol/water (20/80, v/v) and 2 mL of water). The mixtures were then loaded onto the pre-conditioned HLB cartridges (Waters Oasis[®] 60 mg, 3 cc). The cartridges were first washed with 2 mL of methanol/water (10/90, v/v) and then eluted with 2 mL of methanol. The organic solvents were evaporated at 40°C and the dry residues were reconstituted in 200 μl of methanol/water/formic acid (70/29.75/0.25, v/v/v) (Lorenzo-Soler et al., 2021).

An Agilent 1200 series liquid chromatograph coupled with an Agilent 6490 Triple Quad LC/MS (Agilent Technologies Canada, Mississauga, Ontario, Canada) was used for the LC-MS/MS analysis. A 20 μl aliquot of the extracted samples was injected onto an ACE Excel 5 Super C18 column (4.6x150 mm, Advanced Chromatography Technologies, Aberdeen, Scotland) maintained at 25°C for a gradient separation at the flow rate of 0.8 mL/min. Mobile phase A was methanol/ H_2O /formic acid, 70/29.75/0.25 (v/v/v) and the mobile phase B was methanol/ H_2O /formic acid, 90/9.75/0.25 (v/v/v). For gradient elution, 100% mobile phase A was used for the first 4.5 min, followed by 100% mobile B for 1.5 min, and then back to 100% mobile phase A for 2 minutes of re-equilibration, with a total run time of 8 minutes. Candesartan and candesartan- d_4 were eluted at 5.1 minutes and irbesartan and irbesartan- d_4 were eluted at 4.1 minutes. The MS detection was in the positive electrospray ionization (ESI) mode using the MRM transitions (protonated molecule to product ion) of m/z 441–263, 445–267, 429–207, and m/z 433–211 for candesartan, candesartan- d_4 , irbesartan, and irbesartan- d_4 , respectively (Lorenzo-Soler et al., 2021).

The drug quantification was carried out by Nucro-Technics (Scarborough, Ontario, Canada).

3.2 Paper II

3.2.1 Ethical statement

All animal procedures were performed under license by the Icelandic Food and Veterinary Authority (MAST) and the ARVO Statement for the Use of Animals in Ophthalmic and Vision Research. The study was carried out according to the national regulation nr. 460/2017 on animal experiments, according to the national law on animal welfare nr. 80/2016. The Icelandic regulation on animal experiments is based on Directive 86/609/EEC of the European Parliament and of the Council on the protection of animals used for scientific purposes. Professional assistance from veterinarians at the Institute for Experimental Pathology from the University of Iceland was provided (Lorenzo-Soler et al., 2022).

3.2.2 *In vivo* studies

23 French lop rabbits (*Oryctolagus cuniculus*) weighing between 3 and 6 kg were housed in individual cages with a temperature between 16-22°C. They had constant access to hay, pellets, and fresh water during the study. They were acclimatized for a minimum of 7 days and no treatment was administered during the acclimatization. Rabbits were awake during the eye drop administration and no topical anaesthetic was used (Lorenzo-Soler et al., 2022).

Five rabbits were used as a blank group, with no treatment administered, and 18 rabbits were tested with the eye drop micro-suspension containing cediranib maleate 3%, administered only in the left eye. Rabbits were marked with a pen in the left ear, and 50 µl of the eye drop micro-suspension was topically administered. The eye drops were instilled with a calibrated adjustable micropipette fitted with disposable tips into the lower conjunctival sac of the eye by pulling the lower lid away from the eyeball. After instillation, the upper and the lower lids were held together for a few seconds to avoid rapid removal of the eye drop from the ocular surface. Animals were observed for overall health and local tolerance to the formulations until the end of the study (Lorenzo-Soler et al., 2022).

3.2.3 Test compounds

The eye drop nanosuspension containing 3% cediranib maleate was shaken thoroughly until homogeneously suspended, placed into a sonicator at 40°C for 30 minutes and shaken very well before use. This procedure was carried out immediately before eye drops administration to the rabbits. After use, they were stored at controlled room temperature (~25°C) and protected from light (Lorenzo-Soler et al., 2022). Cediranib maleate 3% (w/v) eye drops in γ -cyclodextrin nanoparticle suspension was prepared and obtained from the Faculty of Pharmacy, University of Iceland, by Pitsiree Praphanwittaya, PhD.

3.2.4 Sample preparation

At predetermined time intervals (1, 3 and 6 hours) after administration, the animals were euthanized with pentobarbital. Just before euthanasia, tear fluid was collected from the left and the right eyes of each rabbit with surgical sponges. Blood samples were collected by intracardiac puncture into tubes containing lithium heparin as anticoagulant and processed to obtain plasma by centrifuging at 1300 rpm (Lorenzo-Soler et al., 2022).

The rabbits were euthanized immediately after blood sample extraction. Just after euthanasia, the two eyes of each animal were removed and dissected to extract surgically the different eye tissues. Samples from aqueous humour, cornea, iris, lens, vitreous humour, retina and sclera were obtained from each eye. The ocular tissue and fluid samples were collected into labelled cryotubes and stored frozen (-80°C) until thawed for analysis (Lorenzo-Soler et al., 2022).

Dissection of the different tissues is shown in the pictures below.



Figure 18. Dissected tissues after eye enucleation. Top row, left: aqueous humour; middle and right: cornea. Middle row, left to right: iris, lens and vitreous. Bottom row, left: sclera and retina; right: sclera without retina.

3.2.5 Quantitative determinations

The concentration of cediranib maleate in each tissue was analyzed in a reversed-phase high-performance liquid chromatography (HPLC) system (Dionex, Softron GmbH Ultimate 3000 series, Germany). The analytical instrument composed of a P680 pump with a DG-1210 degasser, an ASI-100 autosampler, VWD-3400 UV-VIS detector, and a

column heater, containing a C18 column (100A 150 × 4.6 mm, 5 μm) from Kinetex Core-shell technology and a guard column (Phenomenex, UK). The HPLC system was operated under 30°C, isocratic condition, flow rate was 1.0 mL/min, detection wavelength was 234 nm, and injection volume was 20 μL. The mobile phase consisted of acetonitrile and 0.05% (v/v) phosphoric acid (volume ratio 35:65) (Lorenzo-Soler et al., 2022).

The drug quantification was carried out by Charles River Laboratories ('s-Hertogenbosch, Netherlands).

3.2.6 Statistical analysis

Shapiro-Wilk and Levene tests were performed on the pharmacokinetic data obtained from the *in vivo* studies to determine whether the assumptions of normal distribution and homogeneity of variances were fulfilled. The tests indicated that our data, for the most part, did not follow a normal distribution nor showed homogeneity of variances. Therefore, to analyze if statistically significant differences existed in drug concentration in the ocular tissues between treated and untreated eyes, a nonparametric Mann-Whitney U test was carried out. The data processing, statistical tests and analysis of the results were performed using Python 3.0 and its open-source libraries, Pandas, NumPy and SciPy (Lorenzo-Soler et al., 2022).

3.3 Paper III

3.3.1 Compounds and sample preparation

The permeability coefficients of 27 drug compounds were experimentally determined across two parts of the eyewall: (1) *ex vivo* full-thickness cornea and (2) conjunctiva-sclera-choroid-retina.

The test solutions for the donor compartment were prepared at different concentrations that were selected based on data found in the literature in similar experiments for better comparison with previously published data. The model compounds were dissolved in PBS, pH 7.4. Those compounds that exhibit poor water solubility were prepared as a 1:10 dimethyl sulfoxide (DMSO) : PBS pH 7.4.

The compounds used in the study were: acetazolamide, ampicillin sodium, atenolol, brimonidine tartrate, bromfenac sodium, caffeine, candesartan, chlorpheniramine maleate, ciprofloxacin hydrochloride, dexamethasone, fluconazole, fluorescein, flurbiprofen, hesperetin, hesperidin, hydroquinone, imidazole, labetalol hydrochloride, lincomycin hydrochloride, metoprolol tartrate, nadolol, pilocarpine hydrochloride, prednisolone, propranolol hydrochloride, riboflavin, timolol maleate and xylometazoline hydrochloride. The compounds were obtained from Sigma-Aldrich (St. Louis, Missouri, US).

3.3.2 Tissue preparation

Fresh porcine eyes were supplied from a local slaughterhouse. Eyes were frozen at -80°C within two hours of collection until used. A previous test was carried out with an aqueous solution of irbesartan to compare the effect of freezing-thawing the eyes against using fresh eyes for permeation assays. Similar to results reported by other authors, no significant differences were obtained between frozen-thawed and fresh eyes, confirming that the freezing procedure did not have any effect on the tissues' integrity (Nicoli et al., 2009). Before dissection, the eyes were kept in PBS, pH 7.4, for approximately fifteen minutes until completely thawed. First, a small cut was made with the scalpel at the limbus and the corneas were dissected from the eyeballs. Full-thickness corneas and the conjunctiva-sclera-choroid-retina complex were isolated and used in the permeability studies. Corneas were excised with approximately 1 cm ring of sclera to properly fix the membrane between the donor and receptor compartments. Lens, aqueous humour and vitreous were discarded and full-thickness sclera, including conjunctiva, choroid and retina, were placed between the donor and receptor compartments. The dissected tissues were kept in PBS until used, which occurred within 5 minutes after dissection.

3.3.3 Permeation experiments

Permeation experiments were performed in jacketed glass Franz-type diffusion cells (area 2.54 cm²). Full-thickness tissues were placed on the cell with the endothelial side facing the receiving compartment. The donor compartment was filled with 1mL of the solution containing the model compound. The receiving phase consisted of 5 mL of PBS buffer, magnetically stirred to avoid any boundary layer effect. The cells were connected to a heater system and kept at 37 ± 0.2 °C during the whole experiment. At predetermined times for up to 6 hours, 100µL of solution was sampled from the receiving side and immediately replaced by an equal volume of fresh PBS. All experiments were carried out in triplicate using always different ocular bulbs from different animals.

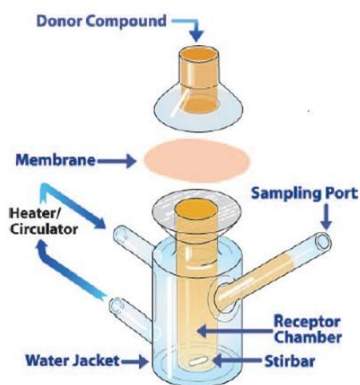


Figure 19. Franz-type diffusion cell (PermeGear Inc., 2014).

3.3.4 Analytical Methods

Samples were analyzed by spectroscopy without any preliminary separation using a microplate reader equipped with a UV–Vis spectrophotometric detector and according to the absorption spectrum of each molecule (SpectraMax, Molecular Devices, San Jose, CA).

Calibration curves were constructed for each compound by measuring the absorption of known substance concentrations, yielding correlation coefficients equal to or higher than 0.9 for all compounds. The calibration curves were prepared with the same solvents used for the preparation of the model compound in the donor solution.

Drug quantifications for each drug and sample were carried out in triplicate and analyses were performed at room temperature unless otherwise indicated.

3.3.5 Calculations of corneal and conjunctiva-sclera-choroid-retina permeability

The mean calculated permeability coefficients for full-thickness cornea and conjunctiva-sclera-choroid-retina were compared to determine differences in the permeability between these two parts of the eye.

Data were presented as the cumulative amount of drug permeated per area ($\mu\text{g}/\text{cm}^2$) as a function of time (min).

Generally, permeation experiments using Franz diffusion cells are performed under sink conditions, where the concentration in the receiver compartment is initially zero and is assumed to increase insignificantly during the experiment. It is generally agreed that the concentration in the receiver compartment should not exceed 10% of the concentration in the donor compartment (Brodin et al., 2010). In some cases, however, this assumption is invalid. When working with highly permeable compounds, for

example, the transport of the drug from the donor to the receiver can cause a first-order decrease of the drug concentration in the donor, causing an increase of the concentration in the receiver above 10% of the donor. In these situations, the concentration gradient cannot be considered constant. These cases require different calculation methods to account for the difference in the concentration gradients.

For those compounds that maintained sink conditions throughout the whole experiment, the fluxes (J , $\mu\text{g/s}$) were calculated as the amount of drug permeated during the steady-state period, whereas the apparent permeability coefficient (P , cm/s) was calculated as:

Equation 15:

$$P = \frac{J_{ss}}{(C_d - C_r) * A}$$

where J_{ss} is the drug flux during steady-state, C_d and C_r are the drug concentrations in the donor and receiver, respectively, and A is the area of exposed tissue.

In some cases, we observed atypical permeation profiles that deviated from the common linear representation, as those described in section 1.5.3.2, or compounds that showed receiver concentrations that exceeded the 10% of the donor concentration established for sink conditions (Tavelin et al., 2002b).

In these situations, the permeability coefficient was calculated using the following equation described in various papers (Hubatsch et al., 2007; Kratz et al., 2011; Mangas-Sanjuan et al., 2014; Teixeira et al., 2020):

Equation 16:

$$C_r(t) = \left(\frac{M_{tot}}{V_d + V_r} \right) + \left(C_r(t-1) - \frac{M_{tot}}{V_d + V_r} \right) * e^{-P_{app} * A * \left(\frac{1}{V_r} + \frac{1}{V_d} \right) * t}$$

where $C_r(t)$ is the drug concentration in the receiver chamber at time t , M_{tot} is the total amount of drug in both chambers, V_r and V_d are the volumes of each chamber, $C_r(t-1)$ is the drug concentration in the receiver chamber at the previous time, A is the surface area of the membrane, t is the time interval and P_{app} is the intermediate permeability coefficient calculated as sink conditions (Hubatsch et al., 2007; Kratz et al., 2011; Mangas-Sanjuan et al., 2014; Teixeira et al., 2020). An example of the calculation applying the non-sink equation is described in Appendix I.

Once the mean permeability coefficient was calculated for each compound and tissue, an independent t-test was performed to observe whether statistically significant differences existed between the tissues' permeabilities for the studied compounds.

3.3.6 Testing of new compounds and formulations

DF003, a newly synthesized molecule, was tested on both full-thickness cornea and

conjunctiva-sclera-choroid-retina as a water-based solution and in a lipid nanocapsules-based formulation.

The molecule is part of a novel class of cGMP (cyclic guanosine- 3',5'-monophosphate) analogues recently developed that have shown to be potentially effective in the treatment of retinal degenerations (Ekström et al., 2019; Vighi et al., 2018). The compound in its naked form, as well as the lipid nanocapsules-based formulation, were kindly provided by RISE (Research Institutes of Sweden, Södertälje, Sweden) and BIOLOG (Biolog Life Science Institute, Bremen, Germany). The formulation has been described in detail in a previous publication (Urimi et al., 2021).

3.3.7 Correlation between permeability and physicochemical properties

Various molecular descriptors were either extracted from different databases (PubChem and DrugBank) or calculated using Mordred and the simplified molecular-input line-entry system (SMILES) of each compound. The descriptors were selected based on those listed in similar papers published previously by other authors. Initial descriptors in the analysis included: molecular weight, molecular radius, polar surface area, number of hydrogen bond donors and acceptors, the logarithm of the octanol-water partition coefficient of the neutral form (logP) and at pH 7.4 (logD), the logarithm of water solubility, number of rings, freely rotatable bonds, pK_a for the most basic and acidic molecular form (Kidron et al., 2010; Prausnitz, 1998; Ramsay et al., 2018b).

We analyzed the correlations between the permeability coefficients for each tissue and the physicochemical properties of the compounds tested using Pearson's correlation coefficient (r) and plotting the data on a scatter plot with the coefficient of determination (r^2). Along with the calculation of Pearson's coefficient, we also performed a t-test to determine the statistical significance of the obtained correlations, where p-values < 0.05 were used to reject the null hypothesis that no significant correlation existed between variables. The final descriptors that showed significant correlations with permeability across full-thickness cornea (logarithm of solubility, logP and number of rings) and conjunctiva-sclera-choroid-retina (logarithm of solubility, logP, logD, molecular weight and number of rings) had all been obtained from DrugBank.

3.3.8 Data analysis and statistics

All calculations and analysis of data, obtention of molecular descriptors and statistical analysis were performed using Python 3.0 and its open-source libraries and packages Pandas, NumPy, Scikit-learn, Seaborn, Mordred and RDKit.

4 Results

4.1 Effect of angiotensin receptor blockers on the intraocular pressure after topical administration

The individual IOP values for each rabbit and the mean change (mmHg; mean \pm SD) of the different groups, from baseline to four hours after administration, are shown in Figure 20.

The greatest effects on IOP caused by candesartan and irbesartan occurred four hours after the eye drop administration. Candesartan lowered the IOP from 24.6 ± 1.6 mmHg to 19 ± 0.9 mmHg ($n = 10$; change of 5.6 mmHg, paired t-test, $p = 0.030$). For irbesartan, the IOP decreased from 24.2 ± 1.7 mmHg to 20.2 ± 0.9 mmHg ($n = 10$; change of 4.0 mmHg, paired t-test, $p = 0.142$). In the same time, the commercial timolol solution lowered the IOP from 24.9 ± 4.2 mmHg to 20.4 ± 4.8 mmHg ($n = 10$, change of 4.6 mmHg, paired t-test, $p = 0.036$).

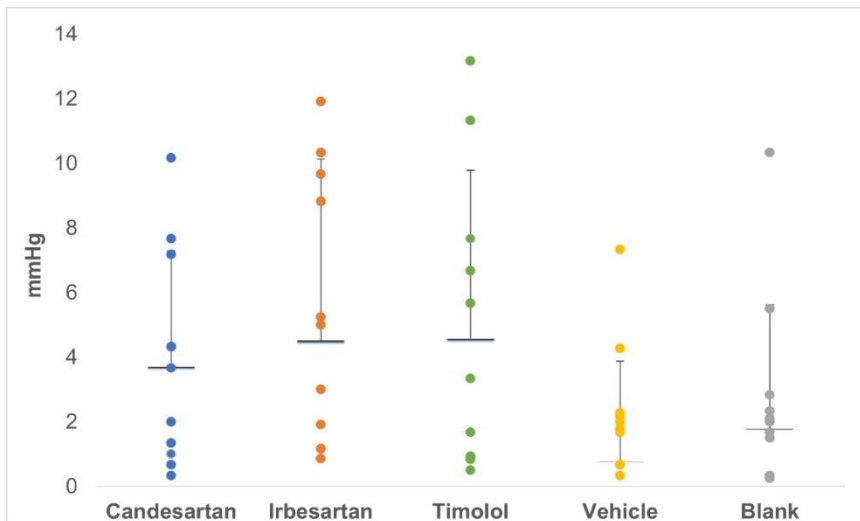


Figure 20. Mean (mmHg, mean \pm SD) and individual values for IOP change for each of the different drug and control groups four hours after eye drop application.

Figure 21 shows the change in IOP at different measured timepoints. The most relevant changes in IOP for both candesartan and irbesartan took place between two and four hours after administration. Candesartan showed a change of 1.8 mmHg in the first two hours of administration and a 3.7 mmHg change from two to four hours after administration. Irbesartan lowered the IOP by 0.48 mmHg during the first two hours

after administration and by 4.5 mmHg from two to four hours after administration. On the other hand, timolol shows a more relevant IOP change during the first two hours of administration, lowering it by 4.3 mmHg compared with a change of 0.3 mmHg from two to four hours after administration.

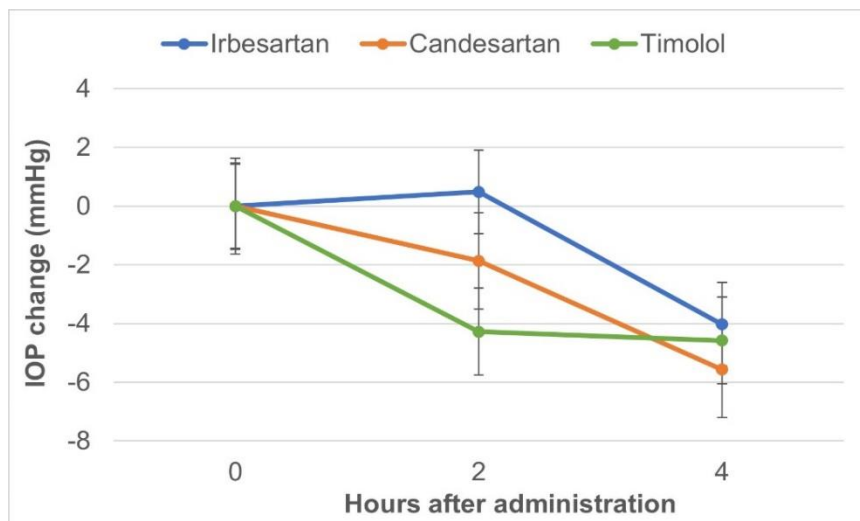


Figure 21. IOP change (mmHg, mean ± SD, n=10) at different timepoints after eye drop administration for each drug.

4.2 Ocular pharmacokinetics of angiotensin receptor blockers in the anterior segment

The drug concentration for irbesartan and candesartan in the cornea and aqueous humour at 1, 2, 3, 6 and 12 hours after administration is shown in Table 2 and Table 3 and Figure 22 and Figure 23.

Table 2. Concentration of irbesartan (ng/g, mean ± SD, n = 26) in the corneal tissue and aqueous humour at different timepoints after eye drop administration.

Hour after administration	Irbesartan			
	Cornea		Aqueous humour	
	Treated eye	Fellow eye	Treated eye	Fellow eye
0.5	3286.1 ± 555.1	32.8 ± 46.8	36.2 ± 41.7	3.4 ± 7.5
1.5	3662.6 ± 987.7	48.8 ± 85.6	99.6 ± 34.8	0.0
3	3127.1 ± 1021.8	14.9 ± 15.1	121.4 ± 68.8	0.0
6	1603.5 ± 369.6	0.0	59.6 ± 20.8	0.0
12	1039.4 ± 279.7	3.3 ± 4.9	33.7 ± 15.6	0.0

Table 3. Concentration of candesartan (ng/g, mean \pm SD, n = 23) in the corneal tissue and aqueous humour at different timepoints after eye drop administration.

Candesartan				
Hour after administration	Cornea		Aqueous humour	
	Treated eye	Fellow eye	Treated eye	Fellow eye
0.5	2905.8 \pm 1193	2.0 \pm 4.0	11.7 \pm 8.8	0.0
1.5	3503.9 \pm 801.5	1.3 \pm 1.6	14.6 \pm 2.5	0.0
3	2761.3 \pm 173.0	0.0	30.4 \pm 13.9	0.0
6	2350.2 \pm 742.0	0.9 \pm 1.2	29.1 \pm 8.8	0.0
12	2341.02 \pm 576.5	0.5 \pm 1.1	26.9 \pm 12.7	0.0

For the objective of the study, which is to evaluate the effectiveness of both drugs as IOP lowering treatments, only pharmacokinetic data corresponding to the anterior segment of the eye are shown. Irbesartan reached a maximum concentration of 121.4 \pm 68.8 ng/g (mean \pm SD, n = 26) in the aqueous humour of the study eye three hours after administration (Figure 22). The highest concentration in the aqueous humour for candesartan was 30.4 \pm 13.9 ng/g (mean \pm SD, n = 23) three hours after administration (Figure 23).

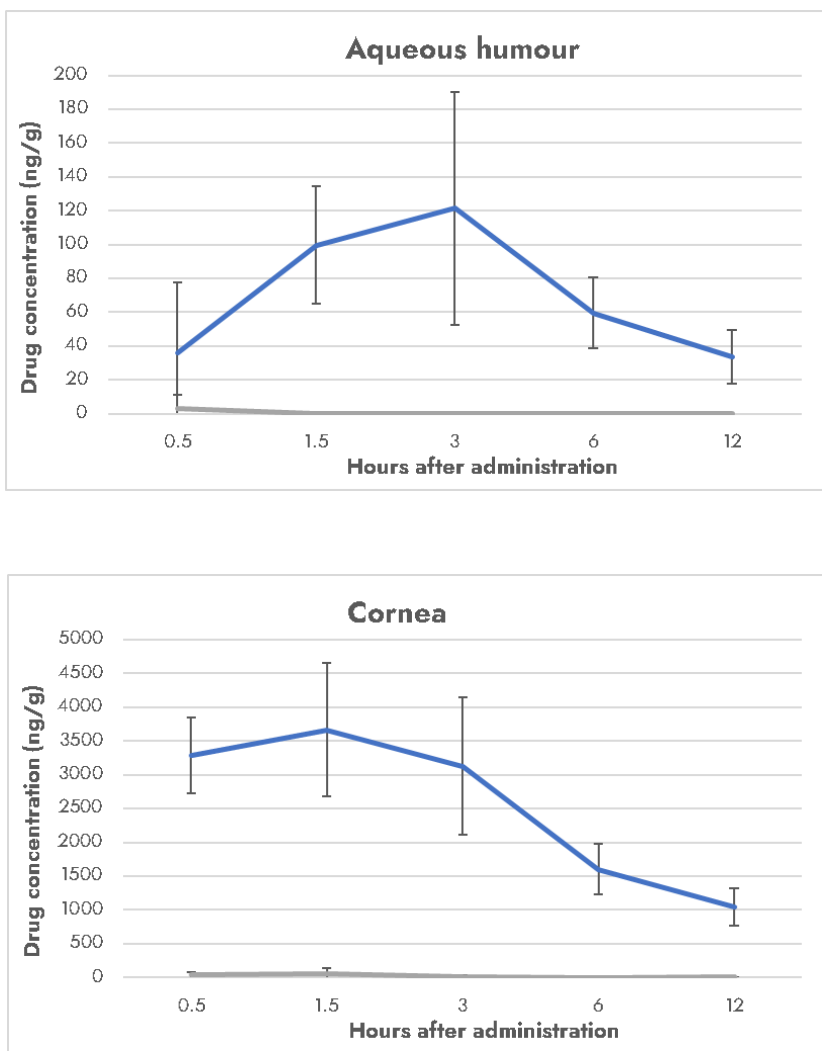


Figure 22. Top: irbesartan concentration (n = 26, mean ± SD; ng/g) in the cornea. Bottom: irbesartan concentration in the aqueous humour. Charts show drug concentration at timepoints (hours) after administration. Study eyes are shown in blue and untreated fellow eyes are shown in grey.

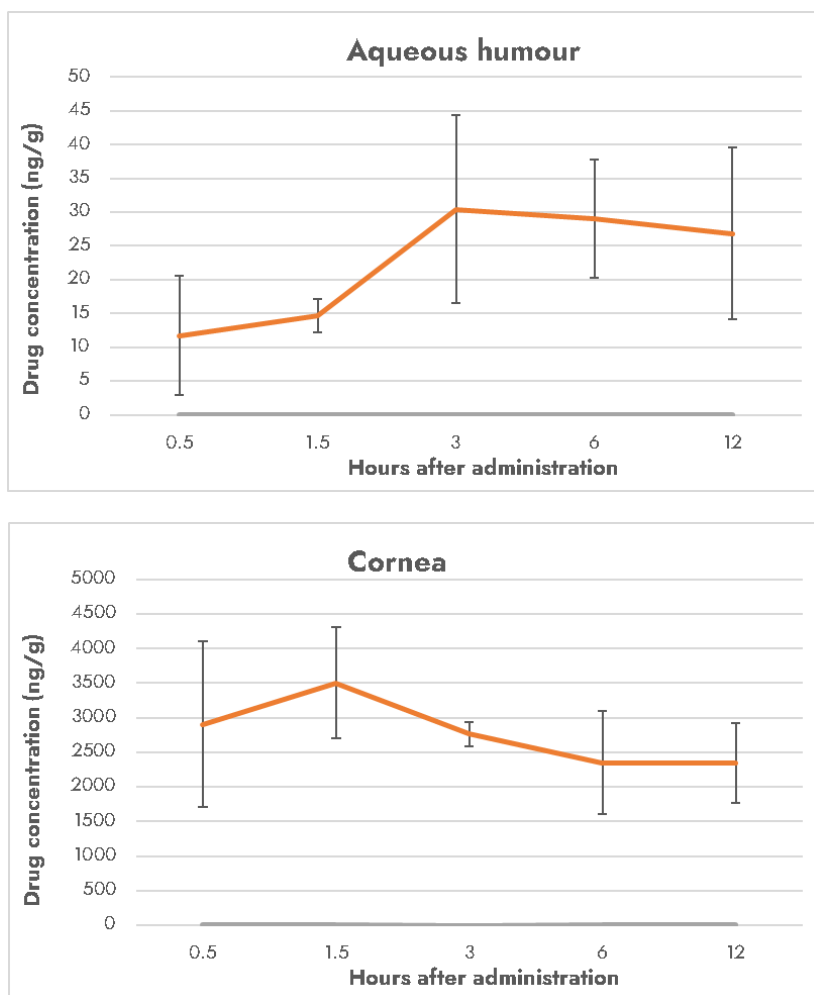


Figure 23. Top: candesartan concentration ($n = 23$, mean \pm SD; ng/g and nmol) in the cornea. Bottom: candesartan concentration in the aqueous humour. Charts show drug concentration at timepoints (hours) after administration. Study eyes are shown in orange and untreated fellow eyes are shown in grey.

4.3 Ocular pharmacokinetics of cediranib maleate in γ -cyclodextrin eye drop nanoparticles

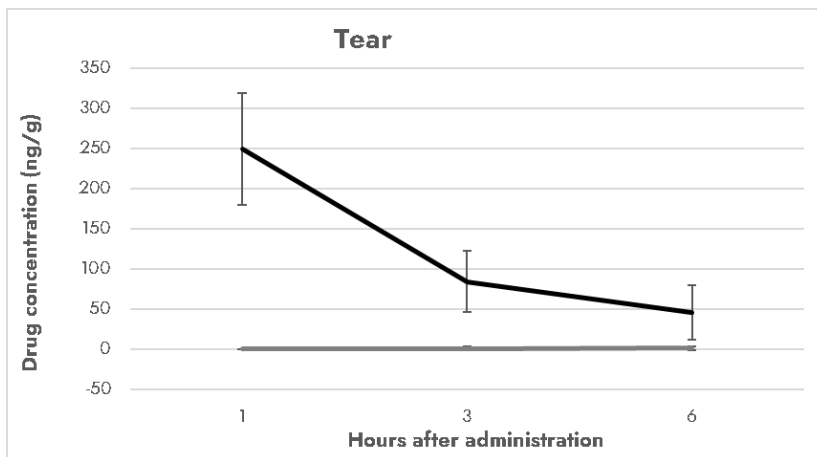
The highest drug concentrations in the retina and vitreous, being 530.8 ± 735.2 ng/g (1070 ± 1404 nM) and 9.3 ± 6.4 ng/g (19 ± 9 nM) (mean \pm SD, $n = 6$), were reached 1 hour after the administration. In the treated eye, the drug concentration in the vitreous was significantly higher at 1 and 3 hours after the administration ($p = 0.02$) when compared with the untreated eye. Regarding the retina, the drug concentration in the treated eye was significantly higher 6 hours after the administration, 429.6 ± 198.5

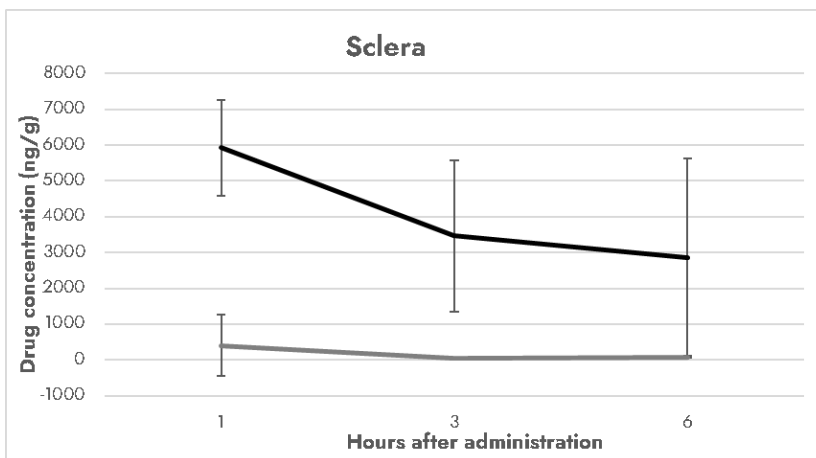
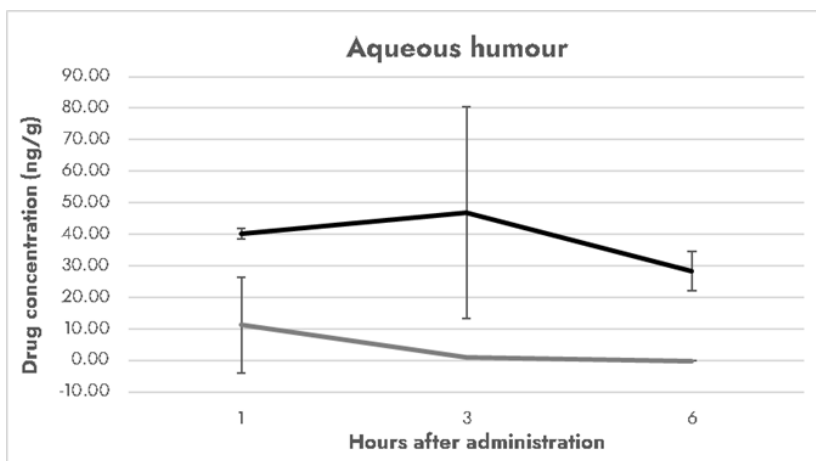
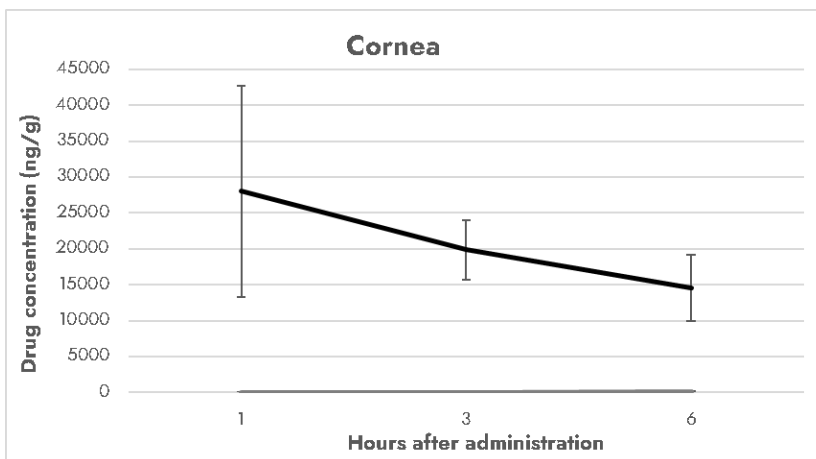
ng/g (758.1 ± 350.5 nM) when compared with the control eye with 210.9 ± 135.5 ng/g (372.3 ± 239.2 nM) ($p = 0.04$).

In the anterior segment, the highest concentrations were obtained in the cornea 1 hour after administration, 28042.1 ± 14709.2 ng/g. Maximum drug concentrations in the iris (3071.6 ± 2655.5 ng/g), lens (26.7 ± 30.3 ng/g) and aqueous humour (28.4 ± 6.1 ng/g) were found 6 hours after administration. Drug concentrations were significantly higher in the treated eye compared with control eyes ($p < 0.05$), except for the concentration found in the lens 6 hours after the administration ($p = 0.082$).

Drug concentrations were also measured in samples of tear and blood, taken immediately before euthanasia. Drug levels in the tear showed a decrease over time, ranging from 249.9 ± 69.2 ng/g to 46.2 ± 33.9 ng/g. Peak concentrations of cediranib maleate in the blood were found 3 hours after the administration with levels of 8.1 ± 4.3 g/g, decreasing to 3.8 ± 0.7 ng/g 6 hours after the administration.

The drug distribution of 3% cediranib maleate in both anterior and posterior segments at different timepoints after the eye drop administration (1, 3 and 6 hours) is shown in the figures below. Table 4 shows the highest drug concentrations for each tissue of the treated eye, compared to the corresponding drug levels in the untreated eye.





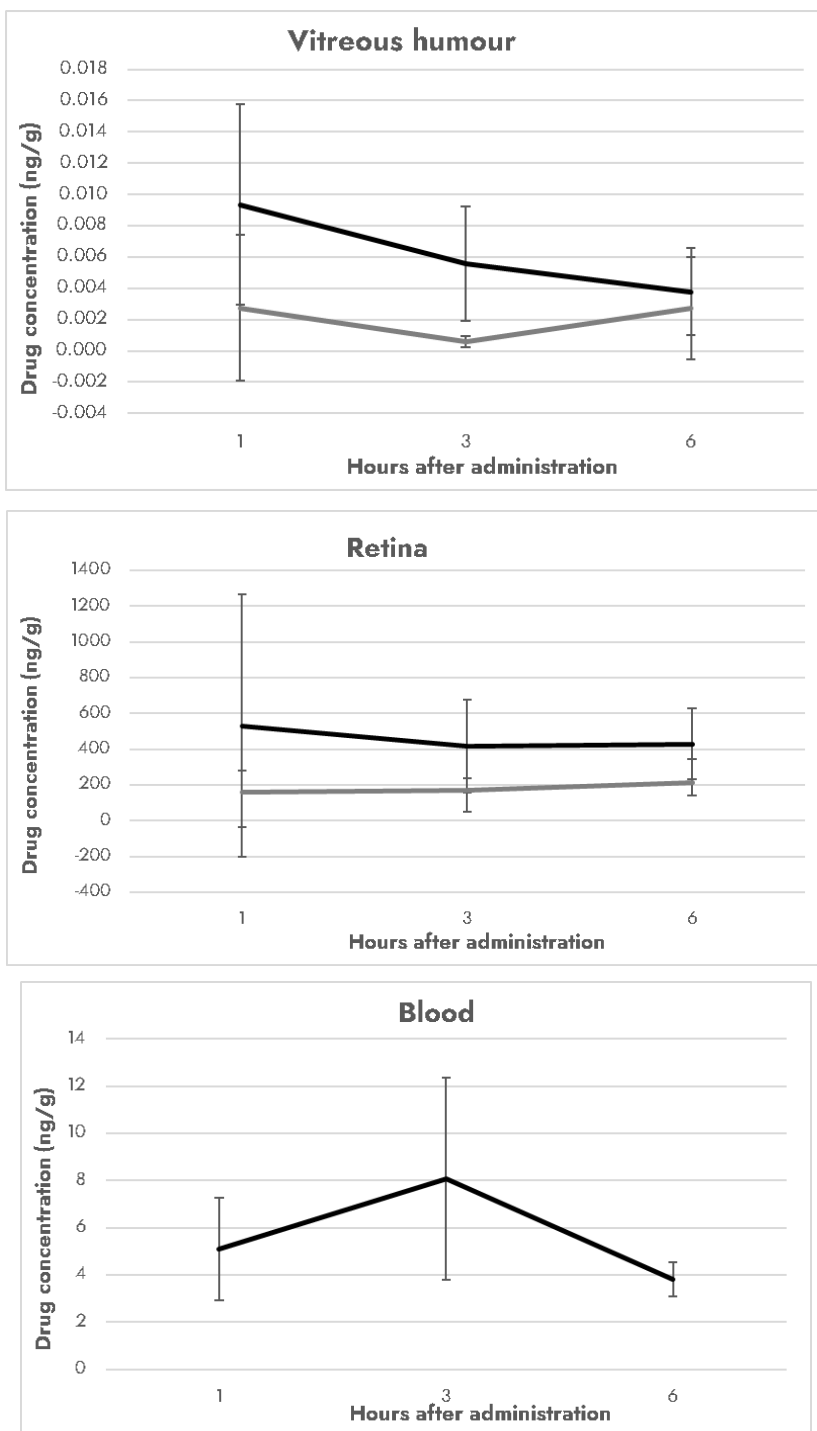


Figure 24. 3% cediranib maleate concentration (mean \pm SD; ng/g, n = 6) in the different eye tissues for the study eye (solid line), the untreated fellow eye (dotted line) and blood samples at different timepoints after administration.

Table 4. Highest concentration of cediranib maleate (nM, mean \pm SD; n = 6) in each tissue for the study eye (left) and corresponding concentration in the fellow eye (right). p-value indicates the difference ($p < 0.05$) in concentration levels of cediranib maleate between the study eye and the untreated fellow eye.

Tissue	Hours after administration	Treated eye (ng/g)	Fellow eye (ng/g)	p-value
Tear	1	249.9 \pm 69.2	0.6 \pm 0.0	< 0.01
Cornea	1	28042.1 \pm 14709.2	3.4 \pm 1.2	0.01
Aqueous humour	3	46.9 \pm 33.5	1.1 \pm 0.0	0.01
Sclera	1	5923.2 \pm 1344.9	409.0 \pm 863.0	0.01
Retina	1	530.8 \pm 735.2	160.6 \pm 120.9	0.06
Vitreous	1	9.3 \pm 6.4	2.7 \pm 4.7	0.02
Blood	3	8.1 \pm 4.3		

4.4 Comparison between fresh and frozen tissues for the permeation experiments

4.4.1 Full-thickness cornea

The permeation profiles for irbesartan obtained from the experiments comparing the use of fresh and frozen-thawed tissues are shown below for both full-thickness cornea and conjunctiva-sclera-choroid-retina. The permeability coefficients for irbesartan calculated at the end of the permeation studies were $2.7 \pm 1.7 \times 10^{-6}$ cm/s for fresh cornea and $2.7 \pm 1.3 \times 10^{-6}$ cm/s for frozen-thawed cornea. An independent t-test was performed to determine whether statistically significant differences existed between the permeability values obtained for fresh and frozen full-thickness cornea, a p-value of 0.7 was obtained.

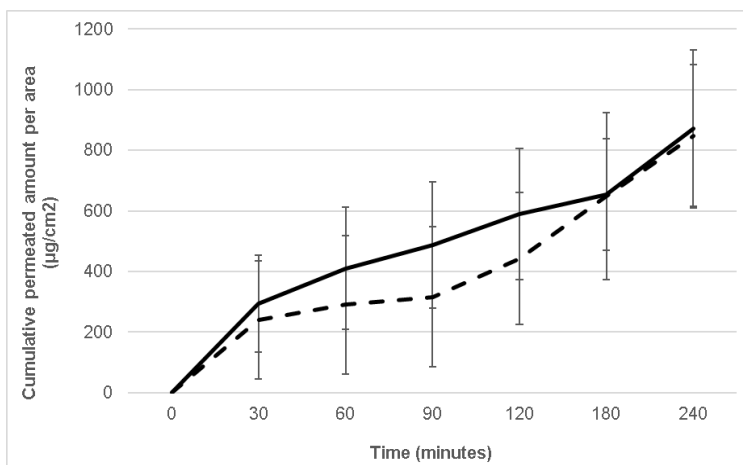


Figure 25. Cumulative permeated amount per area ($\mu\text{g}/\text{cm}^2$, mean \pm SD, $n = 3$) of 2.4% Irbesartan through fresh (dashed line) and frozen-thawed full-thickness cornea (solid line).

4.4.2 Conjunctiva-sclera-choroid-retina

For fresh and frozen-thawed conjunctiva-sclera-choroid-retina the permeability coefficients for irbesartan obtained from the permeation studies were $0.4 \pm 0.2 \times 10^{-6}$ cm/s and $0.6 \pm 0.4 \times 10^{-6}$ cm/s, respectively. The p-value obtained from the independent t-test was 0.5.

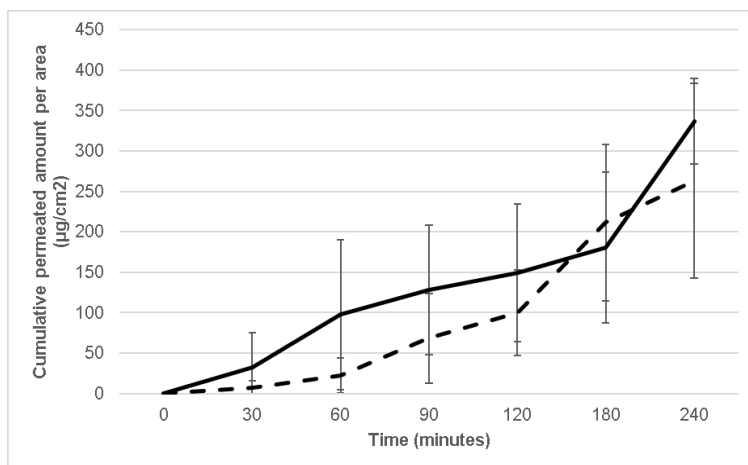


Figure 26. Cumulative permeated amount per area ($\mu\text{g}/\text{cm}^2$, mean \pm SD, $n = 3$) of 2.4% Irbesartan through fresh (dashed line) and frozen-thawed conjunctiva-sclera-choroid-retina (solid line).

4.5 Determination of steady-state flux and permeability coefficient

4.5.1 Sink conditions

For those compounds which maintained sink conditions at all times during the experiment, the permeability coefficient was calculated as slope of the linear part of the steady-state flux divided by time and the donor concentration at each timepoint, calculated as the difference between receiver concentration and initial donor concentration.

The following graph shows an example of the permeation profile for atenolol through full-thickness cornea, represented as the cumulative amount permeated ($\mu\text{g}/\text{cm}^2$) as a function of time.

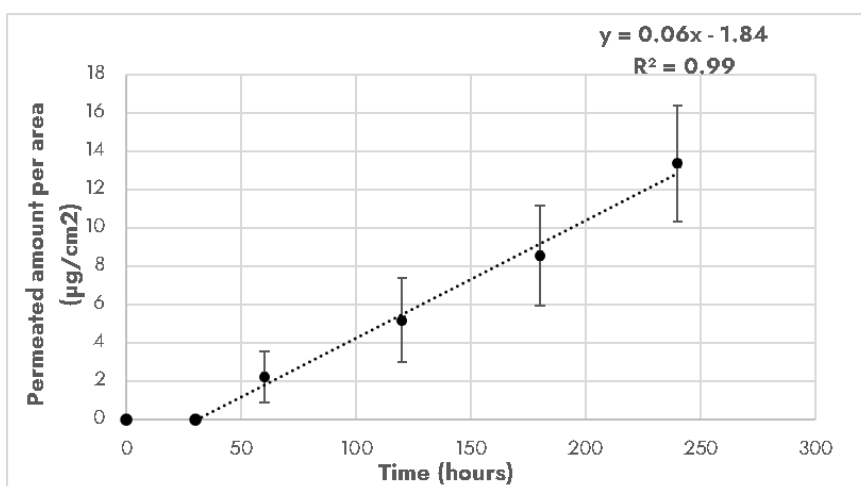


Figure 27. Cumulative amount permeated per area ($\mu\text{g}/\text{cm}^2$, mean \pm SD, $n = 3$) of atenolol through full-thickness cornea.

4.5.2 Non-sink conditions

Non-sink conditions were observed for some compounds, where the drug concentration in the receiver reached a level above 10% of the drug concentration in the donor. This situation can lead to a higher accumulation of the substance in the acceptor compartment which results in a decreasing flux. The figure below shows the permeation profile for dexamethasone through full-thickness cornea, where the concentration of the drug in the receiver surpasses 10% of the concentration in the donor within the first 30 minutes of the experiment.

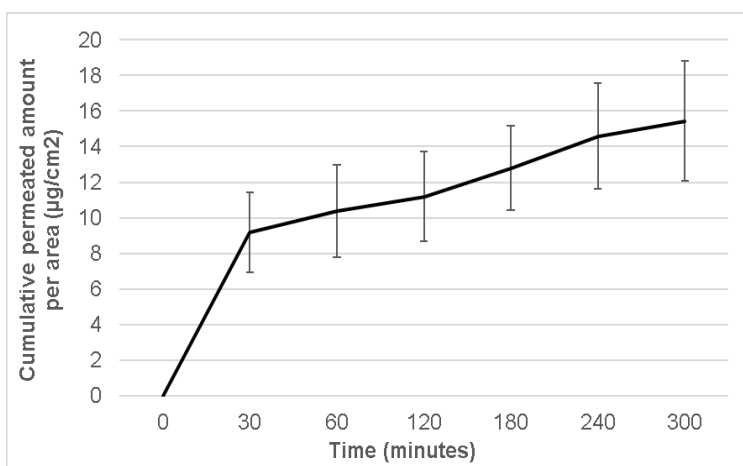


Figure 28. Cumulative amount permeated per area ($\mu\text{g}/\text{cm}^2$, mean \pm SD, $n = 3$) of dexamethasone through full-thickness cornea.

In these cases, the concentration gradient cannot be considered constant, and the non-sink equation described previously (Equation 16:) needs to be applied to take into account the changing in concentration gradient (Brodin et al., 2010; Mangas-Sanjuan et al., 2014; Teixeira et al., 2020):

Using the mentioned equation to calculate the permeability coefficient for dexamethasone, we obtained a value of $3.4 \pm 1.5 \times 10^{-6} \text{ cm/s}$, compared to previously reported values of $7.6 \pm 1.2 \times 10^{-6} \text{ cm/s}$ (Loch et al., 2012) and $0.9 \pm 3.0 \times 10^{-6} \text{ cm/s}$ (Juretić et al., 2018).

4.5.3 Atypical permeation profiles

The non-sink equation was also applied to those compounds that showed atypical permeation profiles (described in section 1.5.3.2), where establishing the linear period corresponding to the steady-state flux was more subjective (Figure 29). Given that, in the figure below, both the first interval (0-30 minutes) or the rest of the experiment (30-360 minutes) could be established as the steady-state fluxes, we chose to make use of Equation 16: to account for the different permeability rates that occurred during the experiment.

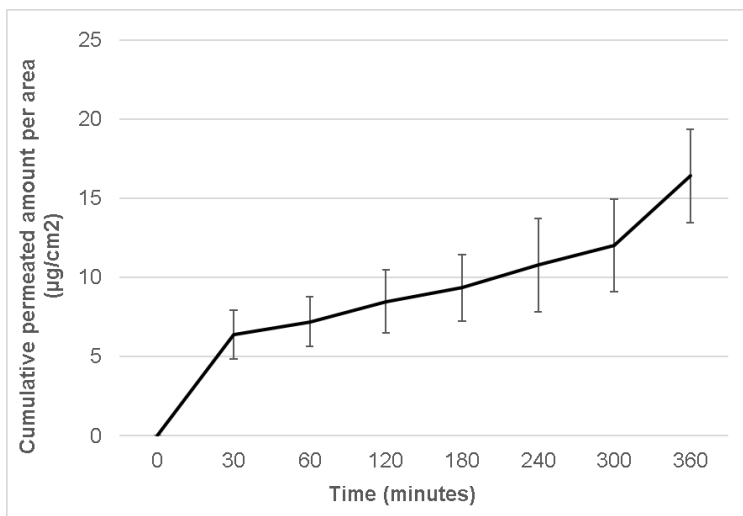


Figure 29. Cumulative amount permeated per area ($\mu\text{g}/\text{cm}^2$, mean \pm SD, $n = 3$) of propranolol hydrochloride through conjunctiva-sclera-choroid-retina.

Using the non-sink equation to calculate the permeability coefficient, we obtain a permeability value for propranolol hydrochloride of $6.5 \pm 2.5 \times 10^{-6} \text{ cm/s}$, which is similar to the one reported in the literature ($5.9 \pm 2.1 \times 10^{-6} \text{ cm/s}$) (Pescina et al., 2012).

4.6 Corneal and conjunctiva-sclera-choroid-retina permeability

Figure 30 shows the differences in permeability between full-thickness cornea and the conjunctiva-sclera-choroid-retina complex for each of the 27 compounds tested. Each permeability coefficient was calculated as the mean value and standard deviation of three replicas for each compound and tissue.

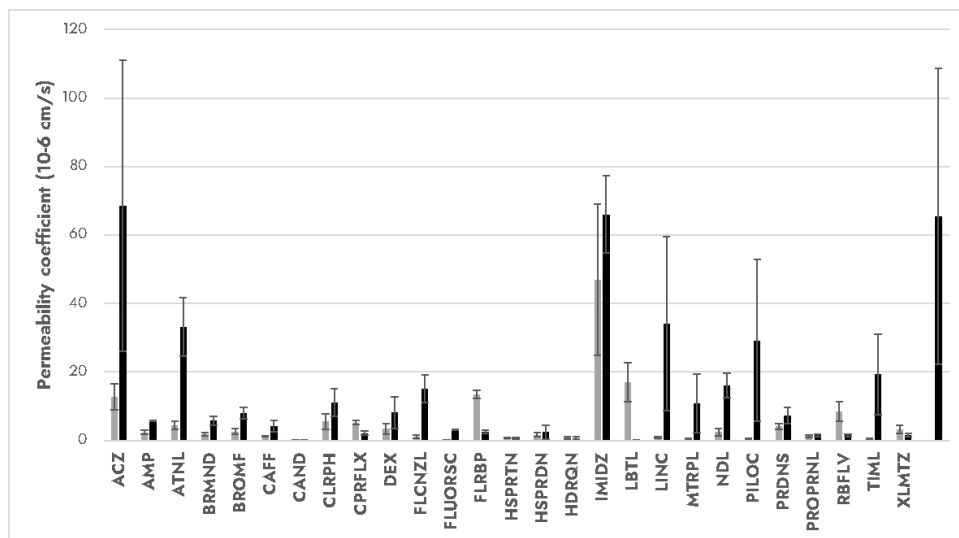


Figure 30. Individual permeability coefficient values (cm/s, mean ± SD, n = 3) for full-thickness cornea (gray) and conjunctiva-sclera-choroid-retina (black) for each compound tested.

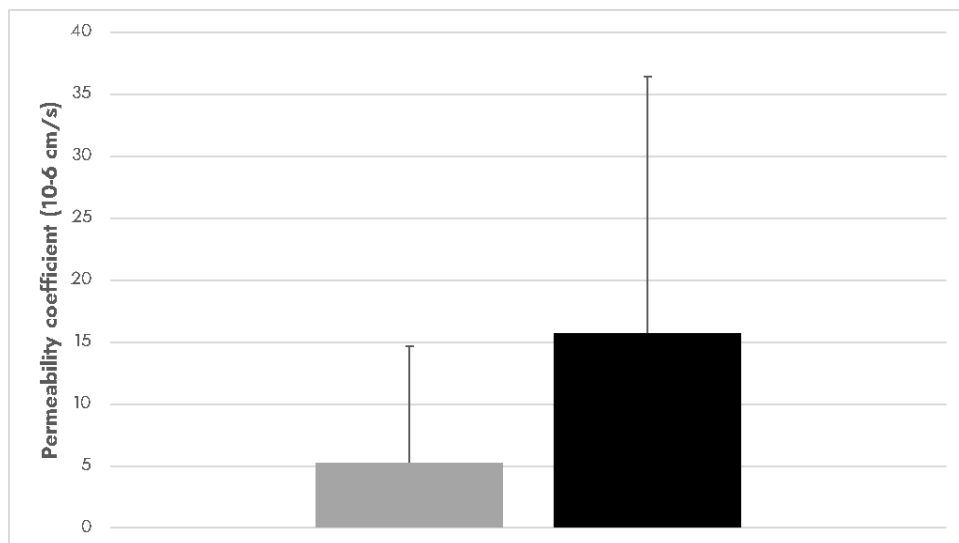


Figure 31. Mean permeability coefficient values (x10⁻⁶ cm/s, mean ± SD, n = 27) for full thickness cornea (gray) and conjunctiva-sclera-choroid-retina (black) for all compounds tested.

The permeability coefficient for each compound and tissue and the p-value obtained from the independent t-test are shown in the table below. p-values lower than 0.05 indicate that the difference in permeability between full-thickness cornea and conjunctiva-sclera-choroid-retina is statistically significant.

Table 5. Permeability coefficient values (10^{-6} cm/s, mean \pm SD, n = 3) for full-thickness cornea and conjunctiva-sclera-retina-choroid for all compounds tested.

Compound	Cornea	Sclera	p-value
Acetazolamide	12.8 \pm 3.8	68.5 \pm 42.5	0.00
Ampicillin sodium	2.3 \pm 0.6	5.7 \pm 0.1	0.00
Atenolol	4.4 \pm 1.2	33.1 \pm 8.5	0.00
Brimonidine tartrate	1.8 \pm 0.5	5.8 \pm 1.3	0.00
Bromfenac sodium	2.6 \pm 0.8	8.0 \pm 1.7	0.00
Caffeine	1.2 \pm 0.1	4.1 \pm 1.7	0.00
Candesartan	0.09 \pm 0.04	0.07 \pm 0.001	0.00
Chlorpheniramine maleate	5.5 \pm 2.3	11.1 \pm 4.0	0.00
Ciprofloxacin hydrochloride	5.2 \pm 0.6	2.1 \pm 0.6	0.03
Dexamethasone	3.4 \pm 1.5	8.1 \pm 4.7	0.00
Fluconazole	1.0 \pm 0.5	15.1 \pm 4.1	0.00
Fluorescein	0.2 \pm 0.05	3.1 \pm 0.2	0.00
Flurbiprofen	13.4 \pm 1.2	2.6 \pm 0.5	0.70
Hesperetin	0.7 \pm 0.2	0.6 \pm 0.3	0.68
Hesperidin	1.7 \pm 0.645	2.4 \pm 1.994	0.06
Hydroquinone	0.8 \pm 0.4	0.7 \pm 0.3	0.33
Imidazole	47.0 \pm 22.1	66.0 \pm 11.3	0.00
Labetalol hydrochloride	17.0 \pm 5.7	34.1 \pm 25.4	0.00
Lincomycin hydrochloride	0.8 \pm 0.2	10.8 \pm 8.5	0.00
Metoprolol tartrate	0.5 \pm 0.2	16.1 \pm 3.5	0.00
Nadolol	2.4 \pm 1.1	29.2 \pm 23.7	0.00
Pilocarpine hydrochloride	0.7 \pm 0.03	7.3 \pm 2.3	0.00
Prednisolone	4.1 \pm 0.8	0.7 \pm 0.2	0.02
Propranolol hydrochloride	1.2 \pm 0.432	6.5 \pm 2.5	0.00
Riboflavin	8.4 \pm 2.8	19.3 \pm 11.7	0.00
Timolol maleate	0.4 \pm 0.1	1.5 \pm 0.5	0.00
Xylometazoline hydrochloride	3.2 \pm 1.2	65.4 \pm 43.2	0.00

On average, the permeability through the scleral complex was 2.7 times higher than the permeability through full-thickness cornea. For some of the tested compounds, the scleral permeability ranged from 2-fold to 30-fold the corneal permeability. On the other hand, full-thickness cornea showed a higher permeability than conjunctiva-sclera-choroid-retina for six out of 27 compounds tested (ciprofloxacin hydrochloride, candesartan, flurbiprofen, hesperetin, hydroquinone and prednisolone) which was statistically significant for candesartan, flurbiprofen and prednisolone.

4.7 cGMP and lipidic nanocapsules

The results of the permeability study with a cGMP as a naked compound and in a lipidic nanocapsule-based formulation across full-thickness cornea and conjunctiva-sclera-choroid-retina are shown below.

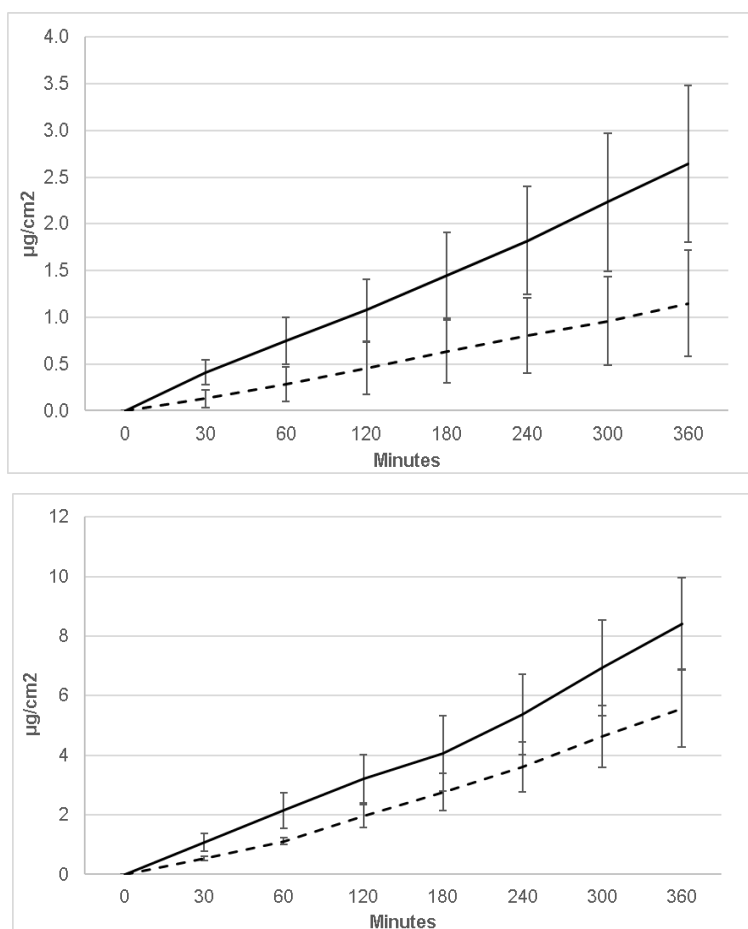


Figure 32. Cumulative amount permeated per area ($\mu\text{g}/\text{cm}^2$, mean \pm SD, $n = 3$) of DF003 as a naked compound (dashed line) and in a formulation with lipidic nanocapsules (solid line) through full-thickness cornea (top) and conjunctiva-sclera-choroid-retina (bottom).

The formulation containing lipid nanocapsules showed a higher permeation of DF003 across both tissues when compared with the naked compound. Moreover, the conjunctiva-sclera-choroid-retina showed a higher permeation to DF003 in both water-based solution and lipid nanocapsules when compared to the cornea.

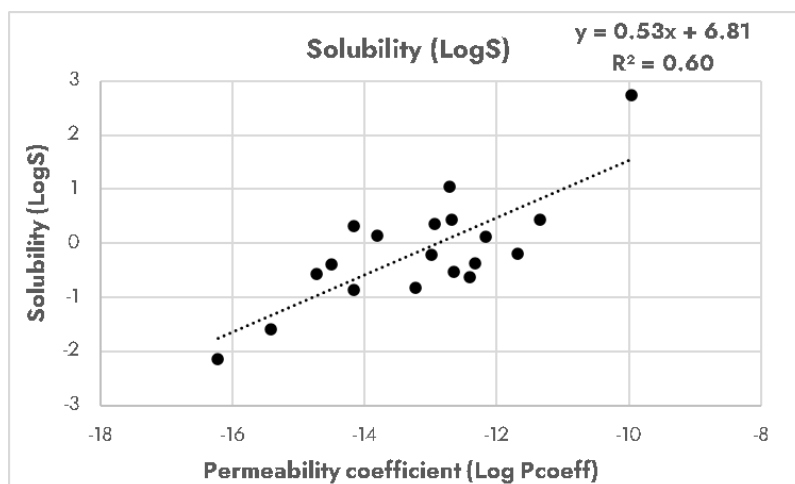
The permeability coefficients across full-thickness cornea for DF003 were $2.2 \pm 1.2 \times 10^{-8}$ cm/s (mean \pm SD, $n = 3$) in water solution and $5.1 \pm 1.7 \times 10^{-8}$ cm/s for the LNCs formulation. For conjunctiva-sclera-choroid-retina DF003 alone showed a permeability coefficient of $1.0 \pm 0.2 \times 10^{-7}$ cm/s and $1.6 \pm 0.4 \times 10^{-7}$ cm/s for the LNCs formulation.

DF003 showed a permeability 4.6 times higher across conjunctiva-sclera-choroid-retina than cornea as a naked compound, and 3 times higher when tested as a lipid nanocapsules-based formulation.

4.8 Correlation between permeability and molecular properties

4.8.1 Full-thickness cornea

Three molecular properties showed to be significantly correlated with the permeability across full-thickness cornea: the logarithm of solubility ($r^2 = 0.60$, $p = 0.002$), the number of rings ($r^2 = -0.52$, $p < 0.001$) and $\log P$ ($r^2 = -0.67$, $p < 0.001$). The logarithm of water solubility showed a positive correlation, indicating that higher water solubilities lead to an increase in permeability. On the other hand, an increase in the number of rings and the $\log P$ of the molecules seem to negatively affect their permeability through full-thickness cornea. The scatter plots with the r^2 and the p -value for each correlation are shown below.



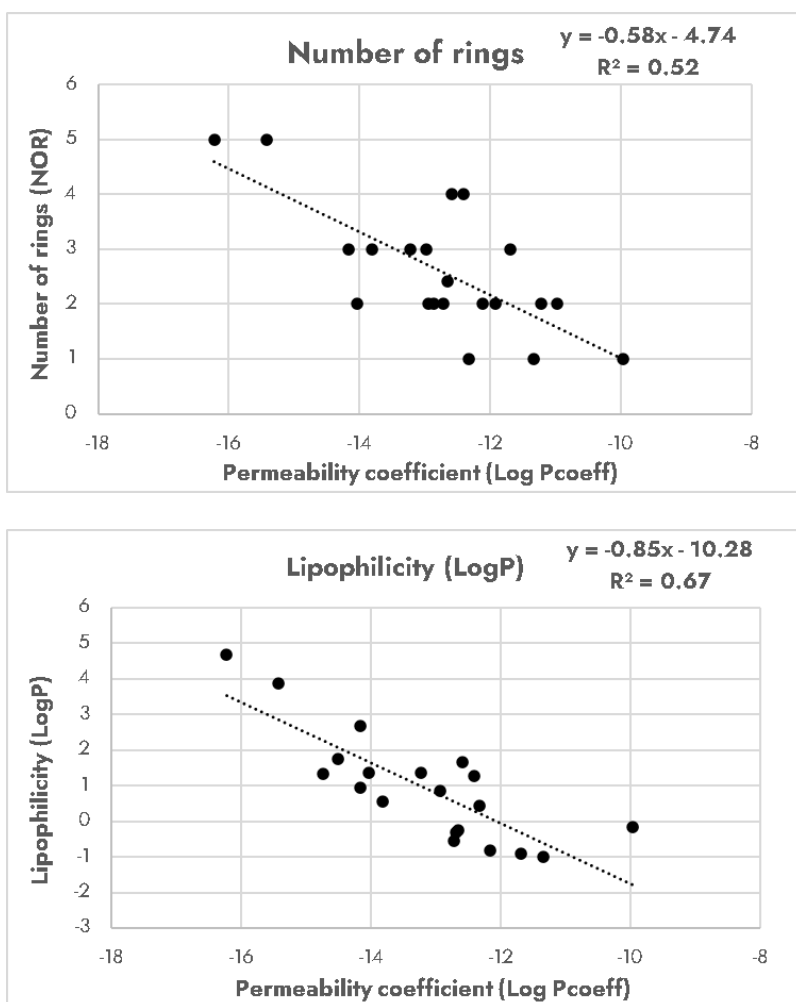
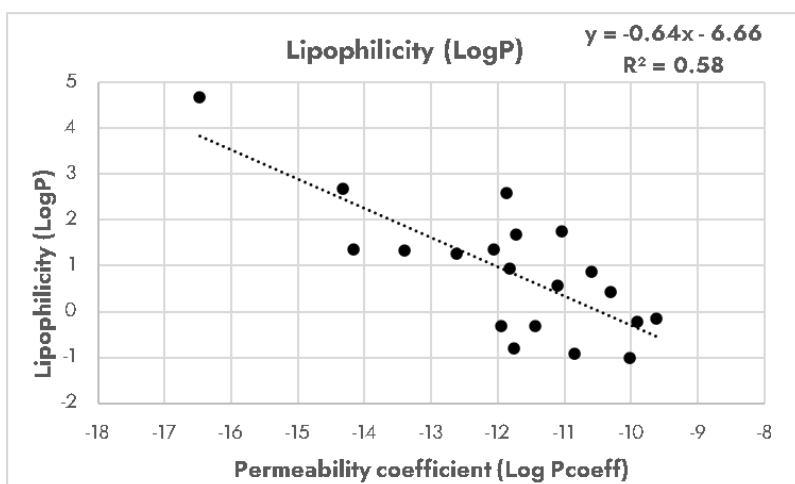
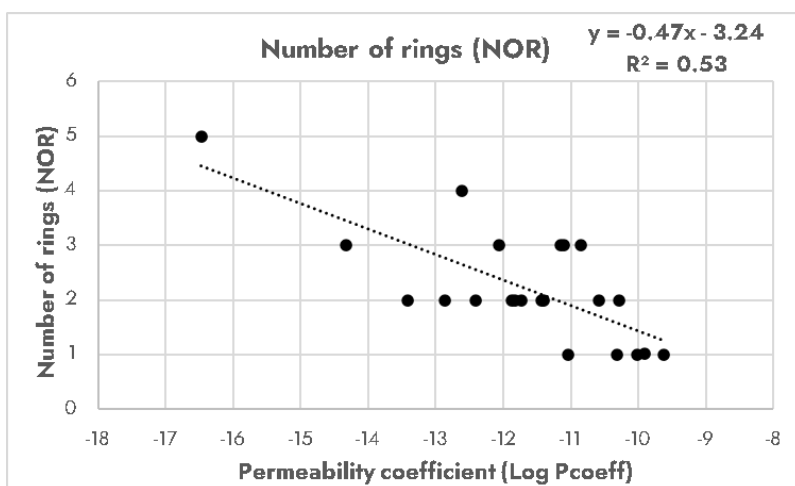
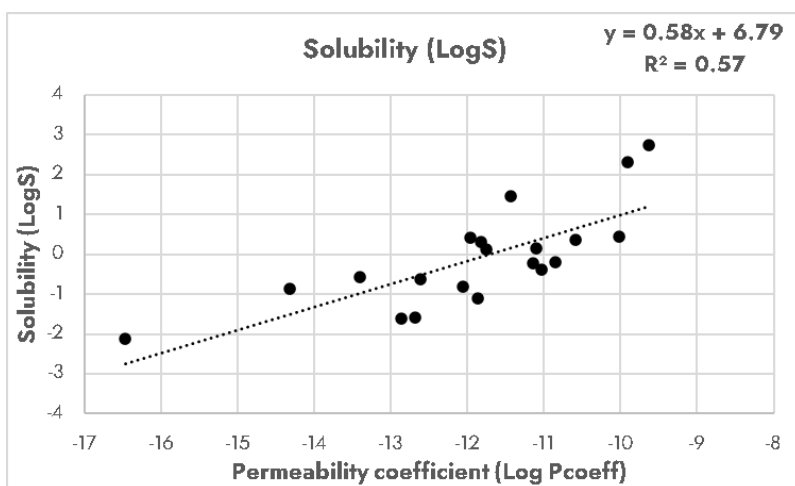


Figure 33. Scatter plots for the correlations between physicochemical properties and the permeability of compounds across full-thickness cornea.

4.8.2 Conjunctiva-sclera-choroid-retina

Five molecular descriptors showed significant correlations with the permeability of the tested compounds through conjunctiva-sclera-choroid-retina. The logarithm of water solubility showed a positive association ($r^2 = 0.57$, $p < 0.001$), while the number of rings ($r^2 = -0.53$, $p < 0.001$), logP ($r^2 = -0.58$, $p < 0.001$), molecular weight ($r^2 = -0.51$, $p < 0.001$) and logD ($r^2 = -0.55$, $p < 0.001$) were negatively correlated with the permeability. The scatterplots for these correlations are shown in the figures below.



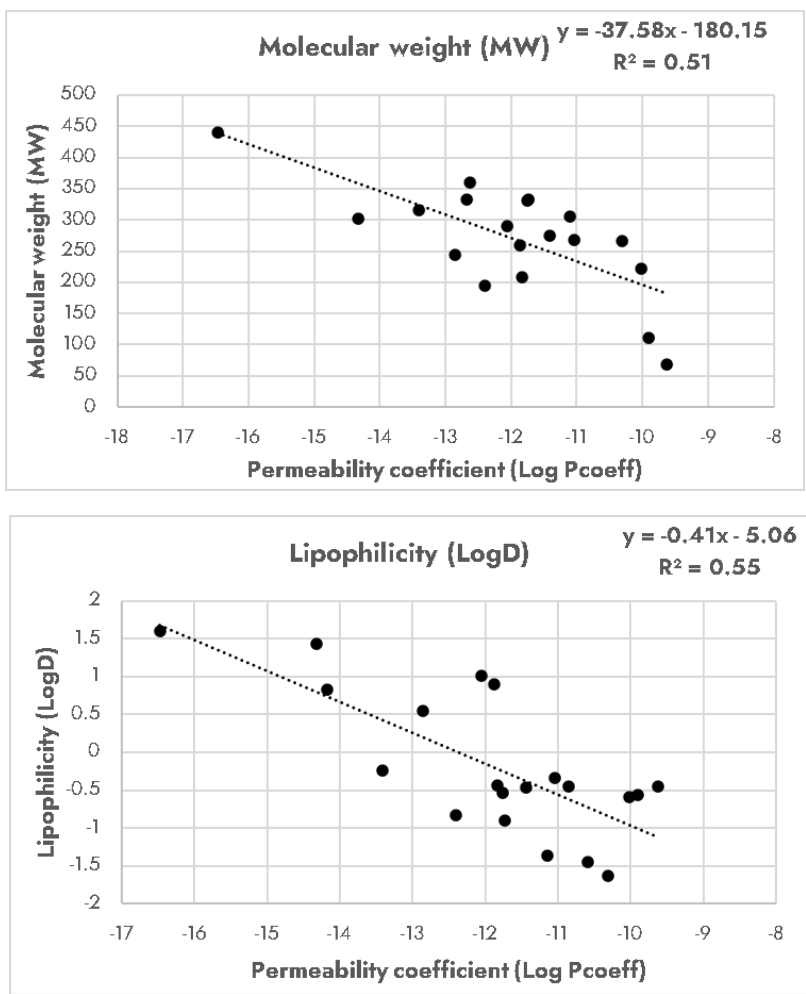


Figure 34. Scatter plots for the correlations between physicochemical properties and the permeability of compounds across conjunctiva-sclera-choroid-retina.

5 Discussion

The objective of the studies described in this thesis was to investigate and further understand the pharmacokinetics of drugs in the ocular tissues following topical administration, which is the preferred route for ophthalmologic treatments.

Topical application of drugs using eye drop formulations is especially common for the treatment of diseases in the anterior segment, however, challenges arise when the target tissues involve those in the back of the eye. Treatment of disorders affecting tissues in the posterior segment, such as the retina and choroid, is hampered by the physiological and anatomical mechanisms that protect the eye from exogenous substances. Invasive techniques, such as the intravitreal injection, are the common procedures used to reach the back of the eye. Although effective and generally safe, this method is uncomfortable for the patient and involves repetitive injections to be performed periodically.

Despite the challenges that surround the topical delivery of drugs to the posterior segment, eye drop formulations using different drug delivery systems have shown to reach the retinal tissues to some extent (Araújo et al., 2011; Cheng et al., 2019; Y. Bin Choy et al., 2019; Gupta et al., 2019; Lajunen et al., 2014; Popov, 2020; Shi et al., 2019; Tahara et al., 2017; X. Xu et al., 2020). This suggests that formulations with appropriate physicochemical properties can traverse the layers and different barriers of the eye and deliver drugs in therapeutically active concentrations to the back of the eye.

In this project, we developed two different *in vivo* studies to investigate and quantify drug delivery using γ -cyclodextrin-based eye drop formulations in both anterior and posterior segments. As shown by our results, and compared with previously reported IC_{50} values, these formulations were able to deliver drugs in pharmacologically active concentrations (D. Kim et al., 2018; Lacy et al., 2017; van Rodijnen et al., 2010). Moreover, we investigated the therapeutic effect of two of these formulations (irbesartan and candesartan), targeting the anterior segment. The positive outcome of the study reinforces the conclusion that the eye drops achieved a localized delivery and effect of the drug.

In vivo studies are key to understanding the absorption, distribution, metabolism and excretion characteristics of drugs. They provide invaluable insight into the pharmacokinetics and pharmacodynamics of drug candidates during development and are reliable assessment tools for the efficacy and safety of drug formulations. However, they are resourcefully and ethically questionable for commonly involving the use of a high number of animals. In this thesis, as an alternative to *in vivo* studies, we performed

multiple *in vitro* experiments using a common and well-described methodology to investigate the permeability of different molecular compounds across the ocular tissues. These experiments aimed to compare the permeability of drugs through full-thickness cornea, the main route used for delivering drugs to the anterior segment, and the conjunctiva-sclera-choroid-retina, which is suggested as a more direct path of drug delivery to the back of the eye. With the data obtained from these experiments, we intended to highlight those physicochemical properties that are more relevant for drug permeability across the eye tissues. Being able to predict the permeability of drugs based on their physicochemical characteristics would provide a useful and valuable screening tool during drug development, potentially reducing both the use of animal studies and failures at different stages of the drug development process.

5.1 *In vivo* pharmacokinetics

In two of the studies described in this thesis, we analyzed the drug pharmacokinetics of γ -cyclodextrin-based eye drop nanosuspensions after topical administration *in vivo* in rabbits. We quantified the drug concentration in tissues of the anterior or posterior segment of the eye depending on the therapeutic target of each drug.

5.1.1 Angiotensin receptor blockers

The first study focused on the use of two different drugs, candesartan and irbesartan, that act as angiotensin receptor blockers and are involved in the regulation of the intraocular pressure. For this purpose, the drug concentration was measured in the cornea and the aqueous humour. Moreover, we also measured the pharmacologic effect of irbesartan and candesartan on the intraocular pressure of normotensive rabbits.

The results from our pharmacokinetic analysis suggest that both irbesartan and candesartan in γ -cyclodextrin nanoparticle eye drops penetrate the eye in pharmacologically relevant concentrations after a single topical application.

Based on a study from Kim et al., the IC_{50} of irbesartan as a specific competitive antagonist of the angiotensin II type 1 receptor is 1.3 nM or 0.6 ng/g of tissue (D. Kim et al., 2018). Van Rodikjen et al. found only a slight difference in potency between candesartan and irbesartan, and their calculations estimate candesartan's IC_{50} values to be between 0.4 and 0.7 nM (0.17-0.3 ng/g) (van Rodijnen et al., 2010). Our results show a concentration in aqueous humour of 100-200 times the IC_{50} for irbesartan and 50 times the IC_{50} for candesartan, suggesting over 99% inhibition of the receptor for both drugs.

In absence of concentration measurements in the ciliary body, where the renin-angiotensin system is located, the drug concentration in the aqueous humour can be used as a substitute. The highest concentrations in the aqueous humour are reached

three hours after the administration, explaining the fact that the most relevant changes observed in the IOP for both drugs take place between two and four hours after the administration.

Thirty minutes after administration, a small amount of irbesartan was also detectable in the fellow control eye, indicating systemic absorption. On the other hand, candesartan was not detected in the control eye, which is probably due to the concentration being lower than the detection limit (5ng/g).

Interestingly, candesartan showed more stable and sustained drug concentrations in both cornea and aqueous humour throughout time. These results are consistent with a study reported previously by van Rodijnen et al., where they suggested a slower dissociation of candesartan from the AT1-receptor than irbesartan (van Rodijnen et al., 2010).

In addition to candesartan and irbesartan, one of the groups in our study was treated with a single eye drop application of timolol, a beta-blocking agent commonly used to lower intraocular hypertension in glaucoma patients. Chiang et al. tested different timolol preparations and measured the effect on the IOP in rabbits. Their results showed a noticeable decrease in the IOP one hour after a 50µl administration of 0.5% timolol. This agrees with our results, where we can see that timolol produced the fastest decrease in the IOP, two hours after the administration (Chiang, Ho, & Chen, 1996). Although candesartan and irbesartan showed a slower effect on the IOP compared to timolol, the effect of both drugs at the end of the study was comparable to that of timolol, suggesting the potential of candesartan and irbesartan as novel glaucoma drugs.

Considerable variations in the intraocular pressure have been reported to take place over 24 hours in both normal and glaucomatous eyes. These short-term fluctuations are mostly associated with circadian rhythms, heart rate, breathing patterns, eye or lid position or physical activity, as well as issues regarding repeatability and reproducibility of rebound tonometry (Weitzman et al., 1975; Shapiro, Dickersin and Lietman, 2006). In our study, a blank group was included as a control for the diurnal effect and other potential variability on the IOP. For this group a decreasing trend in the IOP along the day was observed, however, it showed no statistical significance when compared with the treated groups ($n = 10$, $p > 0.05$). Other factors responsible for short-term IOP fluctuations are water drinking, animal handling and drug administration. Bruccleri et al. observed that IOP increased significantly after water ingestion and remained altered for 45 minutes. They suggested aqueous drainage as a possible explanation for this phenomenon. Accordingly, we intended for the rabbits to have a continuous source of drinking water so the fluid balance was not interrupted and minimal changes in IOP were caused due to water loading (Bruccleri et al., 1999).

Animal handling during *in vivo* studies has also shown to have an impact on the intraocular pressure. According to a study from Dinslage et al. changes in the IOP lasted from a few minutes to several hours after interaction with the rabbits. We used rebound tonometry for the IOP measurements in our study, which, despite being a non-invasive technique, requires handling each animal individually several times a day. Moreover, the measurement is performed by briefly touching the ocular surface using a small probe, which may cause distress to the animal. To ensure that minimal disturbances were caused to the rabbits, they were gently handled before every IOP measurement. As indicated by Ma et al., if any sign of stress was found, IOP measurements were postponed for at least another two minutes before repeating the measurements (Dinslage et al., 1998; Ma et al., 2016).

5.1.2 Cediranib maleate

In the second *in vivo* study, we tested a novel γ -cyclodextrin-based formulation with cediranib maleate, a potent tyrosine kinase inhibitor that has shown potential as an anti-VEGF, acting through inhibition of angiogenesis and neovascularization, when administered orally (Batchelor et al., 2010; Dietrich et al., 2009). When targeting ocular neovascularization, however, anti-VEGF drugs are commonly injected directly into the ocular tissues using intravitreal injections, resulting in an unmet need for alternative and less invasive delivery routes to the posterior segment. Cediranib maleate in γ CD micro-suspension eye drops could provide a new treatment as an anti-VEGF therapy to the back of the eye, potentially replacing invasive intraocular drug delivery procedures.

In this study, we quantified the drug concentration in various ocular tissues from both anterior and posterior segments after a single eye drop administration. Based on our data, cediranib maleate was detected in all measured tissues. When compared to recently reported data, where cediranib has been shown to inhibit VEGF-stimulated proliferation with IC50 values of 0.4-0.5 nM (~0.29 ng/g), our results showed drug concentrations 10 times higher in the vitreous (6.7-16.4 nM, 3.8-9.4 ng/g), and more than 100 times higher in the retina (936.6-758.1 nM, 429.6-530.8 ng/g) (Lacy et al., 2017).

A slow decrease in the drug levels of tear sample showed sustained residence time in the tear film over the course of the study. This indicates that, even if in lower concentrations, there could be a potential continuous release of the drug to the tissues for at least 6 hours after the administration.

The drug levels in blood samples are useful to study to which degree systemic absorption is affecting the distribution of cediranib maleate to the ocular tissues. The highest concentration of cediranib maleate in blood samples was found 3 hours after the administration, with drug levels of 8.1 ± 4.3 ng/ml of plasma. The recommended dose of cediranib maleate for oral administration derived from efficacy and safety

studies is around 25 mg (Ledermann et al., 2016). Given that the single-dose administered in our studies contained 1.5 µg of cediranib maleate, the risk of adverse side effects caused by the drug concentration present in plasma samples due to systemic absorption, seems unlikely.

Our results suggest that cediranib maleate is delivered in therapeutically active concentrations to the posterior segment of the eye when topically administered as γ -cyclodextrin eye drop nanosuspension. In addition, drug concentration levels were significantly higher in the treated eye compared with the untreated eye, indicating that the formulation delivers cediranib maleate locally in the ocular tissues, which could contribute to minimizing side effects caused by systemic absorption.

Several studies have been performed to determine the pharmacokinetic properties of γ -cyclodextrin/drug complexes after topical administration to the eye. Johannsdóttir et al. investigated whether topically applied dexamethasone/ γ CD micro-suspension could deliver dexamethasone to various tissues of the eye in therapeutic concentrations in rabbits. Maximum drug concentrations were reached after 2 hours of administration in all tissues, where the highest to lowest drug concentrations were found in the cornea, iris, sclera, retina, aqueous humour, vitreous and lens (Johannsdottir et al., 2018b). These results are in agreement with those obtained in our study, where the highest concentrations were found in the cornea, iris, sclera and retina, with peak levels generally occurring during the first 2-3 hours after the administration. Moreover, the drug concentration showed sustained levels up to 12 and 6 hours in each of the *in vivo* studies, respectively.

These data support that γ -cyclodextrin eye drop nanosuspensions represent an effective and non-invasive drug delivery system from the surface of the eye to both anterior and posterior segments, allowing the localized administration of therapeutically active drug concentrations in the ocular tissues and, therefore, minimizing the risk of side effects associated to systemic drug administration.

5.2 Comparative permeability of corneal and conjunctiva-scleral delivery routes

The corneal route has traditionally been regarded as the main route of drug penetration into the ocular tissues following topical administration. This route, however, presents various physical and physiological barriers, i.e., eye blinking and tear turnover, that hinder the permeability of molecules, causing only 5% or less of the administered dose to effectively reach the intraocular tissues. These barriers, in addition to the distance a molecule needs to cross from the cornea to the posterior segment, result in the corneal route being highly inefficient for delivering drugs to the tissues in the back of the eye.

The conjunctival-scleral route has been presented as an alternative for topical drug delivery to the posterior segment. This route, in addition to being more closely located

to the posterior segment, has shown to be more permeable to molecules with different physicochemical properties when compared to the cornea. Moreover, it also shows a larger exposed surface, resulting in a greater area for drug diffusion.

To test the hypothesis that the conjunctiva-sclera could be used as an alternative delivery route when administering drugs to the posterior segment, we developed a series of experiments applying a well-described methodology, commonly used at the beginning of most studies involving percutaneous absorption (Salamanca et al., 2018). This methodology aims to predict the *in vivo* permeability of molecules by using *ex vivo* animal tissues or synthetic membranes, providing a good preliminary tool for the screening of drug permeability without the need for *in vivo* animal testing.

Applying the Franz-diffusion cell methodology, we determined the *ex vivo* permeability across full-thickness cornea and conjunctiva-sclera-choroid-retina of 27 different drug molecules, 21 of which showed a higher permeability across conjunctiva-sclera when compared to full-thickness cornea and a mean conjunctival-scleral permeability 2.7-fold higher than the corneal permeability. If we take into account the measurements of the exposed sclera reported by other authors, which is approximately twice as large as the corneal surface, our results suggest that the average permeability across conjunctiva-sclera-choroid-retina is almost 6 times higher than the permeability across full-thickness cornea (Caspar et al., 2021; Danel et al., 2018; Kobayashi & Kohshima, 1997, 2001).

The conclusion that permeability through the scleral complex is generally higher than that of the cornea, is in agreement with the general literature on the field. One of the most exhaustive studies regarding the permeability of different ocular tissues was conducted by Prausnitz and Noonan in 1998, with almost 150 different compounds and 300 permeability measurements of cornea, sclera, and conjunctiva from different species. They observed in the results that the sclera shows a relatively higher permeability compared to the cornea (Prausnitz, 1998). Hämäläinen et al. estimated in their study with polyethylene glycol oligomers that the noncorneal route (conjunctiva and sclera) was 15 to 25 times more permeable than the cornea (Hämäläinen et al., 1997). Several other studies have also shown the sclera to be more permeable than the cornea for different solutes, including compounds with high molecular weights, such as dextrans, antibodies and bovine serum albumin (Ambati et al., 2000; Olsen et al., 1995).

Ex vivo permeability values in porcine tissues have been previously reported by other authors for some of the compounds in our dataset. Hahne et al. reported a corneal permeability coefficient for dexamethasone of $1.51 \pm 0.12 \times 10^{-6}$ cm/s, compared with $7.6 \pm 1.2 \times 10^{-6}$ cm/s reported by Loch et al., $0.9 \pm 0.3 \times 10^{-6}$ cm/s obtained by Juretić et al. and $0.2 \pm 0.07 \times 10^{-6}$ cm/s showed by Ramsay et al. (Hahne et al., 2012; Juretić et al., 2018; Loch et al., 2012; Ramsay et al., 2018b). Our value for full-thickness corneal permeability of dexamethasone was $3.4 \pm 1.5 \times 10^{-6}$ cm/s, which is in range with the mentioned results reported by other authors. For conjunctiva-sclera-choroid-retina, Loch et al. reported a permeability value of $1.0 \pm 0.2 \times 10^{-6}$ cm/s, a value which

is 8-times smaller than our permeability value ($8.1 \pm 4.7 \times 10^{-6}$ cm/s), however, when they calculate the permeability coefficient considering the resistance of the different tissue layers, they obtain a permeability value of 7.8×10^{-6} cm/s. Very similar values of permeability coefficient for fluorescein through full-thickness cornea were obtained by us ($0.2 \pm 0.05 \times 10^{-6}$ cm/s) and Hahne et al. ($0.18 \pm 10.15 \times 10^{-6}$ cm/s), which are almost 3-times lower than the one reported by Pescina et al. ($0.5 \pm 0.2 \times 10^{-6}$ cm/s).

Permeability values for timolol were reported by the same authors: $5.1 \pm 0.6 \times 10^{-6}$ cm/s (Loch et al., 2012), $7.1 \pm 1.8 \times 10^{-6}$ cm/s (Hahne et al., 2012) and $10.7 \pm 2.1 \times 10^{-6}$ cm/s (Juretić et al., 2018). These values range from 10 to 25 times difference compared with our permeability value for full-thickness cornea. For conjunctiva-sclera-choroid-retina, however, our permeability value ($1.5 \pm 0.5 \times 10^{-6}$ cm/s) is very similar to the one obtained by Loch et al. ($1.3 \pm 0.4 \times 10^{-6}$ cm/s) (Loch et al., 2012).

Pescina et al. also determined the permeability of propranolol hydrochloride through full-thickness cornea and conjunctiva-sclera-choroid-retina. Our permeability value for propranolol through full-thickness cornea ($1.2 \pm 0.4 \times 10^{-6}$ cm/s) is around 10 times lower than the value reported by Pescina et al. ($14.6 \pm 0.5 \times 10^{-6}$ cm/s), but very similar to one obtained by Ramsay et al. ($1.5 \pm 1.4 \times 10^{-6}$ cm/s) (Pescina et al., 2015; Ramsay et al., 2018b). Regarding the permeability of propranolol hydrochloride through the scleral complex, our value is 5 times lower than the one reported by Pescina et al. in their study, $7.0 \pm 2.5 \times 10^{-6}$ cm/s compared to $1.4 \pm 0.3 \times 10^{-6}$ cm/s (Pescina et al., 2012).

Our results are in general agreement with those previously reported in the literature. This is, however, to the best of our knowledge, the first study to experimentally test and compare the diffusion of a library of compounds with differing physicochemical properties on both full-thickness cornea and conjunctiva-sclera-choroid-retina.

5.2.1 Ex vivo testing of new compounds

We also used the Franz-diffusion cells methodology to perform an *ex vivo* screening of DF003, a newly synthesized molecule and part of a novel class of cGMP (cyclic guanosine- 3',5'-monophosphate) analogues recently developed as potential treatments for retinal degenerations (Ekström et al., 2019; Vighi et al., 2018). The screening was conducted on both full-thickness cornea and conjunctiva-sclera-choroid-retina. Moreover, we used two different formulations of the drug, an aqueous solution and a lipid nanocapsules-based formulation. Similar to cyclodextrins, lipid nanocapsules (LNC) are widely used drug delivery systems, especially for lipophilic and poorly soluble drugs (Bohley et al., 2019). LNCs have shown to be effective in different *in vitro* and *in vivo* animal models, however, their use as topical delivery systems in ophthalmology has only recently been explored (Formica et al., 2020). The aim of our study was, therefore, not only to compare the permeability of a compound across different tissues but to assess the potential of the *ex vivo* model described above as a preliminary screening tool for new eye drop formulations.

The permeability coefficients of both aqueous solution and the lipid nanocapsules formulation across conjunctiva-sclera-choroid-retina ($1.0 \pm 0.2 \times 10^{-7}$ cm/s and $1.6 \pm 0.4 \times 10^{-7}$ cm/s, mean \pm SD, n = 3) were higher than across full-thickness cornea ($2.2 \pm 1.2 \times 10^{-8}$ cm/s and $5.1 \pm 1.7 \times 10^{-8}$ cm/s), reinforcing our previous conclusion that the noncorneal route might represent a more efficient way of drug delivery to the posterior segment. Moreover, when formulated with lipid nanocapsules, the permeability of DF003 was improved across both tissues, agreeing with previously reported studies where LNCs enhanced corneal permeation and improved residence time when tested *in vivo* (Gaballa et al., 2020; Huang et al., 2018; Khalil et al., 2017). Regarding the posterior segment, several preclinical studies have shown that the use of lipid nanocapsules improves permeation to the posterior segment, increasing the retinal concentration and therapeutic effect of the drugs (Lakhani et al., 2020; Navarro-Partida, Altamirano-Vallejo, et al., 2021; Tatke et al., 2019).

Despite its advantages over the corneal route, drugs that are topically applied to the sclera are subject to a high degree of systemic absorption due to the extense vascularization of the conjunctiva (Ramsay et al., 2017). Increasing the residence time of topically applied compounds, using formulations such as lipid nanocapsules and cyclodextrins, can decrease the effect of systemic absorption, improving the local delivery of drugs to the retinal tissues. Therefore, based on the results of this study, the Franz-cells methodology using *ex vivo* ocular tissues can provide valuable preliminary permeability data during the initial phases of drug development, potentially reducing the use of animal testing and failures in later stages of the development process.

5.2.2 Ocular permeability and physicochemical properties

Computer modelling, high-throughput analysis and cell-based assays are essential tools in the screening of pharmacologic activity and toxicity of drugs. The pharmacokinetic and pharmacodynamic (PK/PD) properties of different drugs, however, are based on ADME studies (absorption, distribution, metabolism and excretion) that are usually developed on *in vivo* studies, which are resourceful, time-consuming and require the use of alive animals (Y. Bin Choy & Prausnitz, 2011). Drug pharmacokinetics present a strong dependence on the physicochemical properties of each compound, such as solubility, lipophilicity and molecular weight. Although PK/PD analysis requires data that can only be obtained using *in vivo* systems, an early triage of drugs based on favourable physicochemical properties could be a useful tool in predicting the PK properties and selecting potential drug candidates. Therefore, in the last part of our *ex vivo* permeability study, we aimed to establish a relationship between the data obtained on permeability across the different ocular tissues, full-thickness cornea and conjunctiva-sclera-choroid-retina, and the physicochemical properties of the different compounds tested.

Based on our results, the permeability of compounds across full-thickness cornea and conjunctiva-sclera-choroid-retina is similarly affected by water solubility, lipophilicity and the number of rings present in a molecule. Our data shows that an increase in the lipophilicity of the compounds (logP and logD) negatively affects their permeation across full-thickness cornea and conjunctiva-sclera-choroid-retina. LogP is the descriptor of lipophilicity for neutral compounds, or where the compound exists in a single form. On the other hand, logD measures the lipophilicity for ionizable solutes, or compounds that can exist as a variety of different species in a pH-dependent manner (Bhal, 2019).

When crossing the cornea, drugs must partition from the epithelium, a lipophilic membrane with tight junctions, to the stroma, a hydrophilic layer composed of collagen fibrils. For highly lipophilic drugs, transitioning from the lipophilic epithelium to the hydrophilic stroma is rate-limiting and, in most cases, determines the corneal permeability (P. Agarwal & Rupenthal, 2016; Ramsay et al., 2018b; Shih & Lee, 1990; Shirasaki, 2008). Permeation through the cornea has been shown to follow a parabolic relationship with an optimal logP of 2–3 and that, at high lipophilicity values (logP > 4), the corneal permeability decreases, presumably due to the poor desorption from the lipoidal epithelium to the hydrophilic stroma (Rimpelä, Reunanen, et al., 2018; Schoenwald & Ward, 1978). Regarding the sclera, its structure is comparable to the corneal stroma, with a high degree of water content rendering it conducive to hydrophilic molecules (Miao et al., 2013; Pitkänen et al., 2005). Kadam et al. studied the influence of permeant lipophilicity on the permeability across the full-thickness sclera, showing higher permeability for hydrophilic molecules when compared to lipophilic ones (Kadam et al., 2011). Similarly, Cheruvu and Kompella found that the solute permeability coefficients measured in both bovine and porcine tissues exhibited a negative correlation with the logarithm of distribution coefficients (Cheruvu & Kompella, 2006).

The higher the lipophilicity of a molecule, the lower its water solubility, which explains the opposite correlation between these descriptors and permeability. Low aqueous solubility of drugs is one of the main challenges in drug development. Poorly soluble compounds are restricted in solubility by their hydrophobicity, which hinders their ability to combine with the surrounding water phase and partition into the tissues, causing low bioavailabilities after administration (Bergström & Larsson, 2018; Praphanwittaya et al., 2020). Studies have conclusively proved that the conjunctiva–scleral layer plays a role in the drug absorption of hydrophilic molecules and that the permeability through isolated conjunctiva for hydrophilic molecules is twice that of the sclera and higher than the cornea (Ghate & Edelhauser, 2006). Thakur et al. studied the permeability of different corticosteroids related to their lipophilicity and solubility. They concluded that higher transscleral diffusion correlated with higher aqueous solubilities and decreased with increasing lipophilicity (Thakur et al., 2011).

The molecular weight and the number of rings also showed to be relevant descriptors in dictating the permeation of compounds across conjunctiva-sclera-choroid-retina. The effect of molecular weight on the permeation of compounds through conjunctiva-sclera has been reported previously. Miao et al. studied the permeability of macromolecules through the sclera and concluded that larger molecules are more likely to accumulate on the outer surface, hampering their permeability across the tissue. They suggested that differences in thickness between topographical locations of the sclera may have pharmacokinetic implications when considering transscleral diffusion of macromolecules (Miao et al., 2013).

The number of rings counts the number of cyclic structures present in a compound, where one or more series of atoms are connected forming a ring. This descriptor shows a high positive correlation with the molecular weight of the compound ($r^2 = 0.64$), indicating that a greater number of rings lead to an increase in the mass and size of a compound. This association between the number of rings and molecular weight explains the negative effect of this descriptor on the permeability through the noncorneal route.

In conclusion, our results indicate that solubility, logP and the number of rings, are the main characteristics affecting the permeability of compounds across both full-thickness cornea and conjunctiva-sclera-choroid-retina. LogD and molecular weight, however, only seem to affect the permeability of our compounds across the noncorneal route. In a similar study by Kidron et al., the results reflected that corneal permeability has a stronger correlation with LogD than LogP, opposite to our results (Kidron et al., 2010). Ramsay et al., on the other hand, did not find any relationship between corneal permeability and lipophilicity descriptors. They obtained, instead, that the permeability of molecular compounds across cornea depends on the polar surface area, the number of hydrogen bond donors and the halogen ratio of the molecules (Ramsay et al., 2018b). Differences in the results of each study can be attributed to different factors, such as the chemical space represented by the compounds used and the source of molecular descriptors.

In 1997, Lipinski developed a widely accepted rule to predict the pharmacokinetic properties of drug compounds (Lipinski et al., 1997). This Rule of Five establishes that permeation or absorption of compounds increases with molecular weight < 500 , logP < 5 , number of hydrogen bond donors < 5 and number of hydrogen bond acceptors < 10 . Although this rule was developed to assess the oral absorption of drugs, Choy and Prausnitz tested whether the Rule of Five was applicable to predict the permeation of drugs through non-oral delivery routes (Y. Bin Choy & Prausnitz, 2011). They concluded that a modified Rule of Five (MW < 500 , logP < 4.2 , number of hydrogen bond donors < 3 and number of hydrogen bond acceptors < 8) was applicable for predicting the absorption of ophthalmologic drugs.

Our results are in general agreement with the modified Rule of Five suggested by Choy and Prausnitz, indicating that lipophilicity (LogP, LogD and, consequently, solubility) and molecular weight (strongly related to the number of rings) are relevant descriptors in the prediction of drug absorption in the ocular tissues (Y. Bin Choy & Prausnitz, 2011). No correlation was found in our study between the number of hydrogen bonds and/or donors and the permeability of compounds, which might be caused by a limited chemical space represented by our molecules.

Although the compounds included in our study show differing physicochemical properties, allowing us to establish some significant correlations with the permeability across full-thickness cornea and conjunctiva-sclera-choroid-retina, a more extensive library of compounds, covering a wider range of molecular descriptors, would reveal other important properties and, most likely, stronger correlations. Performing these experiments with a high number of molecules would require a considerable amount of time and resources. However, it could contribute to avoiding major failures in later stages of the process, minimizing the waste of expensive resources and, more importantly, reducing the number of animal studies employed in the early phases of drug discovery (del Amo, 2015; Deng et al., 2016; Moiseev et al., 2019; Sellick, 2011).

6 Conclusions

We have investigated the pharmacokinetics of different drugs across ocular tissues, including both the anterior and posterior segments of the eye, applying both *in vivo* and *in vitro* methods.

In vivo studies are essential when investigating the pharmacokinetics and pharmacodynamics of drugs, allowing us to determine different aspects of drug delivery such as drug distribution, elimination, systemic absorption and pharmacologic effect. Based on our studies, we can conclude that drug delivery using eye drop formulations is an effective way of delivering drugs to the ocular tissues. We show that drugs can reach tissues in both anterior and posterior segments of the eye in pharmacologically relevant concentrations, based on the IC₅₀ values reported by other authors for the different drugs tested. This conclusion is also reinforced by the IOP-lowering effect produced by candesartan and irbesartan after a single-drop administration. Moreover, our data demonstrate that different delivery systems, such as cyclodextrins and lipid nanocapsules, can be used to modify drug properties and enhance the permeation of compounds across the layers of the eye.

On the other hand, *in vitro* and *ex vivo* models can provide helpful preliminary data for screening and choosing new drug candidates, before being tested using *in vivo* models. Using a porcine model and a well-described *in vitro* methodology we were able to confirm our initial hypothesis, suggested also by other authors, that the noncorneal route might represent an alternative and more efficient way of delivering drugs to the posterior segment of the eye. Although previous studies have reported the higher permeability of conjunctiva-sclera compared with the cornea, these studies are generally focused on groups of drugs with similar properties, which, as shown by our analysis, can impact and limit the permeability of compounds across tissues. This is, to the best of our knowledge, the first study comparing the permeability between full-thickness cornea and conjunctiva-sclera-choroid-retina for a library of molecular compounds with different physicochemical properties. From our results, we conclude that the higher permeability of the non-corneal route applies to most compounds. Moreover, our correlation analysis agrees with results obtained by other authors, proving that both the methodology used and the data obtained in our studies are reliable and reproducible.

Regarding the screening of new compounds, we have no means to determine how the data obtained in our *ex vivo* experiments for the formulations including DF003 translates into *in vivo* models, since no studies exist where this compound has been tested. Our results, however, agree with the general conclusion that the conjunctiva-

sclera is more permeable than the cornea, and that the use of delivery systems, such as lipid nanocapsules, can improve permeability across the ocular tissues, which has been shown in different *in vivo* studies with other drugs.

An unmet need exists to improve ocular drug delivery following topical administration, offering patients alternative and less invasive delivery methods than the commonly used, such as intravitreal injections. From our studies, we can suggest that drug delivery platforms that improve the penetration of compounds into the ocular tissues are a step toward providing safer and more comfortable treatments for ophthalmology patients, especially those who require repeated or regular administration. In addition, an alternative and more efficient way to deliver drugs compared to the corneal route might be achieved by localizing delivery through the conjunctiva-sclera.

References

- Abdelkader, H., Longman, M. R., Alany, R. G., & Pierscionek, B. (2016). Phytosome-hyaluronic acid systems for ocular delivery of L-carnosine. *International Journal of Nanomedicine*, *11*, 2815–2827.
- Achouri, D., Alhanout, K., Piccerelle, P., & Andrieu, V. (2013). Recent advances in ocular drug delivery. *Drug Development and Industrial Pharmacy*, *39*(11), 1599–1617.
- Acott, T. S., & Kelley, M. J. (2008). Extracellular matrix in the trabecular meshwork. *Experimental Eye Research*, *86*(4), 543–561.
- Agarwal, P., & Agarwal, R. (2018). Trabecular meshwork ECM remodeling in glaucoma: could RAS be a target? *Expert Opinion on Therapeutic Targets*, *22*(7), 629–638.
- Agarwal, P., & Rupenthal, I. D. (2016). In vitro and ex vivo corneal penetration and absorption models. *Drug Delivery and Translational Research*, *6*(6), 634–647.
- Agarwal, R., Krasilnikova, A. V., Intan, R., & Agarwal, P. (2014). Mechanisms of angiotensin converting enzyme inhibitor-induced IOP reduction in normotensive rats. *730*, 8–13.
- Agrahari, V., Mandal, A., Agrahari, V., Trinh, H. M., Joseph, M., Ray, A., Hadji, H., Mitra, R., Pal, D., & Mitra, A. K. (2016). A comprehensive insight on ocular pharmacokinetics. *Drug Delivery and Translational Research*, *6*(6), 735–754.
- Ahmed, I., & Gokhale, D. (1972). Pharmaceutical sciences. *The American Journal of Digestive Diseases*, *17*(10), 918–918.
- Ahmed, I., & Patton, T. F. (1985). Importance of the noncorneal absorption route in topical ophthalmic drug delivery. *Investigative Ophthalmology and Visual Science*, *26*(4), 584–587.
- Ako-Adounvo, A. M., & Karla, P. K. (2018). Transscleral drug delivery to retina and posterior segment disease. *Drug Delivery for the Retina and Posterior Segment Disease*, 215–227.
- Al Sabbah, Z., Mansoor, A., & Kaul, U. (2013). Angiotensin receptor blockers - Advantages of the new sartans. *Journal of Association of Physicians of India*, *61*(7), 464–470.

- Amadio, M., Govoni, S., & Pascale, A. (2016). Targeting VEGF in eye neovascularization: What's new?: A comprehensive review on current therapies and oligonucleotide-based interventions under development. *Pharmacological Research*, *103*, 253–269.
- Ambati, J., & Adamis, A. P. (2002). Transscleral drug delivery to the retina and choroid. *Progress in Retinal and Eye Research*, *21*(2), 145–151.
- Ambati, J., Canakis, C. S., Miller, J. W., Gragoudas, E. S., Edwards, A., Weissgold, D. J., Kim, I., Delori, F. C., & Adamis, A. P. (2000). Diffusion of high molecular weight compounds through sclera. *Investigative Ophthalmology and Visual Science*, *41*(5), 1181–1185.
- Anderson, D. H., & Fisher, S. K. (1979). The relationship of primate foveal cones to the pigment epithelium. *Journal of Ultrastructure Research*, *67*(1), 23–32.
- Araie, M., & Kimura, M. (1997). Intraocular irrigating solutions and barrier function of retinal pigment epithelium. *British Journal of Ophthalmology*, *81*(2), 150–153.
- Araie, M., & Maurice, D. M. (1991). The loss of fluorescein, fluorescein glucuronide and fluorescein isothiocyanate dextran from the vitreous by the anterior and retinal pathways. *Experimental Eye Research*, *52*(1), 27–39.
- Araújo, J., Nikolic, S., Egea, M. A., Souto, E. B., & Garcia, M. L. (2011). Nanostructured lipid carriers for triamcinolone acetonide delivery to the posterior segment of the eye. *Colloids and Surfaces B: Biointerfaces*, *88*(1), 150–157.
- Ascher, K. W. (1954). Veins of the aqueous humor in glaucoma. *Bolletino d'Oculistica*, *33*(3), 129–144.
- Augusteyn, R. C. (2007). Growth of the human eye lens. *Molecular Vision*, *13*(February), 252–257.
- Awwad, S., Mohamed Ahmed, A. H. A., Sharma, G., Heng, J. S., Khaw, P. T., Brocchini, S., & Lockwood, A. (2017). Principles of pharmacology in the eye. *British Journal of Pharmacology*, *174*(23), 4205–4223.
- Barar, J., Javadzadeh, A. R., & Omid, Y. (2008). Ocular novel drug delivery: Impacts of membranes and barriers. *Expert Opinion on Drug Delivery*, *5*(5), 567–581.
- Barathi, A., Thu, M. K., & Beuerman, R. W. (2002). Dimensional growth of the rabbit eye. *Cells Tissues Organs*, *171*(4), 276–285.
- Batchelor, T. T., Duda, D. G., Di Tomaso, E., Ancukiewicz, M., Plotkin, S. R., Gerstner, E., Eichler, A. F., Drappatz, J., Hochberg, F. H., Benner, T., Louis, D. N., Cohen, K. S., Chea, H., Exarhopoulos, A., Loeffler, J. S., Moses, M. A., Ivy, P., Sorensen, A. G., Wen, P. Y., & Jain, R. K. (2010). Phase II study of cediranib, an oral pan-vascular endothelial growth factor receptor tyrosine kinase inhibitor, in patients with recurrent glioblastoma. *Journal of Clinical Oncology*, *28*(17), 2817–2823.

- Beljanski, V. (2007). Bevacizumab. *XPharm: The Comprehensive Pharmacology Reference*, 1–6.
- Bennion, B. J., Be, N. A., McNerney, M. W., Lao, V., Carlson, E. M., Valdez, C. A., Malfatti, M. A., Enright, H. A., Nguyen, T. H., Lightstone, F. C., & Carpenter, T. S. (2017). Predicting a Drug's Membrane Permeability: A Computational Model Validated with in Vitro Permeability Assay Data. *Journal of Physical Chemistry B*, 121(20), 5228–5237.
- Bergström, C. A. S., & Larsson, P. (2018). Computational prediction of drug solubility in water-based systems: Qualitative and quantitative approaches used in the current drug discovery and development setting. *International Journal of Pharmaceutics*, 540(1–2), 185–193.
- Bhal, S. K. (2019). Understanding When to Use Log P & Log D. *ACD/Labs - Advanced Chemistry Development, Inc. Toronto, Canada.*, 3–6.
- Bill, A., & Helsing, K. (1965). Production and drainage of aqueous humor in the cynomolgus monkey (*Macaca irus*). *Investigative Ophthalmology and Visual Science*, 4(5), 920–926.
- Boddu, S., Gupta, H., & Patel, S. (2014). Drug Delivery to the Back of the Eye Following Topical Administration: An Update on Research and Patenting Activity. *Recent Patents on Drug Delivery & Formulation*, 8(1), 27–36.
- Bohley, M., Haunberger, A., & Goepferich, A. M. (2019). Intracellular availability of poorly soluble drugs from lipid nanocapsules. *European Journal of Pharmaceutics and Biopharmaceutics*, 139(December 2018), 23–32.
- Boote, C., Sigal, I. A., Grytz, R., Hua, Y., Nguyen, T. D., & Girard, M. J. A. (2020). Scleral structure and biomechanics. *Progress in Retinal and Eye Research*, 74(August).
- Borges- Giampani, A. S., & Giampani, J. (2013). Anatomy of Ciliary Body, Ciliary Processes, Anterior Chamber Angle and Collector Vessels. *Glaucoma - Basic and Clinical Aspects, figure 1*, 3–14.
- Borrás, T. (2014). The Cellular and Molecular Biology of the Iris, an Overlooked Tissue. *Journal of Glaucoma*, S39–S42.
- Bowman, R. J. C., Cope, J., & Nischal, K. K. (2004). Ocular and systemic side effects of brimonidine 0.2% eye drops (Alphagan) in children. *Eye (London, England)*, 18(1), 24–26.
- Brodin, B., Steffansen, B., & Nielsen, C. U. (2010). Passive diffusion of drug substances: The concepts of flux and permeability. *Molecular Biopharmaceutics: Aspects of Drug Characterization, Drug Delivery and Dosage Form Evaluation*, 135–151.

- Bruculeri, M., Hammel, T., Harris, A., Malinovsky, V., & Martin, B. (1999). Regulation of intraocular pressure after water drinking. *Journal of Glaucoma*, 8(2), 111–116.
- Busse, D., Yakes, F. M., Lenferink, A. E. G., & Arteaga, C. L. (2001). Tyrosine kinase inhibitors: Rationale, mechanisms of action, and implications for drug resistance. *Seminars in Oncology*, 28(5 SUPPL. 16), 47–55.
- Cabral-Pacheco, G. A., Garza-Veloz, I., Castruita-De la Rosa, C., Ramirez-Acuña, J. M., Perez-Romero, B. A., Guerrero-Rodriguez, J. F., Martinez-Avila, N., & Martinez-Fierro, M. L. (2020). The Roles of Matrix Metalloproteinases and Their Inhibitors in Human Diseases. *International Journal of Molecular Sciences*, 21(24).
- Campbell, D. J. (2014). Clinical relevance of local renin angiotensin systems. *Frontiers in Endocrinology*, 5(JUL), 1–5.
- Cantor, L. B. (2000). The evolving pharmacotherapeutic profile of brimonidine, an alpha 2-adrenergic agonist, after four years of continuous use. *Expert Opinion on Pharmacotherapy*, 1(4), 815–834.
- Cantor, L. B. (2006). Brimonidine in the treatment of glaucoma and ocular hypertension. *Therapeutics and Clinical Risk Management*, 2(4), 337–346.
- Caspar, K. R., Biggemann, M., Geissmann, T., & Begall, S. (2021). Ocular pigmentation in humans, great apes, and gibbons is not suggestive of communicative functions. *Scientific Reports*, 11(1).
- Chen, G., Shen, Z., & Li, Y. (2020). A machine-learning-assisted study of the permeability of small drug-like molecules across lipid membranes. *Physical Chemistry Chemical Physics*, 22(35), 19687–19696.
- Chen, H. (2015). Recent developments in ocular drug delivery. *Journal of Drug Targeting*, 23(7–8), 597–604.
- Cheng, T., Li, J., Cheng, Y., Zhang, X., & Qu, Y. (2019). Triamcinolone acetonide-chitosan coated liposomes efficiently treated retinal edema as eye drops. *Experimental Eye Research*, 188(April).
- Cheruvu, N. P. S., & Kompella, U. B. (2006). Bovine and Porcine Transscleral Solute Transport. *Investigative Ophthalmology & Visual Science*, 47(10), 1–7.
- Chiang, C. H., Ho, J. I., & Chen, J. L. (1996). Pharmacokinetics and intraocular pressure lowering effect of timolol preparations in rabbit eyes. *Journal of Ocular Pharmacology and Therapeutics*, 12(4), 471–480.
- Cholkar, K., Dasari, S. R., Pal, D., & Mitra, A. K. (2013). Eye: Anatomy, physiology and barriers to drug delivery. In *Ocular Transporters and Receptors: Their Role in Drug Delivery*.

- Choy, Y. Bin, & Prausnitz, M. R. (2011). The rule of five for non-oral routes of drug delivery: Ophthalmic, inhalation and transdermal. *Pharmaceutical Research*, 28(5), 943–948.
- Choy, Y. Bin, Ryu, W. M., Kim, S. N., & Min, C. H. (2019). Dry tablet formulation of plga nanoparticles with a preocular applicator for topical drug delivery to the eye. *Pharmaceutics*, 11(12).
- Choy, E. P. Y., To, T. S. S., Cho, P., Benzie, I. F. F., & Choy, C. K. M. (2004). Viability of porcine corneal epithelium ex vivo and effect of exposure to air: A pilot study for a dry eye model. *Cornea*, 23(7), 715–719.
- Civan, M. M., & Macknight, A. D. C. (2004). The ins and outs of aqueous humour secretion. *Experimental Eye Research*, 78(3), 625–631.
- Collantes, E. R., Tong, W., Welsh, W. J., & Zielinski, W. L. (1996). Use of moment of inertia in comparative molecular field analysis to model chromatographic retention of nonpolar solutes. *Analytical Chemistry*, 68(13), 2038–2043.
- Coons, S. J., Sheahan, S. L., Martin, S. S., Hendricks, J., Robbins, C. A., & Johnson, J. A. (1994). Predictors of medication noncompliance in a sample of older adults. *Clinical Therapeutics*, 16(1), 110–117.
- Cruysberg, L. P. J., Nuijts, R. M. M. A., Gilbert, J. A., Geroski, D. H., Hendrikse, F., & Edelhauser, H. F. (2005). In vitro sustained human transscleral drug delivery of fluorescein-labeled dexamethasone and methotrexate with fibrin sealant. *Current Eye Research*, 30(8), 653–660.
- Cullinane, A. B., Leung, P. S., Ortego, J., Coca-Prados, M., & Harvey, B. J. (2002). Renin-angiotensin system expression and secretory function in cultured human ciliary body non-pigmented epithelium. *The British Journal of Ophthalmology*, 86(6), 676–683.
- Danel, D. P., Waciewicz, S., Lewandowski, Z., Żywicznyński, P., & Perea-Garcia, J. O. (2018). Humans do not perceive conspecifics with a greater exposed sclera as more trustworthy: a preliminary cross-ethnic study of the function of the overexposed human sclera. *Acta Ethologica*, 21(3), 203–208.
- De Groef, L., Van Hove, I., Dekeyser, E., Stalmans, I., & Moons, L. (2013). MMPs in the trabecular meshwork: promising targets for future glaucoma therapies? *Investigative Ophthalmology & Visual Science*, 54(12), 7756–7763.
- del Amo, E. M. (2015). *Ocular and systemic pharmacokinetic models for drug discovery and development* [University of Helsinki].
- Delamere, N. A. (2005). Ciliary Body and Ciliary Epithelium. *Advanced Organ Biology*, 1(10), 127–148.

- Deng, F., Ranta, V. P., Kidron, H., & Urtti, A. (2016). General Pharmacokinetic Model for Topically Administered Ocular Drug Dosage Forms. *Pharmaceutical Research*, 33(11), 2680–2690.
- Dietrich, J., Wang, D., & Batchelor, T. T. (2009). Cediranib - Profile of a novel anti-angiogenic agent in patients with glioblastoma. *Expert Opinion on Investigational Drugs*, 18(10), 1549–1557.
- Dinslage, S., McLaren, J., & Brubaker, R. (1998). Intraocular pressure in rabbits by telemetry II: Effects of animal handling and drugs. *Investigative Ophthalmology and Visual Science*, 39(12), 2485–2489.
- Djebli, N., Khier, S., Griguer, F., Coutant, A. L., Tavernier, A., Fabre, G., Leriche, C., & Fabre, D. (2017). Ocular Drug Distribution After Topical Administration: Population Pharmacokinetic Model in Rabbits. *European Journal of Drug Metabolism and Pharmacokinetics*, 42(1), 59–68.
- Downie, L. E., Vessey, K., Miller, A., Ward, M. M., Pianta, M. J., Vingrys, A. J., Wilkinson-Berka, J. L., & Fletcher, E. L. (2009). Neuronal and glial cell expression of angiotensin II type 1 (AT1) and type 2 (AT2) receptors in the rat retina. *Neuroscience*, 161(1), 195–213.
- Durairaj, C. (2017). Ocular Pharmacokinetics. In *Handbook of Experimental Pharmacology* (Issue January, pp. 31–55).
- Edelhauser, H. F., Rowe-Rendleman, C. L., Robinson, M. R., Dawson, D. G., Chader, G. J., Grossniklaus, H. E., Rittenhouse, K. D., Wilson, C. G., Weber, D. A., Kuppermann, B. D., Csaky, K. G., Olsen, T. W., Kompella, U. B., Holers, V. M., Hageman, G. S., Gilger, B. C., Campochiaro, P. A., Whitcup, S. M., & Wong, W. T. (2010). Ophthalmic Drug Delivery Systems for the Treatment of Retinal Diseases: Basic Research to Clinical Applications. *Investigative Ophthalmology & Visual Science*, 51(11), 5403.
- Edwards, A., & Prausnitz, M. R. (1998). Fiber Matrix Model of Sclera and Corneal Stroma for Drug Delivery to the Eye. *AIChE Journal*, 44(1), 214–225.
- Edwards, A., & Prausnitz, M. R. (2001). Predicted permeability of the cornea to topical drugs. *Pharmaceutical Research*, 18(11), 1497–1508.
- Ekström, P., Paquet-Durand, F., Gaillard, P., Marigo, V., Genieser, H. G., Rentsch, A., Trifunović, D., & Tekgoz, A. S. (2019). *Targeted liposomal delivery of cGMP analogues*.
- Falavarjani, K. G., & Nguyen, Q. D. (2013). Adverse events and complications associated with intravitreal injection of anti-VEGF agents: A review of literature. *Eye (Basingstoke)*, 27(7), 787–794.
- Formica, M. L., Ullio Gamboa, G. V., Tártara, L. I., Luna, J. D., Benoit, J. P., & Palma, S. D. (2020). Triamcinolone acetonide-loaded lipid nanocapsules for ophthalmic applications. *International Journal of Pharmaceutics*, 573(June 2019), 118795.

- Franz, T. J. (1975). Percutaneous absorption. On the relevance of in vitro data. *Journal of Investigative Dermatology*, 64(3), 190–195.
- Friend, D. R. (1992). In vitro skin permeation techniques. *Journal of Controlled Release*, 18(3), 235–248.
- Frisch, H. L. (1957). The time lag in diffusion. *Journal of Physical Chemistry*, 61(1), 93–95.
- Fuchs, H., & Igney, F. (2017). Binding to Ocular Albumin as a Half-Life Extension Principle for Intravitreally Injected Drugs: Evidence from Mechanistic Rat and Rabbit Studies. *Journal of Ocular Pharmacology and Therapeutics*, 33(2), 115–122.
- Gaballa, S. A., El Garhy, O. H., Moharram, H., & Abdelkader, H. (2020). Preparation and Evaluation of Cubosomes/Cubosomal Gels for Ocular Delivery of Beclomethasone Dipropionate for Management of Uveitis. *Pharmaceutical Research*, 37(10).
- Gaudana, R., Ananthula, H. K., Parenky, A., & Mitra, A. K. (2010). Ocular drug delivery. *The AAPS Journal*, 12(3), 348–360.
- Geroski, D. H., & Edelhauser, H. F. (2001). Transscleral drug delivery for posterior segment disease. *Advanced Drug Delivery Reviews*, 52(1), 37–48.
- Ghate, D., & Edelhauser, H. F. (2006). Ocular drug delivery. *Expert Opinion on Drug Delivery*, 3(2), 275–287.
- Gisladottir, S., Loftsson, T., & Stefansson, E. (2009). Diffusion characteristics of vitreous humour and saline solution follow the Stokes Einstein equation. *Graefe's Archive for Clinical and Experimental Ophthalmology*, 247(12), 1677–1684.
- Goel, M. (2010). Aqueous Humor Dynamics: A Review. *The Open Ophthalmology Journal*, 4(1), 52–59.
- Goel, M., Picciani, R. G., Lee, R. K., & Bhattacharya, S. K. (2010). Aqueous humor dynamics: a review. *The Open Ophthalmology Journal*, 4, 52–59.
- Göktürk, S., Çalişkan, E., Talman, R. Y., & Var, U. (2012). A study on solubilization of poorly soluble drugs by cyclodextrins and micelles: Complexation and binding characteristics of sulfamethoxazole and trimethoprim. *The Scientific World Journal*, 2012.
- Gorthy, W. C., Snaveley, M. R., & Berrong, N. D. (1971). Some aspects of transport and digestion in the lens of the normal young adult rat. *Experimental Eye Research*, 12(1), 112–119.
- Grant, W. M. (1963). Experimental Aqueous Perfusion in Enucleated Human Eyes. *Archives of Ophthalmology*, 69(6), 783–801.

- Gupta, A., Nayak, K., & Misra, M. (2019). Cow ghee fortified ocular topical microemulsion; in vitro, ex vivo, and in vivo evaluation. *Journal of Microencapsulation*, 36(7), 603–621.
- Hahne, M., Zorn-Kruppa, Mi., Guzman, G., Brandner, J. M., Haltner-Ukomado, E., Wätzig, H., & Reichl, S. (2012). Prevalidation of a Human Cornea Construct as an Alternative to Animal Corneas for InVitro Drug Absorption Studies. *Journal of Pharmaceutical Sciences*, 101(8), 2976–2988.
- Hämäläinen, K. M., Kananen, K., Auriola, S., Kontturi, K., & Urtti, A. (1997). Characterization of paracellular and aqueous penetration routes in cornea, conjunctiva, and sclera. *Investigative Ophthalmology and Visual Science*, 38(3), 627–634.
- Heikkinen, A. T., Korjamo, T., & Mönkkönen, J. (2010). Modelling of drug disposition kinetics in in vitro intestinal absorption cell models. *Basic and Clinical Pharmacology and Toxicology*, 106(3), 180–188.
- Hejtmancik, J. F., & Shiels, A. (2015). Overview of the Lens. *Progress in Molecular Biology and Translational Science*, 134, 119–127.
- Hennequin, L. F., Thomas, A. P., Johnstone, C., Stokes, E. S. E., Plé, P. A., Lohmann, J. J. M., Ogilvie, D. J., Dukes, M., Wedge, S. R., Curwen, J. O., Kendrew, J., & Lambert-Van Der Brempt, C. (1999). Design and structure-activity relationship of a new class of potent VEGF receptor tyrosine kinase inhibitors. *Journal of Medicinal Chemistry*, 42(26), 5369–5389.
- Heys, J. J., & Barocas, V. H. (2002). A Boussinesq model of natural convection in the human eye and the formation of Krukenberg's spindle. *Annals of Biomedical Engineering*, 30(3), 392–401.
- Holappa, M., Vapaatalo, H., & Vaajanen, A. (2015). *World Journal of Ophthalmology* © 2015. 5(3), 110–125.
- Holappa, M., Vapaatalo, H., & Vaajanen, A. (2020a). Local ocular renin–angiotensin–aldosterone system: any connection with intraocular pressure? A comprehensive review. *Annals of Medicine*, 0(0), 000.
- Holappa, M., Vapaatalo, H., & Vaajanen, A. (2020b). Local ocular renin-angiotensin-aldosterone system: any connection with intraocular pressure? A comprehensive review. *Annals of Medicine*, 52(5), 191–206.
- Honda, M., Asai, T., Oku, N., Araki, Y., Tanaka, M., & Ebihara, N. (2013). Liposomes and nanotechnology in drug development: Focus on ocular targets. *International Journal of Nanomedicine*, 8(May 2014), 495–504.
- Hoon, M., Okawa, H., Della Santina, L., & Wong, R. O. L. (2014). Functional architecture of the retina: Development and disease. *Progress in Retinal and Eye Research*, 42(i), 44–84.

- Huang, D., Chen, Y. S., & Rupenthal, I. D. (2018). Overcoming ocular drug delivery barriers through the use of physical forces. In *Advanced Drug Delivery Reviews* (Vol. 126).
- Hubatsch, I., Ragnarsson, E. G. E., & Artursson, P. (2007). Determination of drug permeability and prediction of drug absorption in Caco-2 monolayers. *Nature Protocols*, 2(9), 2111–2119.
- Jackson, T. L., Antcliff, R. J., Hillenkamp, J., & Marshall, J. (2003). Human retinal molecular weight exclusion limit and estimate of species variation. *Investigative Ophthalmology and Visual Science*, 44(5), 2141–2146.
- Jansook, P., Muankaew, C., Stefánsson, E., & Loftsson, T. (2015). Development of eye drops containing antihypertensive drugs: Formulation of aqueous irbesartan/ γ CD eye drops. *Pharmaceutical Development and Technology*, 20(5), 626–632.
- Jansook, P., Stefánsson, E., Thorsteinsdóttir, M., Sigurdsson, B. B., Kristjánsdóttir, S. S., Bas, J. F., Sigurdsson, H. H., & Loftsson, T. (2010). Cyclodextrin solubilization of carbonic anhydrase inhibitor drugs: Formulation of dorzolamide eye drop microparticle suspension. *European Journal of Pharmaceutics and Biopharmaceutics*, 76(2), 208–214.
- Jayanetti, V., Sandhu, S., & Lusthaus, J. A. (2020). The Latest Drugs in Development That Reduce Intraocular Pressure in Ocular Hypertension and Glaucoma. *Journal of Experimental Pharmacology*, 12, 539–548.
- Johannsdóttir, S., Jansook, P., Stefansson, E., Kristinsdóttir, I. M., Fulop, Z., Asgrimsdóttir, G. M., Thorsteinsdóttir, M., Eiriksson, F. F., & Loftsson, T. (2018a). Topical drug delivery to the posterior segment of the eye: Dexamethasone concentrations in various eye tissues after topical administration for up to 15 days to rabbits. *Journal of Drug Delivery Science and Technology*, 45(April), 449–454.
- Johannsdóttir, S., Jansook, P., Stefansson, E., Kristinsdóttir, I. M., Fulop, Z., Asgrimsdóttir, G. M., Thorsteinsdóttir, M., Eiriksson, F. F., & Loftsson, T. (2018b). Topical drug delivery to the posterior segment of the eye: Dexamethasone concentrations in various eye tissues after topical administration for up to 15 days to rabbits. *Journal of Drug Delivery Science and Technology*, 45.
- Johnson, M. (2006). “What controls aqueous humour outflow resistance?”. *Experimental Eye Research*, 82(4), 545–557.
- Johnson, M., & Erickson, K. (2000). Mechanisms and routes of aqueous humor drainage. In D. M. Albert, & F. A. Jakobiec (Eds.), *Principles and Practice of Ophthalmology*. WB Saunders Co.
- Juretić, M., Cetina-Čižmek, B., Filipović-Grčić, J., Hafner, A., Lovrić, J., & Pepić, I. (2018). Biopharmaceutical evaluation of surface active ophthalmic excipients using in vitro and ex vivo corneal models. *European Journal of Pharmaceutical Sciences*, 120(November 2017), 133–141.

- Kadam, R. S., Cheruvu, N. P. S., Edelhauser, H. F., & Kompella, U. B. (2011). Sclera-choroid-RPE transport of eight β -blockers in human, bovine, porcine, rabbit, and rat models. *Investigative Ophthalmology and Visual Science*, 52(8), 5387–5399.
- Käsdorf, B. T., Arends, F., & Lieleg, O. (2015). Diffusion Regulation in the Vitreous Humor. *Biophysical Journal*, 109(10), 2171–2181.
- Keller, K. E., & Acott, T. S. (2013). The Juxtacanalicular Region of Ocular Trabecular Meshwork: A Tissue with a Unique Extracellular Matrix and Specialized Function. *Journal of Ocular Biology*, 1(1), 3.
- Kels, B. D., Grzybowski, A., & Grant-Kels, J. M. (2015). Human ocular anatomy. *Clinics in Dermatology*, 33(2), 140–146.
- Khalil, R. M., Abdelbary, G. A., Basha, M., Awad, G. E. A., & el-Hashemy, H. A. (2017). Enhancement of lomefloxacin Hcl ocular efficacy via niosomal encapsulation: in vitro characterization and in vivo evaluation. *Journal of Liposome Research*, 27(4), 312–323.
- Khier, S., Griguer, F., Tavernier, A., Leriche, C., Djebli, N., Coutant, A.-L., Fabre, G., & Fabre, D. (2016). Ocular Drug Distribution After Topical Administration: Population Pharmacokinetic Model in Rabbits. *European Journal of Drug Metabolism and Pharmacokinetics*, 42(1), 59–68.
- Kidron, H., Vellonen, K. S., Del Amo, E. M., Tissari, A., & Urtti, A. (2010). Prediction of the corneal permeability of drug-like compounds. *Pharmaceutical Research*, 27(7), 1398–1407.
- Kim, D., Pattamatta, U., Kelly, E., Healey, P. R., Carnt, N., Zoellner, H., & White, A. J. R. (2018). Inhibitory Effects of Angiotensin II Receptor Blockade on Human Tenon Fibroblast Migration and Reactive Oxygen Species Production in Cell Culture. *Translational Vision Science & Technology*, 7(2), 20.
- Kim, S. H., Lutz, R. J., Wang, N. S., & Robinson, M. R. (2007). Transport barriers in transscleral drug delivery for retinal diseases. *Ophthalmic Research*, 39(5), 244–254.
- Kobayashi, H., & Kohshima, S. (1997). Unique morphology of the human eye. *Nature*, 387(1992), 766–767.
- Kobayashi, H., & Kohshima, S. (2001). Unique morphology of the human eye and its adaptive meaning: Comparative studies on external morphology of the primate eye. *Journal of Human Evolution*, 40(5), 419–435.
- Kolb, H. (1995). Simple Anatomy of the Retina. *Webvision: The Organization of the Retina and Visual System*, 1–24.
- Kratz, J. M., Teixeira, M. R., Koester, L. S., & Simões, C. M. O. (2011). An HPLC-UV method for the measurement of permeability of marker drugs in the Caco-2 cell assay. *Brazilian Journal of Medical and Biological Research*, 44(6), 531–537.

- Krishnamoorthy, M. K., Park, J., Augsburger, J. J., & Banerjee, R. K. (2008). Effect of retinal permeability, diffusivity, and aqueous humor hydrodynamics on pharmacokinetics of drugs in the eye. *Journal of Ocular Pharmacology and Therapeutics*, 24(3), 255–267.
- la Cour, M., & Tezel, T. (2005). The Retinal Pigment Epithelium. *Advances in Organ Biology*, 10(15), 253–272.
- Lacy, S. A., Miles, D. R., & Nguyen, L. T. (2017). Clinical Pharmacokinetics and Pharmacodynamics of Cabozantinib. *Clinical Pharmacokinetics*, 56(5), 477–491.
- Lajunen, T., Hisazumi, K., Kanazawa, T., Okada, H., Seta, Y., Yliperttula, M., Urtti, A., & Takashima, Y. (2014). Topical drug delivery to retinal pigment epithelium with microfluidizer produced small liposomes. *European Journal of Pharmaceutical Sciences*, 62, 23–32.
- Lakhani, P., Akash, P., Wu, K.-W., Sweeney, C., Tripathi, S., Avula, B., Taskar, P., Khan, S., & Majumdar, S. (2020). Optimization, stabilization, and characterization of amphotericin B loaded nanostructured lipid carriers for ocular drug delivery. *International Journal Of Pharmaceutical*, 572(118771).
- Ledermann, J. A., Embleton, A. C., Raja, F., Perren, T. J., Jayson, G. C., Rustin, G. J. S., Kaye, S. B., Hirte, H., Eisenhauer, E., Vaughan, M., Friedlander, M., González-Martín, A., Stark, D., Clark, E., Farrelly, L., Swart, A. M., Cook, A., Kaplan, R. S., & Parmar, M. K. B. (2016). Cediranib in patients with relapsed platinum-sensitive ovarian cancer (ICON6): a randomised, double-blind, placebo-controlled phase 3 trial. *Lancet (London, England)*, 387(10023), 1066–1074.
- Lin, C., Stone, R. A., & Wax, M. B. (1990). Angiotensin binding sites in rabbit anterior uvea and human ciliary epithelial cells. *Investigative Ophthalmology & Visual Science*, 31(1), 147–152.
- Lipinski, C., Lombardo, F., Dominy, B., & Feeney, P. (1997). Experimental and computational approaches to estimate solubility and permeability in drug discovery and development settings. *Advanced Drug Delivery Reviews*, 23, 3–25.
- Loch, C., Zakelj, S., Kristl, A., Nagel, S., Guthoff, R., Weitschies, W., & Seidlitz, A. (2012). Determination of permeability coefficients of ophthalmic drugs through different layers of porcine, rabbit and bovine eyes. *European Journal of Pharmaceutical Sciences*, 47(1), 131–138.
- Lofsson, T., & Stefánsson, E. (2002). Cyclodextrins in eye drop formulations: Enhanced topical delivery of corticosteroids to the eye. *Acta Ophthalmologica Scandinavica*, 80(2), 144–150.
- Lofsson, T., & Stefánsson, E. (2017). Cyclodextrins and topical drug delivery to the anterior and posterior segments of the eye. *International Journal of Pharmaceutics*, 531(2), 413–423.

- Lorenzo-Soler, L., Olafsdottir, O. B., Garhöfer, G., Jansook, P., Kristinsdottir, I. M., Tan, A., Loftsson, T., & Stefansson, E. (2021). Angiotensin Receptor Blockers in cyclodextrin nanoparticle eye drops: Ocular pharmacokinetics and pharmacologic effect on intraocular pressure. *Acta Ophthalmologica*, 99(4), 376–382.
- Lorenzo-Soler, L., Praphanwittaya, P., Olafsdottir, O. B., Kristinsdottir, I. M., Asgrimsdottir, G. M., Loftsson, T., & Stefansson, E. (2022). Topical noninvasive retinal drug delivery of a tyrosine kinase inhibitor: 3% cediranib maleate cyclodextrin nanoparticle eye drops in the rabbit eye. *Acta Ophthalmologica*, 1–9.
- Ma, D., Chen, C. B., Liang, J., Lu, Z., Chen, H., & Zhang, M. (2016). Repeatability, reproducibility and agreement of intraocular pressure measurement in rabbits by the TonoVet and Tono-Pen. *Scientific Reports*, 6(October), 1–7.
- Mälkiä, A., Murtomäki, L., Urtti, A., & Kontturi, K. (2004). Drug permeation in biomembranes: In vitro and in silico prediction and influence of physicochemical properties. *European Journal of Pharmaceutical Sciences*, 23(1), 13–47.
- Mangas-Sanjuan, V., González-Álvarez, I., González-Álvarez, M., Casabó, V. G., & Bermejo, M. (2014). Modified nonsink equation for permeability estimation in cell monolayers: Comparison with standard methods. *Molecular Pharmaceutics*, 11(5), 1403–1414.
- Marino, M., Jamal, Z., & Zito, P. M. (2022). *Pharmacodynamics*. StatPearls [Internet].
- Matthyssen, S., Van den Bogerd, B., Dhubhghaill, S. N., Koppen, C., & Zakaria, N. (2018). Corneal regeneration: A review of stromal replacements. *Acta Biomaterialia*, 69(January), 31–41.
- Maurice, D. M., & Polgar, J. (1977). Diffusion across the sclera. *Experimental Eye Research*, 25(6), 577–582.
- McMenamin, P. G., & Steptoe, R. J. (1991). Normal anatomy of the aqueous humour outflow system in the domestic pig eye. *Journal of Anatomy*, 178, 65–77.
- Miao, H., Wu, B. D., Tao, Y., & Li, X. X. (2013). Diffusion of macromolecules through sclera. *Acta Ophthalmologica*, 91(1), 1–6.
- Miyamoto, S., & Shimono, K. (2020). Molecular Modeling to Estimate the Diffusion Coefficients of Drugs and Other Small Molecules. *Molecules (Basel, Switzerland)*, 25(22).
- Mohammadian, M., Salami, M., Emam-Djomeh, Z., & Alavi, F. (2017). Nutraceutical properties of dairy bioactive peptides. *Dairy in Human Health and Disease across the Lifespan*, December, 325–342.
- Moiseev, R. V., Morrison, P. W. J., Steele, F., & Khutoryanskiy, V. V. (2019). Penetration enhancers in ocular drug delivery. *Pharmaceutics*, 11(7).

- Moisseiev, E., & Loewenstein, A. (2017a). Drug delivery to the posterior segment of the eye. *Developments in Ophthalmology*, *58*, 87–101.
- Moisseiev, E., & Loewenstein, A. (2017b). Drug delivery to the posterior segment of the eye. *Developments in Ophthalmology*, *58*(5–6), 87–101.
- Moisseiev, E., & Loewenstein, A. (2019). INTRAVITREAL INJECTION - A SMALL PROCEDURE FOR THE EYE, A GIANT LEAP FOR OPHTHALMOLOGY. *The Israel Medical Association Journal*, *158*(2), 121–125.
- Molday, R. S., & Moritz, O. L. (2015). Photoreceptors at a glance. *Journal of Cell Science*, *128*(22), 4039–4045.
- Morrison, P. W. J., Connon, C. J., & Khutoryanskiy, V. V. (2013). Cyclodextrin-mediated enhancement of riboflavin solubility and corneal permeability. *Molecular Pharmaceutics*, *10*(2), 756–762.
- Muankaew, C., Jansook, P., Stefánsson, E., & Loftsson, T. (2014). Effect of γ -cyclodextrin on solubilization and complexation of irbesartan: Influence of pH and excipients. *International Journal of Pharmaceutics*, *474*(1–2), 80–90.
- Murgatroyd, H., & Bembridge, J. (2008). Intraocular pressure. *Continuing Education in Anaesthesia, Critical Care and Pain*, *8*(3), 100–103.
- Murthy, K. R., Goel, R., Subbannayya, Y., Jacob, H. K. C., Murthy, P. R., Manda, S. S., Patil, A. H., Sharma, R., Sahasrabuddhe, N. A., Parashar, A., Nair, B. G., Krishna, V., Prasad, T. S. K., Gowda, H., & Pandey, A. (2014). Proteomic analysis of human vitreous humor. *Clinical Proteomics*, *11*(1), 1–11.
- Navarro-Partida, J., Altamirano-Vallejo, J. C., Rosa, A. G. D. la, Armendariz-Borunda, J., Castro-Castaneda, C. R., & Santos, A. (2021). Safety and tolerability of topical ophthalmic triamcinolone acetone-loaded liposomes formulation and evaluation of its biologic activity in patients with diabetic macular edema. *Pharmaceutics*, *13*(3), 1–17.
- Navarro-Partida, J., Castro-Castaneda, C. R., Cruz-Pavlovich, F. J. S., Aceves-Franco, L. A., Guy, T. O., & Santos, A. (2021). Lipid-based nanocarriers as topical drug delivery systems for intraocular diseases. *Pharmaceutics*, *13*(678), 1–25.
- Nesterova, A. P., Klimov, E. A., Zharkova, M., Sozin, S., Sobolev, V., Ivanikova, N. V., Shkrob, M., & Yuryev, A. (2020). Diseases of the eye. In *Disease Pathways* (pp. 259–296). Elsevier.
- Nickla, D. L., & Wallman, J. (2010). The multifunctional choroid. *Prog.Retin.Eye Res.*, *29*(2), 144–168.
- Nicoli, S., Ferrari, G., Quarta, M., Macaluso, C., Govoni, P., Dallatana, D., & Santi, P. (2009). Porcine sclera as a model of human sclera for in vitro transport experiments: histology, SEM, and comparative permeability. *Molecular Vision*, *15*(November 2008), 259–266.

- Niedorf, F., Schmidt, E., & Kietzmann, M. (2008). The automated, accurate and reproducible determination of steady-state permeation parameters from percutaneous permeation data. *ATLA Alternatives to Laboratory Animals*, 36(2), 201–213.
- Noecker, R. J. (2006). The management of glaucoma and intraocular hypertension: current approaches and recent advances. *Therapeutics and Clinical Risk Management*, 2(2), 193–206.
- Olsen, T. W., Edelhauser, H. F., Lim, J. I., & Geroski, D. H. (1995). Human scleral permeability: Effects of age, cryotherapy, transscleral diode laser, and surgical thinning. *Investigative Ophthalmology and Visual Science*, 36(9), 1893–1903.
- Olsen, T. W., Sanderson, S., Feng, X., & Hubbard, W. C. (2002). Porcine sclera: Thickness and surface area. *Investigative Ophthalmology and Visual Science*, 43(8), 2529–2532.
- Overby, D. R., Stamer, W. D., & Johnson, M. (2009). The changing paradigm of outflow resistance generation: towards synergistic models of the JCT and inner wall endothelium. *Experimental Eye Research*, 88(4), 656–670.
- Patel, A., Cholkar, K., Agrahari, V., & Mitra, A. K. (2013). Ocular drug delivery systems: An overview. *World Journal of Pharmacology*, 2(2), 47–64.
- Patel, S. C., & Spaeth, G. L. (1995). Compliance in patients prescribed eyedrops for glaucoma. *Ophthalmic Surgery*, 26(3), 233–236.
- Pescina, S., Govoni, P., Potenza, A., Padula, C., Santi, P., & Nicoli, S. (2015). Development of a convenient ex vivo model for the study of the transcorneal permeation of drugs: Histological and permeability evaluation. *Journal of Pharmaceutical Sciences*, 104(1), 63–71.
- Pescina, S., Santi, P., Ferrari, G., Padula, C., Cavallini, P., Govoni, P., & Nicoli, S. (2012). Ex vivo models to evaluate the role of ocular melanin in trans-scleral drug delivery. *European Journal of Pharmaceutical Sciences*, 46(5), 475–483.
- Peyman, G. A., Lad, E. M., & Moshfeghi, D. M. (2009). Intravitreal injection of therapeutic agents. *Retina*, 29(7), 875–912.
- Pitkänen, L., Ranta, V. P., Moilanen, H., & Urtti, A. (2005). Permeability of retinal pigment epithelium: Effects of permeant molecular weight and lipophilicity. *Investigative Ophthalmology and Visual Science*, 46(2), 641–646.
- Popov, A. (2020). Mucus-Penetrating Particles and the Role of Ocular Mucus as a Barrier to Micro- And Nanosuspensions. *Journal of Ocular Pharmacology and Therapeutics*, 36(6), 366–375.

- Praphanwittaya, P., Saokham, P., Jansook, P., & Loftsson, T. (2020). Aqueous solubility of kinase inhibitors: I the effect of hydrophilic polymers on their γ -cyclodextrin. *Journal of Drug Delivery Science and Technology*, 55(December 2019).
- Prasanna, M. R. (1998). Permeability of cornea, sclera, and conjunctiva: A literature analysis for drug delivery to the eye. *Journal of Pharmaceutical Sciences*, 87(12), 1479–1488.
- R. Sparrow, J., Hicks, D., & P. Hamel, C. (2010). The Retinal Pigment Epithelium in Health and Disease. *Current Molecular Medicine*, 10(9), 802–823.
- Radu, C. D., Parteni, O., & Ochiuz, L. (2016). Applications of cyclodextrins in medical textiles — review. *Journal of Controlled Release*, 224, 146–157.
- Ram, C. V. S. (2008). Angiotensin Receptor Blockers: Current Status and Future Prospects. *American Journal of Medicine*, 121(8), 656–663.
- Ramsay, E., del Amo, E. M., Toropainen, E., Tengvall-Unadike, U., Ranta, V. P., Urtti, A., & Ruponen, M. (2018a). Corneal and conjunctival drug permeability: Systematic comparison and pharmacokinetic impact in the eye. *European Journal of Pharmaceutical Sciences*, 119(April), 83–89.
- Ramsay, E., del Amo, E. M., Toropainen, E., Tengvall-Unadike, U., Ranta, V. P., Urtti, A., & Ruponen, M. (2018b). Corneal and conjunctival drug permeability: Systematic comparison and pharmacokinetic impact in the eye. *European Journal of Pharmaceutical Sciences*, 119(April), 83–89.
- Ramsay, E., Ruponen, M., Picardat, T., Tengvall, U., Tuomainen, M., Auriola, S., Toropainen, E., Urtti, A., & del Amo, E. M. (2017). Impact of Chemical Structure on Conjunctival Drug Permeability: Adopting Porcine Conjunctiva and Cassette Dosing for Construction of In Silico Model. *Journal of Pharmaceutical Sciences*, 106(9), 2463–2471.
- Ranta, V. P., & Urtti, A. (2006a). Transscleral drug delivery to the posterior eye: Prospects of pharmacokinetic modeling. *Advanced Drug Delivery Reviews*, 58(11), 1164–1181.
- Ranta, V. P., & Urtti, A. (2006b). Transscleral drug delivery to the posterior eye: Prospects of pharmacokinetic modeling. *Advanced Drug Delivery Reviews*, 58(11), 1164–1181.
- Reitsamer, H. A., Posey, M., & Kiel, J. W. (2006). Effects of a topical α_2 adrenergic agonist on ciliary blood flow and aqueous production in rabbits. *Experimental Eye Research*, 82(3), 405–415.
- Rimpelä, A. K., Reinisalo, M., Hellinen, L., Grazhdankin, E., Kidron, H., Urtti, A., & del Amo, E. M. (2018). Implications of melanin binding in ocular drug delivery. *Advanced Drug Delivery Reviews*, 126, 23–43.

- Rimpelä, A. K., Reunanen, S., Hagström, M., Kidron, H., & Urtti, A. (2018). Binding of Small Molecule Drugs to Porcine Vitreous Humor. *Molecular Pharmaceutics*, *15*(6), 2174–2179.
- Rizzolo, L. J. (2007). Development and Role of Tight Junctions in the Retinal Pigment Epithelium. *International Review of Cytology*, *258*(07), 195–234.
- Robinson, R. (1997). *Ocular pharmacokinetics/pharmacodynamics*. *44*(1627), 71–83.
- Romero, F. J., Nicolaissen, B., & Peris-Martinez, C. (2014). New Trends in Anterior Segment Diseases of the Eye. *Journal of Ophthalmology*, *2014*(5), 2012–2014.
- Salamanca, C. H., Barrera-Ocampo, A., Lasso, J. C., Camacho, N., & Yarce, C. J. (2018). Franz diffusion cell approach for pre-formulation characterisation of ketoprofen semi-solid dosage forms. *Pharmaceutics*, *10*(3), 1–10.
- Scahill, L. (2009). Alpha-2 adrenergic agonists in children with inattention, hyperactivity and impulsiveness. *CNS Drugs*, *23* Suppl 1, 43–49.
- Schoenwald, R. D., & Ward, R. L. (1978). Relationship between steroid permeability across excised rabbit cornea and octanol-water partition coefficients. *Journal of Pharmaceutical Sciences*, *67*(6), 786–788.
- Schwartz, S. D., Pan, C. K., Klimanskaya, I., & Lanza, R. (2013). Retinal Degeneration. In *Principles of Tissue Engineering: Fourth Edition* (Fourth Edi, Vol. 000). Elsevier.
- Sellick, J. (2011). Enhancing the protection of animals used for scientific purposes. In *Environmental Law and Management* (Vol. 23, Issue 2).
- Senanayake, P. deS, Drazba, J., Shadrach, K., Milsted, A., Rungger-Brandle, E., Nishiyama, K., Miura, S.-I., Karnik, S., Sears, J. E., & Hollyfield, J. G. (2007). Angiotensin II and its receptor subtypes in the human retina. *Investigative Ophthalmology & Visual Science*, *48*(7), 3301–3311.
- Shah, J. C. (1993). Analysis of permeation data: evaluation of the lag time method. *International Journal of Pharmaceutics*, *90*(2), 161–169.
- Shapiro, B., Dickersin, K., & Lietman, T. (2006). Trachoma, antibiotics and randomised controlled trials. *British Journal of Ophthalmology*, *90*(12), 1443–1444.
- Shastri, D., Shelat, P., Shukla, A., & Patel, P. (2010). Ophthalmic drug delivery system: Challenges and approaches. *Systematic Reviews in Pharmacy*, *1*(2), 113.
- Shi, S., Peng, F., Zheng, Q., Zeng, L., Chen, H., Li, X., & Huang, J. (2019). Micelle-solubilized axitinib for ocular administration in anti-neovascularization. *International Journal of Pharmaceutics*, *560*(December 2018), 19–26.
- Shibuya, M., & Claesson-Welsh, L. (2006). Signal transduction by VEGF receptors in regulation of angiogenesis and lymphangiogenesis. *Experimental Cell Research*, *312*(5), 549–560.


- Shih, R. L., & Lee, V. H. L. (1990). Rate Limiting Barrier to the Penetration of Ocular Hypotensive Beta Blockers Across the Corneal Epithelium in the Pigmented Rabbit. *Journal of Ocular Pharmacology*, 6(4), 329–336.
- Shikamura, Y., Yamazaki, Y., Matsunaga, T., Sato, T., Ohtori, A., & Tojo, K. (2016). Hydrogel Ring for Topical Drug Delivery to the Ocular Posterior Segment. *Current Eye Research*, 41(5), 653–661.
- Shin, K., Fogg, V. C., & Margolis, B. (2006). Tight Junctions and Cell Polarity. *Annual Review of Cell and Developmental Biology*, 22(1), 207–235.
- Shirasaki, Y. (2008). Molecular design for enhancement of ocular penetration. *Journal of Pharmaceutical Sciences*, 97(7), 2462–2496.
- Short, B. G. (2008). Safety Evaluation of Ocular Drug Delivery Formulations: Techniques and Practical Considerations. *Toxicologic Pathology*, 36(1), 49–62.
- Singh, M., Guzman-Aranguez, A., Hussain, A., Srinivas, C. S., & Kaur, I. P. (2019). Solid lipid nanoparticles for ocular delivery of isoniazid: Evaluation, proof of concept and in vivo safety & kinetics. *Nanomedicine*, 14(4), 465–491.
- Souza, J. G., Dias, K., Pereira, T. A., Bernardi, D. S., & Lopez, R. F. V. (2014). Topical delivery of ocular therapeutics: Carrier systems and physical methods. *Journal of Pharmacy and Pharmacology*, 66(4), 507–530.
- Sridhar, M. S. (2018). Anatomy of cornea and ocular surface. *Indian Journal of Ophthalmology*, 66(2), 190–194.
- Sunderland, D. K., & Sapra, A. (2022). *Physiology, Aqueous Humor Circulation*.
- Tahara, K., Karasawa, K., Onodera, R., & Takeuchi, H. (2017). Feasibility of drug delivery to the eye's posterior segment by topical instillation of PLGA nanoparticles. *Asian Journal of Pharmaceutical Sciences*, 12(4), 394–399.
- Tamm, E. R. (2009a). The trabecular meshwork outflow pathways: Structural and functional aspects. *Experimental Eye Research*, 88(4), 648–655.
- Tamm, E. R. (2009b). The trabecular meshwork outflow pathways. Functional morphology and surgical aspects. *Glaucoma*, 2, 31 – 44.
- Tamm, E. R., Braunger, B. M., & Fuchshofer, R. (2015). Chapter Eighteen - Intraocular Pressure and the Mechanisms Involved in Resistance of the Aqueous Humor Flow in the Trabecular Meshwork Outflow Pathways. In J. F. Hejtmancik & J. M. Nickerson (Eds.), *Molecular Biology of Eye Disease* (Vol. 134, pp. 301–314). Academic Press.
- Tatke, A., Dudhipala, N., Janga, K. Y., Balguri, S. P., Avula, B., Jablonski, M. M., & Majumdar, S. (2019). In situ gel of triamcinolone acetate-loaded solid lipid nanoparticles for improved topical ocular delivery: Tear kinetics and ocular disposition studies. *Nanomaterials*, 9(1), 1–17.

- Tavelin, S., Gråsjö, J., Taipalensuu, J., Ocklind, G., & Artursson, P. (2002a). Applications of epithelial cell culture in studies of drug transport. *Methods in Molecular Biology (Clifton, N.J.)*, 188, 233–272.
- Tavelin, S., Gråsjö, J., Taipalensuu, J., Ocklind, G., & Artursson, P. (2002b). Applications of epithelial cell culture in studies of drug transport. *Methods in Molecular Biology (Clifton, N.J.)*, 188, 233–272.
- Teixeira, L. de S., Chagas, T. V., Alonso, A., Gonzalez-alvarez, I., Bermejo, M., Polli, J., & Rezende, K. R. (2020). Biomimetic artificial membrane permeability assay over franz cell apparatus using bcs model drugs. *Pharmaceutics*, 12(10), 1–16.
- Thakur, A., Kadam, R. S., & Kompella, U. B. (2011). Influence of drug solubility and lipophilicity on transscleral retinal delivery of six corticosteroids. *Drug Metabolism and Disposition*, 39(5), 771–781.
- Thrimawithana, T. R., Young, S., Bunt, C. R., Green, C., & Alany, R. G. (2011). Drug delivery to the posterior segment of the eye. *Drug Discovery Today*, 16(5–6), 270–277.
- To, C. H., Kong, C. W., Chan, C. Y., Shahidullah, M., & Do, C. W. (2002). The mechanism of aqueous humour formation. *Clinical and Experimental Optometry*, 85(6), 335–349.
- Törnquist, P., Alm, A., & Anders, B. (1990). Permeability of Ocular Vessels and Transport Across the Blood-Retinal-Barrier. *Eye*, 4, 303–309.
- Touyz, R. M., & Berry, C. (2002). Recent advances in angiotensin II signaling. *Brazilian Journal of Medical and Biological Research*, 35(9), 1001–1015.
- Urmi, D., Widenbring, R., Pérez García, R. O., Gedda, L., Edwards, K., Loftsson, T., & Schipper, N. (2021). Formulation development and upscaling of lipid nanocapsules as a drug delivery system for a novel cyclic GMP analogue intended for retinal drug delivery. *International Journal of Pharmaceutics*, 602(April), 120640.
- Urtti, A., & Salminen, L. (1993). Minimizing systemic absorption of topically administered ophthalmic drugs. *Survey of Ophthalmology*, 37(6), 435–456.
- Vaajanen, A. (2009). *EXPRESSION AND FUNCTION OF ANGIOTENSINS IN THE REGULATION OF INTRAOCULAR PRESSURE - AN EXPERIMENTAL STUDY*. University of Helsinki.
- Van de Waterbeemd, H., Smith, D. A., Beaumont, K., & Walker, D. K. (2001). Property-based design: Optimization of drug absorption and pharmacokinetics. *Journal of Medicinal Chemistry*, 44(9), 1313–1333.

- van der Spek, P. J., Bergen, A. A., Jansonius, N. M., Janssen, S. F., & Gorgels, T. G. (2013). In silico analysis of the molecular machinery underlying aqueous humor production: potential implications for glaucoma. *Journal of Clinical Bioinformatics*, 3(1), 21.
- van Rodijnen, W. F., van Lambalgen, T. A., van Teijlingen, M. E., Tangelder, G.-J., & ter Wee, P. M. (2010). Comparison of the AT1-receptor blockers candesartan, irbesartan and losartan for inhibiting renal microvascular constriction. *Journal of the Renin-Angiotensin-Aldosterone System*, 2(1_suppl), S204–S210.
- Vighi, E., Trifunovic, D., Veiga-Crespo, P., Rentsch, A., Hoffmann, D., Sahaboglu, A., Strasser, T., Kulkarni, M., Bertolotti, E., Van Den Heuvel, A., Peters, T., Reijkerkerk, A., Euler, T., Ueffing, M., Schwede, F., Genieser, H. G., Gaillard, P., Marigo, V., Ekström, P., & Paquet-Durand, F. (2018). Combination of cGMP analogue and drug delivery system provides functional protection in hereditary retinal degeneration. *Proceedings of the National Academy of Sciences of the United States of America*, 115(13), E2997–E3006.
- Watson, P. G., & Young, R. D. (2004). Scleral structure, organisation and disease. A review. *Experimental Eye Research*, 78(3), 609–623.
- Wedge, S. R., Kendrew, J., Hennequin, L. F., Valentine, P. J., Barry, S. T., Brave, S. R., Smith, N. R., James, N. H., Dukes, M., Curwen, J. O., Chester, R., Jackson, J. A., Boffey, S. J., Kilburn, L. L., Barnett, S., Richmond, G. H. P., Wadsworth, P. F., Walker, M., Bigley, A. L., ... Ogilvie, D. J. (2005). AZD2171: A highly potent, orally bioavailable, vascular endothelial growth factor receptor-2 tyrosine kinase inhibitor for the treatment of cancer. *Cancer Research*, 65(10), 4389–4400.
- Wilson, S. E. (2020). Bowman's layer in the cornea— structure and function and regeneration. *Experimental Eye Research*, 195(April), 108033.
- Xu, J., Heys, J. J., Barocas, V. H., & Randolph, T. W. (2000). Permeability and diffusion in vitreous humor: Implications for drug delivery. *Pharmaceutical Research*, 17(6), 664–669.
- Xu, X., Sun, L., Zhou, L., Cheng, Y., & Cao, F. (2020). Functional chitosan oligosaccharide nanomicelles for topical ocular drug delivery of dexamethasone. *Carbohydrate Polymers*, 227(June 2019), 115356.
- Y. Zernii, E., E. Baksheeva, V., N. Iomdina, E., A. Averina, O., E. Permyakov, S., P. Philippov, P., A. Zamyatnin, A., & I. Senin, I. (2016). Rabbit Models of Ocular Diseases: New Relevance for Classical Approaches. *CNS & Neurological Disorders - Drug Targets*, 15(3), 267–291.
- Yellepeddi, V. K., & Palakurthi, S. (2016). Recent Advances in Topical Ocular Drug Delivery. *Journal of Ocular Pharmacology and Therapeutics*, 32(2), 67–82.
- Zimmerman, T. J. (1993). Topical ophthalmic beta blockers: a comparative review. *Journal of Ocular Pharmacology*, 9(4), 373–384.

Paper I

Angiotensin Receptor Blockers in cyclodextrin nanoparticle eye drops: Ocular pharmacokinetics and pharmacologic effect on intraocular pressure

Laura Lorenzo-Soler,¹  Olof Birna Olafsdottir,^{1,2,3} Gerhard Garhöfer,⁴ Phatsawee Jansook,⁵ Iris Myrdal Kristinsdottir,³ Aimin Tan,⁶ Thorsteinn Loftsson⁷ and Einar Stefansson^{1,2,3}

¹Faculty of Medicine, University of Iceland, Reykjavík, Iceland

²Department of Ophthalmology, Landspítali University Hospital, Reykjavík, Iceland

³Oculus ehf., Reykjavík, Iceland

⁴Department of Clinical Pharmacology, Medical University of Vienna, Vienna, Austria

⁵Faculty of Pharmaceutical Sciences, Chulalongkorn University, Bangkok, Thailand

⁶Nucro-Technics, Toronto, ON, Canada

⁷Faculty of Pharmacy, University of Iceland, Reykjavík, Iceland

ABSTRACT.

Purpose: Orally administered angiotensin II receptor blockers (ARBs) decrease intraocular pressure (IOP). Topical administration may reduce systemic side effects and result in a useful glaucoma drug. The aim of this study is to test the ocular delivery and pharmacologic effect of nanoparticle eye drops containing ARBs (e.g. irbesartan and candesartan).

Methods: 1.5% irbesartan and 0.15% candesartan eye drops were applied to rabbits. The pharmacokinetics in cornea and aqueous humour after single eye drop application were studied in 49 rabbits. The effect of the eye drops on IOP was studied in 10 rabbits using an iCare (®) TonoVet Plus, iCare, Finland) tonometer and compared with 0.5% timolol eye drops.

Results: Candesartan lowered IOP from 24.6 ± 5.1 mmHg at baseline to 19.0 ± 2.9 mmHg (mean \pm SD, $p = 0.030$, $n = 10$) 4 hr after application. Irbesartan lowered IOP from 24.2 ± 1.7 mmHg to 20.2 ± 0.9 mmHg ($p = 0.14$, $n = 10$). Timolol decreased the IOP from 24.9 ± 4.2 mmHg to 20.4 ± 4.8 mmHg (mean \pm SD, $p = 0.036$, $n = 10$). The pharmacokinetics data show that both formulations deliver effective amounts of drug into the intraocular tissues, with irbesartan and candesartan reaching concentrations of 121 ± 69 and 30.43 ± 13.93 ng/g (mean \pm SD), respectively, in the aqueous humour 3 hr after a single-dose administration.

Conclusions: Topical application of irbesartan and candesartan eye drops delivers effective drug concentrations to the anterior segment of the eye in rabbits, achieving drug concentrations 100 times above the IC₅₀ for angiotensin II receptor and showing an IOP-lowering effect. Angiotensin receptor blocker (ARB) eye drops have potential as a new class of glaucoma drugs.

Key words: angiotensin receptor blockers – glaucoma – intraocular pressure – pharmacokinetics

Acta Ophthalmol. 2021; 99: 376–382

© 2020 Acta Ophthalmologica Scandinavica Foundation. Published by John Wiley & Sons Ltd

doi: 10.1111/aos.14639

Introduction

The renin-angiotensin system (RAS) plays a role in aqueous humour secretion. The presence of RAS components, as well as enzyme activities of angiotensin-converting enzyme (ACE), have been reported in the eye of several species including human, suggesting that local ocular RAS is involved in the regulation of IOP (Holappa et al., 2020). The primary mechanism of action of an angiotensin receptor blocker (ARB) involves selectively blocking the binding of angiotensin II (Ang II) to the angiotensin type I receptor. This affects the aqueous humour formation signalling process and reduces IOP by decreasing aqueous humour production (Van Haeringen, 1996; Campbell, 2014).

While current glaucoma eye drops are effective in lowering IOP, each has local or systemic side effects, that limit their use. Beta-blockers affect respiratory and cardiac function and prostaglandin analogs and carbonic anhydrase inhibitors show potential eye irritation (Inoue, 2014). This is especially limiting for patients who need multiple drugs to control IOP. This group of patients will benefit from the option of new classes of glaucoma drugs, especially if they have little or no side effects, such as cough, low blood

pressure, headache, rashes and indigestion.

Angiotensin-converting enzyme (ACE) inhibitors (ACE-I) have also been shown to lower IOP by inhibiting the formation of Ang II and thereby reducing the stimulation of angiotensin type I receptors. However, the production of Ang II can occur through non-ACE pathways which remain unaffected by ACE inhibition (Brunner, 2007). Moreover, ARBs show some advantages over ACE-I, including an absence of significant adverse reactions and a favourable side effect profile (Al Sabbah et al., 2013).

Eye drops are the preferred route of ocular drug administration, but the bioavailability of topically applied formulations is limited by the various protective mechanisms and barriers of the eye (Patel et al., 2013). Furthermore, the physicochemical properties of ARBs and ACE inhibitors, such as poor aqueous solubility and instability in aqueous solutions, have prevented their formulation and use as clinically effective eye drops (Chiang, Ho, & Chen, 1996; Agarwal et al., 2014; Muankaew et al., 2014). Our group has now solved this with a novel formulation based on cyclodextrin nanoparticles. Cyclodextrins enable formulation of lipophilic poorly soluble drugs as aqueous eye drop solutions increasing their bioavailability by enhancing drug permeation through the aqueous tear film and eye wall (Jansook et al., 2015).

The γ -cyclodextrin nanoparticle technology was used to develop 1.5% (w/v) irbesartan and 0.15% (w/v) candesartan microsuspension eye drop formulations (Jansook et al., 2015).

The aims of this study are (1) to examine the pharmacokinetics of irbesartan and candesartan in γ -cyclodextrin nanoparticle eye drops in the anterior segment of the rabbit eye and (2) test the hypothesis that irbesartan and candesartan eye drops lower IOP in rabbits.

Materials and methods

Ethical statement

This research followed the ARVO Statement for the Use of Animals in Ophthalmic and Vision Research. For the IOP study, professional assistance by veterinarians at the Institute for

Experimental Pathology from the University of Iceland was provided and approval by the Icelandic Food and Veterinary Authority (MAST) was obtained. The pharmacokinetics study was approved by the local animal welfare committee (GZ BMWFW-66.009/0163-V/3b/2018).

Animals

59 New Zealand rabbits (*Oryctolagus cuniculus*; weight, 3.0–6 kg) were used in studies. 10 rabbits were used in the IOP study and 49 rabbits (26 for irbesartan and 23 for candesartan) were used in the pharmacokinetic study. They were housed in groups by two in cages with raised areas, kept under controlled, standardized conditions (artificial L/D cycle 12:12, room temperature $22 \pm 2^\circ\text{C}$, humidity $55 \pm 10\%$) and had *ad libitum* access to complete feed for rabbits. They were acclimatized for a minimum of 7 days.

The rabbits were not anaesthetized during the procedures and no topical agent was used before the eye drops administration.

Test compounds

1.5% irbesartan, 0.15% candesartan and vehicle eye drops in γ -cyclodextrin nanoparticle suspensions were tested. The difference in concentration for the two ARBs is due to solubility and stability. The formulations have been described previously (Jansook et al., 2015). The eye drops were placed into a sonicator at 40°C for 30 min and shaken thoroughly until homogeneously suspended immediately before eye drops administration to the rabbits (Muankaew et al., 2014). After use, they were stored at controlled room temperature ($\sim 25^\circ\text{C}$) and protected from light.

For the IOP study, a commercial 0.5% timolol solution (Optimol, Oftan, Japan) was also tested, administering the eye drops directly from the vial.

Intraocular pressure study

Ten rabbits were tested repeatedly with five different drugs or controls in eye drop applications with one application per day (treatment 1: 0.15% candesartan, treatment 2: 1.5% irbesartan, treatment 3: 0.5% timolol, treatment 4: blank, treatment 5: vehicle). 50 μl of each suspension was topically

administered to the left eye of each rabbit using a pipette. Timolol solution was administered as one drop directly from the vial. The blank group received no treatment. A minimum of a 2-day washout period was observed between study days.

Four measurement time-points were established for each treatment group: baseline (right before eye drop administration), 1 min, 2 hr and 4 hr after administration. Baseline and one minute after administration measurements were averaged due to the closeness of values and time-points. Intraocular pressure (IOP) was measured only on the left eye (treated eye) using a rebound tonometer ($\text{\textcircled{R}}$ TonoVet Plus, iCare, Finland) and IOP measurements were taken at the same time of the day for all groups to minimize fluctuations due to circadian rhythm. All ten rabbits were tested with all study drugs and controls at different times.

Pharmacokinetic study

A total of 49 animals were used, 26 rabbits for irbesartan and 23 for candesartan, and 35 μl of the ophthalmic solution was administered into the conjunctival sac of the (left) study eye of each rabbit with no drug application to the fellow eye. Rabbits were euthanized in anaesthesia (ketamine 60 mg/kg, xylazine 16 mg/kg, s.c.) by an overdose of pentobarbitone sodium at five predefined time-points (0.5h, 1.5h, 3h, 6h, 12h) after drug administration. Immediately after euthanasia, both eyes were enucleated from each animal. The study eye demonstrates the combination of topical and systemic absorption, whereas the fellow eye shows systemic absorption alone. Enucleated eyes were frozen immediately and stored at -80°C until further processing. For separation of the different ocular tissues, the eyeball was removed from storage and dissected into different parts: cornea, aqueous humour, vitreous body and the retina/choroid, each of which was stored separately in different tubes. All tissues were collected and separately weighted upon collection and stored in separated tubes. Tissue samples including aqueous humour, cornea, retina and vitreous were sent to NuCro-Technics (Scarborough, Ontario, Canada) for assessment of the study drug concentrations.

Weighed rabbit eye tissue samples were homogenized in H₂O-diluted rabbit plasma (rabbit plasma/water, 1/14, v/v) in a ratio of 1–19 (i.e. 1 g or 1 ml of rabbit eye tissue in 19 ml of diluted rabbit plasma. A 200 µl aliquot of rabbit tissue homogenate supernatants was mixed sequentially with 100 µl of internal standards (8 ng/ml of candesartan-d₄ and 20 ng/ml of irbesartan-d₄ in methanol/water (20/80, v/v) and 2 ml of water). The mixtures were then loaded onto the preconditioned HLB cartridges (Waters Oasis® 60 mg, 3 cc). The cartridges were first washed with 2 ml of methanol/water (10/90, v/v) and then eluted with 2 ml of methanol. The organic solvents were evaporated at 40°C and the dry residues were reconstituted in 200 µl of methanol/water/formic acid (70/29.75/0.25, v/v/v).

An Agilent 1200 series liquid chromatograph coupled with an Agilent 6490 Triple Quad LC/MS (Agilent Technologies Canada, Mississauga, Ontario, Canada) was used for the LC-MS/MS analysis. A 20 µl aliquot of the extracted samples was injected onto an ACE Excel 5 Super C18 column (4.6 × 150 mm, Advanced Chromatography Technologies, Aberdeen, Scotland) maintained at 25°C for a gradient separation at the flow rate of 0.8 ml/min. The mobile phase A was methanol/H₂O/formic acid, 70/29.75/0.25 (v/v/v) and the mobile phase B was methanol/H₂O/formic acid, 90/9.75/0.25 (v/v/v). For gradient elution, 100% mobile phase A was used for the first 4.5 min, followed by 100% mobile phase B for 1.5 min, and then back to 100% mobile phase A for 2 min of re-equilibration, with a total run time of 8 min. Candesartan and candesartan-d₄ were eluted at 5.1 min and irbesartan and irbesartan-d₄ were eluted at 4.1 min. The MS detection was in the positive electrospray ionization (ESI) mode using the MRM transitions (protonated molecule to product ion) of *m/z* 441 → 263, 445 → 267, 429 → 207, and *m/z* 433 → 211 for candesartan, candesartan-d₄, irbesartan, and irbesartan-d₄, respectively.

Statistical analysis

For the statistical analysis regarding IOP measurements data, GraphPad Prism 8.0 for Windows (GraphPad, California, USA) was used and t-test

analysis was applied to compare the groups, the significance level was set at *p* < 0.05.

Results

Intraocular pressure

Figure 1A shows the individual values for each rabbit in the different groups and the mean change in IOP (mmHg; mean ± SD) for each group, from baseline to 4 hr after administration. Candesartan showed an IOP-lowering effect, from 24.6 ± 1.6 mmHg at baseline to 19 ± 0.9 mmHg (*n* = 10; change of 5.6 mmHg) 4 hr postinstillation (paired *t*-test, *p* = 0.030).

Irbesartan decreased the IOP from 24.2 ± 1.7 mmHg to 20.2 ± 0.9 mmHg (*n* = 10; change of 4.0 mmHg) 4 hr after the eye drops administration (paired *t*-

test, *p* = 0.142). For timolol, the observed change in IOP was from 24.9 ± 4.2 mmHg to 20.4 ± 4.8 mmHg (*n* = 10, change of 4.6 mmHg) 4 hr after eye drops administration (paired *t*-test, *p* = 0.036).

Figure 1B shows the change in IOP at different measured time-points. The highest changes in IOP for both candesartan and irbesartan occur between 2 and 4 hr after administration. Candesartan showed a change of 1.8 mmHg in the first 2 hr of administration and a 3.7 mmHg change from 2 to 4 hr after administration. Irbesartan lowered the IOP by 0.48 mmHg during the first 2 hr after administration and by 4.5 mmHg from 2 to 4 hr after administration.

On the other hand, timolol shows a more relevant IOP change during the first 2 hr of administration, lowering it

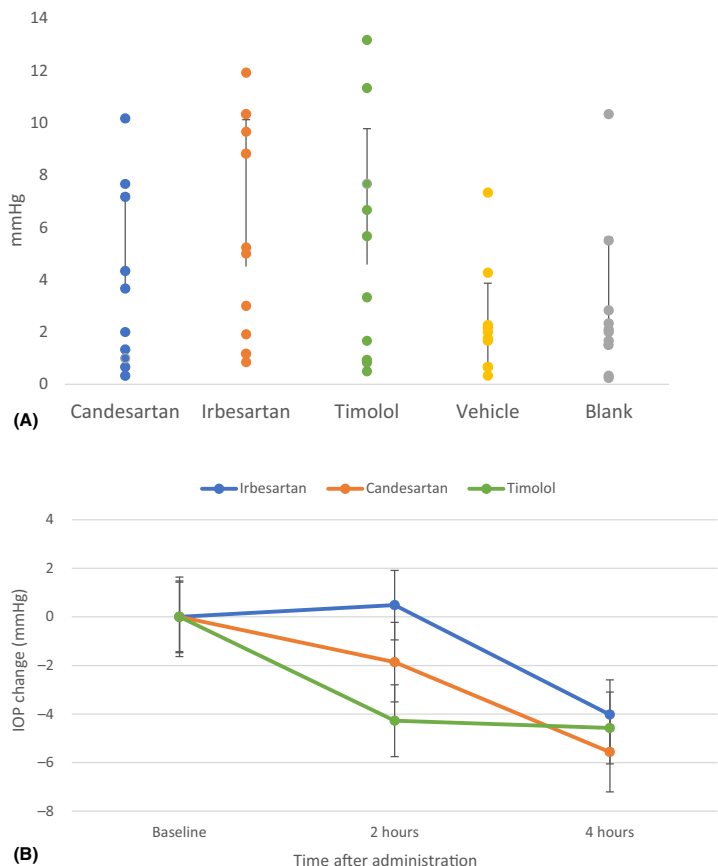


Fig. 1. (A) Mean (mmHg, mean ± SD) and individual values for IOP change for each of the different drug and control groups 4 hr after eye drop application. (B) IOP change (mmHg, mean ± SD, *n* = 10) at different time-points after eye drop administration for each drug.

by 4.3 mmHg compared with a change of 0.3 mmHg from 2 to 4 hr after administration.

Pharmacokinetics

The data from the pharmacokinetic study regarding tissue distribution of both drugs in the cornea and aqueous humour at different time-points after administration (0.5, 1.5, 3, 6 and 12 hr) is shown in Figs 2 and 3.

For the purpose of the study, which is to evaluate the effectiveness of both drugs as IOP-lowering treatments, only pharmacokinetic data regarding the anterior segment of the eye are shown. Irbesartan reached a maximum concentration of 282 ± 159 nM (mean \pm SD, $n = 26$) in the aqueous humour of the study eye 3 hr after administration (Fig. 2A) and candesartan's maximum concentration in the aqueous humour was 70 ± 73 nM

(mean \pm SD, $n = 23$) 3 hr after administration (Fig. 3A).

Discussion

Our data demonstrate that irbesartan and candesartan in γ -cyclodextrin nanoparticle eye drops penetrate the rabbit eye in pharmacologically relevant concentrations after a single topical application and lower IOP comparably to timolol eye drops. Several publications support the efficacy of ARBs and ACEs as IOP-lowering treatments. Relevant studies and their results are listed in Table 1.

Based on a study from Kim et al., the IC50 of irbesartan as an angiotensin II type 1 receptor-specific competitive antagonist is 1.3 nM (Kim et al., 2018). van Rodijnen et al., (2010) found only a slight difference in potency between candesartan and irbesartan, and their calculations estimate

candesartan's IC50 values to be between 0.4 and 0.7 nM. Our results show a concentration in aqueous humour of 100 times the IC50, suggesting over 99% inhibition of the receptor for both drugs.

In a study by Lee et al., 30 rabbits received an intravitreal single injection of 1 mg of candesartan and analysed the concentration in the vitreous at different time-points, calculating a half-life of candesartan of approximately 6.83 hr. In our study, the single dose administered to the rabbits was equal to 0.05 mg. Considering Lee et al. calculations and the difference in the routes of administration, the 48 hr washout period we established between treatments is enough to eliminate residual drugs from previous administrations and avoid a cumulative effect. They also indicated that the common daily oral dose of candesartan for humans is 16 mg and, compared with that, the intraocular concentration after a topical administration of a 0.5 mg dose of candesartan is approximately 200 times higher than that after taking 16 mg orally (Lee et al., 2011).

Several studies have been performed to determine the pharmacokinetic properties of γ -cyclodextrin/drug complexes after topical administration to the eye. In a study by Johannsdóttir et al., dexamethasone in cyclodextrin microsuspension was topically applied in rabbits to determine the pharmacokinetics. Their results showed a maximum concentration of 7506 ± 1067 nM in the cornea and 438 ± 107 nM in the aqueous humour 2 hr after the administration (Johannsdóttir et al., 2018). Our pharmacokinetic profiles for irbesartan and candesartan in the corneal tissue and aqueous humour are in general agreement with those reported by Johannsdóttir et al. regarding dexamethasone, showing an increase of the drug concentration during the first 2–3 hr after administration and a slow decrease after that. This similarity supports our hypothesis that cyclodextrin nanoparticle ensures a sustained release of the drug in the eye tissues and enables penetration of the drug to the anterior chamber.

The pharmacokinetic profiles observed with irbesartan and candesartan also coincide with data reported in previous studies by Djebli et al. and Mishima using different drugs, where

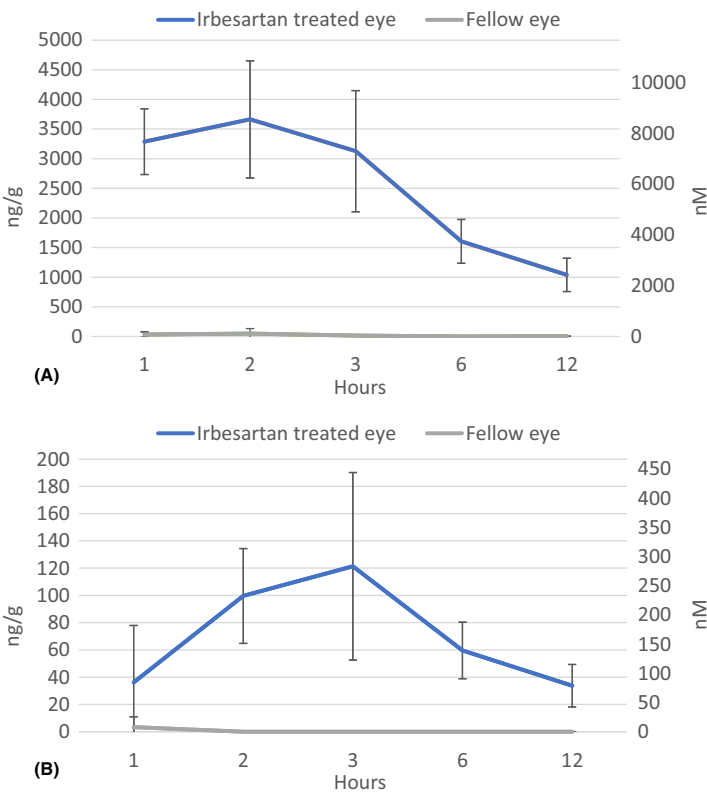


Fig. 2. A (top): irbesartan concentration ($n = 26$, mean \pm SD; ng/g and nM) in the cornea. B (bottom): irbesartan concentration in the aqueous humour. Charts show drug concentration at time-points (hours) after administration. Study eyes are shown in blue and untreated fellow eyes are shown in grey.

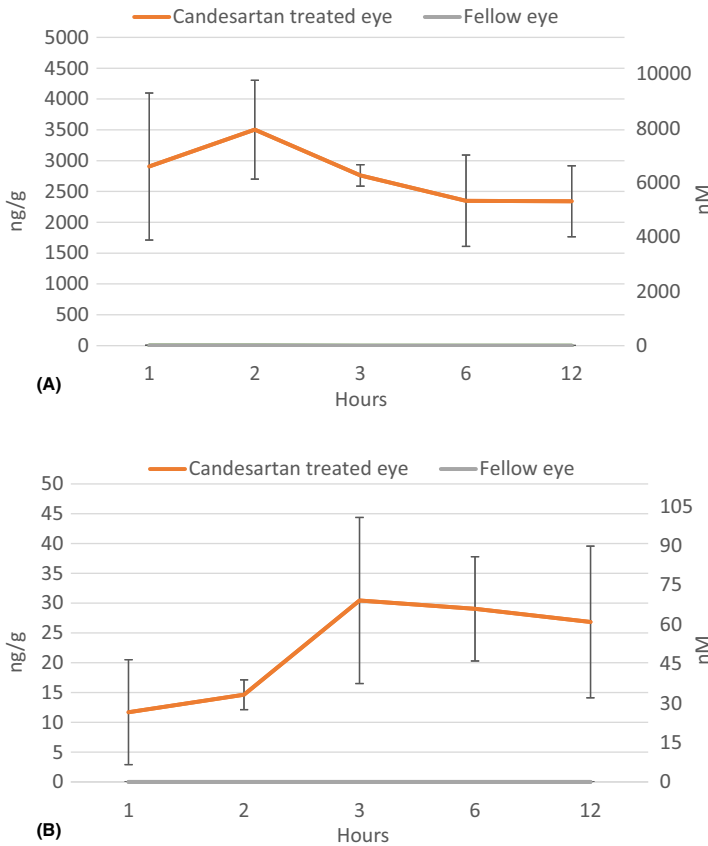


Fig. 3. A (top): candesartan concentration ($n = 23$, mean \pm SD; ng/g and nmol) in the cornea. B (bottom): candesartan concentration in the aqueous humour. Charts show drug concentration at time-points (hours) after administration. Study eyes are shown in orange and untreated fellow eyes are shown in grey.

the drug concentration follows a progressive decrease in the corneal tissue while it peaks in the aqueous humour around 2 hr after administration

(Mishima, 1981; Djebli et al., 2017). As stated by Djebli et al., these findings are consistent with the physiology of the eye (i.e. aqueous humour being a

fluid with a higher turnover compared to the cornea tissue). However, there are perceptible differences between the pharmacokinetic profiles of irbesartan and candesartan, the latter showing more stable and sustained drug concentrations in both cornea and aqueous humour throughout time. These results are consistent with those reported by van Rodijnen et al. that suggested a slower dissociation of candesartan from the AT1-receptor than irbesartan and losartan (van Rodijnen et al., 2010).

Chiang et al. tested different timolol preparations and measured the effect on the IOP in rabbits. Their results showed a noticeable decrease in the IOP 1 hr after a 50 μ l administration of 0.5% timolol, which is consistent to our results where we can see that timolol is the group that shows the greatest decrease 2 hr after the administration (Chiang et al., 1996).

In our study, a blank group was also monitored as a control for a diurnal effect and other variability, as both normal and glaucomatous human eyes can show considerable variation in intraocular pressure (Wilensky, 1991). Although a decreasing trend along the day was observed for the blank group in our study, this change did not reach statistical significance compared with the treated groups ($n = 10$, $p > 0.05$). According to Cervino et al., in addition to the circadian rhythm, IOP short-term fluctuations are associated with heart rate, breathing patterns, eye or lid position or physical activity, as well as issues regarding repeatability and reproducibility of rebound tonometry (Shapiro et al., 2006). Other potential factors influencing IOP fluctuations

Table 1. List of published reports on the IOP-lowering effect of ARBs and ACEs using different experimental models and routes of administration

Drug	References	Route of administration	Model	Effect
SCH 33861 (ACE inhibitor)	Watkins RW et al., (1987)	Topical	Rabbits	Well tolerated and effective in lowering intraocular pressure in patients with ocular hypertension or primary open-angle glaucoma.
Captopril (ACE inhibitor)	Costagliola et al., (1995)	Oral	Human	Significantly lowers IOP in all patients by increasing the outflow of aqueous humour.
Enalaprilat nanoparticle eye drops (ACE inhibitor)	Loftsson et al., (2010)	Topical	Rabbits	The decrease in the IOP was proportional to the concentration of the drug dissolved in the formulation.
CS-088 (ARB)	Inoue et al., (2001)	Topical	Rabbits	IOP-lowering effect in two models of hypertensive rabbits.
Losartan (ARB)	Iaccarino et al., (2002)	Oral	Human	Decrease in the IOP in hypertensive humans mainly due to a reduction in the production of aqueous humour.
Irbesartan and Telmisartan (ARBs)	Hazlewood et al., (2018)	Oral	Human	Both ARBs lower IOP and suggested that delivery of ARBs by eye drops would help to achieve localized effective drug concentrations.

such as water drinking, animal handling and drug administration must be considered. Brucculeri et al. observed that IOP increased significantly after water ingestion and remained altered for 45 min (Brucculeri et al., 1999).

Furthermore, Dinslage et al., (1998) studied the effect of animal handling on IOP, observing an increase followed by a decrease from the normal pressure for a period lasting from a few minutes to several hours. In our study, rebound tonometry requires handling each animal individually several times a day, however, rabbits were handled gently before IOP measurement to cause them minimal disturbances. As indicated by Ma et al., if any sign of stress was found, IOP measurements were postponed for at least another two minutes before repeating the measurements. Regarding water supply, we intended for the rabbits to have a continuous source of drinking water so fluid balance was not interrupted and minimal changes in IOP were caused due to water loading (Ma et al., 2016).

Although the outcome of the study was positive, it shows some potential limitations such as the small sample size of animals used in the IOP study. Individual values for IOP show variability that could affect the robustness of the statistical test and provide deviation in the analysis of the results. Another limitation is the duration of the IOP measurements, with the last one taken 4 hr after the administration while pharmacokinetic data shows that drug can be detected in the tissues at least until 12 hr after the administration.

Conclusion

Irbesartan and candesartan eye drops deliver drug into the eye in pharmacologically relevant concentration, achieving drug concentrations 100 times above the IC₅₀ for angiotensin II receptor and showing an IOP-lowering effect. Our data suggest that both ARBs could have potential as a new class of eye drops to lower IOP in glaucoma. Clinical trials are needed to confirm and develop this thesis.

References

Agarwal R, Krasilnikova AV, Raja IS, Agarwal P & Mohd Ismail N. Mechanisms of

angiotensin converting enzyme inhibitor-induced IOP reduction in normotensive rats. *Eur J Pharmacol* **730**: 8–13.

Al Sabbah Z, Mansoor A & Kaul U (2013): Angiotensin receptor blockers - Advantages of the new sartans. *J Assoc Physicians India* **61**(7): 464–470.

Brucculeri M, Hammel T, Harris A, Malinovsky V & Martin B (1999): Regulation of intraocular pressure after water drinking. *J Glaucoma* **8**(2): 111–116.

Brunner HR (2007): Angiotensin II receptor blockers. *Compr Hypertens* **75246**: 1003–1017.

Campbell DJ (2014): Clinical relevance of local renin angiotensin systems. *Front Endocrinol (Lausanne)* **5**(6): 1–5.

Chiang CH, Ho JI & Chen JL (1996): Pharmacokinetics and intraocular pressure lowering effect of timolol preparations in rabbit eyes. *J Ocul Pharmacol Ther* **12**(4): 471–480.

Costagliola C, Di Benedetto R, DeCaprio L, Verde R & Mastropasqua R (1995): Effect of oral captopril (SQ 14225) on intraocular pressure in man. *Eur J Ophthalmol* **5**(1): 19–25.

Dinslage S, McLaren J & Brubaker R (1998): Intraocular pressure in rabbits by telemetry II: Effects of animal handling and drugs. *Investig Ophthalmol Vis Sci* **39**(12): 2485–2489.

Djebli N, Khier S, Griguer F, Coutant AL, Tavernier A, Fabre G, Leriche C & Fabre D (2017): Ocular drug distribution after topical administration: population pharmacokinetic model in rabbits. *Eur J Drug Metab Pharmacokinet* **42**(1): 59–68.

Hazlewood RJ, Chen Q, Clark F, Kuchtey J & Kuchtey RW (2018): Differential effects of angiotensin II type I receptor blockers on reducing intraocular pressure and TGF β signaling in the mouse retina. *PLoS One* **13**(8): 1–18.

Holappa M, Vapaatalo H & Vaajanen A (2020): Local ocular renin-angiotensin-aldosterone system: any connection with intraocular pressure? A comprehensive review. *Ann Med* **52**(5): 191–206.

Iaccarino G, Mastropasqua L, Costagliola C, Leonarda De Rosa M, Ciancaglini M & Verolino M (2002): Effect of oral losartan potassium administration on intraocular pressure in normotensive and glaucomatous human subjects. *Exp Eye Res* **71**(2): 167–171.

Inoue K (2014): Managing adverse effects of glaucoma medications. *Clin Ophthalmol* **8**: 903–913.

Inoue T, Yokoyama T, Mori Y, Sasaki Y, Hosokawa T, Yanagisawa H & Koike H (2001): The effect of topical CS-088, an angiotensin AT1 receptor antagonist, on intraocular pressure and aqueous humor dynamics in rabbits. *Curr Eye Res* **23**(2): 133–138.

Jansook P, Muankaew C, Stefánsson E & Loftsson T (2015): Development of eye drops containing antihypertensive drugs: Formulation of aqueous irbesartan/ γ CD eye drops. *Pharm Dev Technol* **20**(5): 626–632.

Johannsdóttir S, Jansook P, Stefánsson E et al. (2018): Topical drug delivery to the posterior segment of the eye: Dexamethasone concentrations in various eye tissues after topical administration for up to 15 days to rabbits. *J Drug Deliv Sci Technol* **45**: 449–454.

Kim D, Pattamatta U, Kelly E, Healey PR, Carnt N, Zoellner H & White AJR (2018): Inhibitory effects of angiotensin II receptor blockade on human tenon fibroblast migration and reactive oxygen species production in cell culture. *Transl Vis Sci Technol* **7**(2): 20.

Lee JE, Lim DW, Park HJ, Shin JH, Lee SM & Oum BS (2011): Intraocular toxicity and pharmacokinetics of candesartan in a rabbit model. *Investig Ophthalmol Vis Sci* **52**(6): 2924–2929.

Loftsson T, Thorisdóttir S, Fridriksdóttir H & Stefánsson E (2010): Enalaprilat and enalapril maleate eyedrops lower intraocular pressure in rabbits. *Acta Ophthalmol* **88**(3): 337–341.

Ma D, Chen CB, Liang J, Lu Z, Chen H & Zhang M (2016): Repeatability, reproducibility and agreement of intraocular pressure measurement in rabbits by the TonoVet and Tono-Pen. *Sci Rep* **6**(10): 1–7.

Mishima S (1981): Clinical pharmacokinetics of the eye. Proctor lecture. *Investig Ophthalmol Vis Sci* **21**(4): 504.

Muankaew C, Jansook P, Stefánsson E & Loftsson T (2014): Effect of γ -cyclodextrin on solubilization and complexation of irbesartan: Influence of pH and excipients. *Int J Pharm* **474**(1–2): 80–90.

Patel A, Cholkar K, Agrahari V & Mitra AK (2013): Ocular drug delivery systems: An overview. *World J Pharmacol* **2**(2): 47–64.

van Rodijnen WF, van Lambalgen TA, van Teijlingen ME, Tangelder G-J & ter Wee PM (2010): Comparison of the AT1-receptor blockers candesartan, irbesartan and losartan for inhibiting renal microvascular constriction. *J Renin Angiotensin-Aldosterone Syst* **2**(1_suppl): S204–S210.

Shapiro B, Dickersin K & Lietman T (2006): Trachoma, antibiotics and randomised controlled trials. *Br J Ophthalmol* **90**(12): 1443–1444.

Van Haeringen N (1996): The renin-angiotensin. *Br J Ophthalmol* **80**(2): 99–100.

Watkins RWBaum T, Cedeno K, Smith EM, Yuen PH, Ahn HS, & Barnett A (1987): Topical ocular hypotensive effects of the novel angiotensin converting enzyme inhibitor SCH 33861 in conscious rabbits. *J Ocul Pharmacol* **3**(4): 295–307.

Wilensky JT (1991): Diurnal variations in intraocular pressure. *Trans Am Ophthalmol Soc* **89**: 757–790.

Received on March 11th, 2020.

Accepted on September 8th, 2020.

Correspondence:

Laura Lorenzo-Soler, MSc

Faculty of Medicine
University of Iceland
Vatnsmýrarvegur 16
101 Reykjavík
Phone: +354 7677313
Email: lls10@hi.is

We thank Martin Kallab and Kornelia Schützenberger for their help in performing the PK

experiments. Further, the support of the Department of Biomedical Research, Medical University of Vienna is gratefully acknowledged.

The following author(s) indicated a financial or other interest:



Employment or Leadership Position: Olof B. Olafsdóttir, Iris M. Kristinsdóttir, Aimin Tan.

Stock Ownership: Thorsteinn Loftsson, Einar Stefansson.

This study has received partial funding from the European Union's programme Eurostar under the project No PREVIN E11008 and the Horizon 2020 research and innovation programme under the Marie Skłodowska-Curie grant agreement No 765441.

Paper II

Topical noninvasive retinal drug delivery of a tyrosine kinase inhibitor: 3% cediranib maleate cyclodextrin nanoparticle eye drops in the rabbit eye

Laura Lorenzo-Soler,¹  Pitsiree Praphanwittaya,² Olof Birna Olafsdottir,^{1,3,4} Iris Myrdal Kristinsdottir,⁴ Gudrun Marta Asgrimsdottir,⁴ Thorsteinn Loftsson^{2,4} and Einar Stefansson^{1,3,4} 

¹Faculty of Medicine, University of Iceland, Reykjavík, Iceland

²Faculty of Pharmaceutical Sciences, University of Iceland, Reykjavík, Iceland

³Department of Ophthalmology, Landspítali University Hospital, Reykjavík, Iceland

⁴Oculus ehf., Reykjavík, Iceland

ABSTRACT.

Purpose: Tyrosine kinase inhibitors inhibit VEGF receptors. If delivered to the retina, they might inhibit oedema and neovascularization such as in age-related macular degeneration and diabetic retinopathy. The aim of this study was to formulate cediranib maleate, a potent VEGF inhibitor, as γ -cyclodextrin nanoparticle eye drops and measure the retinal delivery and overall ocular pharmacokinetics after a single-dose administration in rabbits.

Methods: A novel formulation technology with 3% cediranib maleate as γ -cyclodextrin micro-suspension was prepared by autoclaving method. Suitable stabilizers were tested for heat-stable eye drops. The ophthalmic formulation was topically applied to one eye in rabbits. The pharmacokinetics in ocular tissues, tear film and blood samples were studied at 1, 3 and 6 hr after administration.

Results: γ -cyclodextrin formed complex with cediranib maleate. The formation of γ -cyclodextrin nanoparticles occurred in concentrated complexing media. Combined stabilizers prevented the degradation of drug during the autoclaving process. Three hours after administration of the eye drops, treated eyes showed cediranib levels of 737 ± 460 nM (mean \pm SD) in the retina and 10 ± 6 nM in the vitreous humour.

Conclusions: Cediranib maleate in γ -cyclodextrin nanoparticles were stable to heat in presence of stabilizers. The drug as eye drops reached the retina in concentrations that are more than 100 times higher than the 0.4 nM IC₅₀ value reported for the VEGF type-II receptor and thus, presumably, above therapeutic level. These results suggest that γ -cyclodextrin-based cediranib maleate eye drops deliver effective drug concentrations to the retina in rabbits after a single-dose administration.

Key words: cediranib – cyclodextrins – drug delivery – *in vivo* – neovascularization – pharmacokinetics – topical administration

This work was supported by Oculus ehf, Reykjavík, Iceland.

Laura Lorenzo-Soler, Pitsiree Praphanwittaya (none), Olof B. Olafsdottir, Gudrun M. Asgrimsdottir and Iris M. Kristinsdottir, (employees), Thorsteinn Loftsson and Einar Stefansson (financial).

Acta Ophthalmol.

© 2022 Acta Ophthalmologica Scandinavica Foundation. Published by John Wiley & Sons Ltd

doi: 10.1111/aos.15101

1. Introduction

Angiogenesis is the formation and maintenance of blood vessel structures and is essential for the physiological functions of tissues and the progression

of diseases such as cancer and inflammation (Shibuya, 2011). Neovascular age-related macular degeneration (AMD) and diabetic retinopathy (DR) are the leading causes of blindness in many developed countries

affecting elderly and working-age people, respectively, and these pathologies are associated with neovascularization and oedema in the posterior segment of the eye (Cook et al 2008; Cheung et al 2010). Both neovascular AMD and DR

are characterized by endothelial cell proliferation and migration, increase in vascular permeability and inflammation, all processes in which vascular endothelial growth factor-A (VEGF-A) plays a role (Amadio et al 2016). Current protein-based anti-VEGF therapies (ranibizumab, bevacizumab and aflibercept) bind VEGF and, because of their large molecular size, are administered by repeated intraocular injections, with discomfort and risk of injury and infection to patients (Falavarjani & Nguyen 2013; Moisseiev & Loewenstein 2017).

Tyrosine kinase inhibitors (TKIs) are a group of small molecules that inhibit tyrosine kinase targets including VEGFR-1, VEGFR-2, VEGFR-3 and platelet-derived growth factors (PDGFR). Its mechanism of action consists of blocking various signalling molecules in downstream pathways (Shi et al 2019). As TKIs are small lipophilic molecules, they present a potential for topical delivery to the retina by eye drops. However, most small-molecule protein kinase inhibitors are neutral or weakly basic lipophilic compounds with very poor solubility in aqueous media, which decreases their ability to permeate biological membranes (Prapathanwittaya et al 2020).

Several technologies have tried to overcome the barriers of topical drug delivery using emulsions, contact lenses, microneedles and nanoparticles (Patel et al 2013). A promising approach to addressing problems in drug solubility is the complexation with cyclodextrins (CDs) to form inclusion complexes (Göktürk et al 2012; Radu et al 2016).

Cyclodextrins (CDs) are cyclic oligosaccharides that can form water-soluble complexes with many lipophilic drugs and can be used to increase the solubility of lipophilic molecules in aqueous eye drop solutions. The higher drug concentration in such formulations enhances the drug concentration gradient and thereby the flux of drugs from the aqueous tear film through the lipophilic epithelium. Cyclodextrins can increase a drug's aqueous solubilization without changing the intrinsic properties that enable them to permeate lipophilic biological membranes, thus making it possible to topically apply drugs that could previously only be delivered systemically

(Loftsson et al 2007; Johannsdottir et al 2018).

Many studies have shown that CDs can be used to enhance water solubility of kinase inhibitors such as erlotinib, lapatinib and gefitinib (Phillip Lee et al. 2009; Tóth Gerg Jánoska et al 2017; Tóth Gerg Jánoska et al 2016). Cediranib maleate is a potent and reversible small-molecule tyrosine kinase inhibitor of all three VEGF receptors (VEGFR-1, VEGFR-2 and VEGFR-3) at nanomolar concentrations. Furthermore, it has been shown to be generally well tolerated with a manageable and dose-dependent toxicity profile (Dietrich et al 2009).

A previous study has reported that cediranib maleate was heat-labile in concentrated γ -cyclodextrin solution, with riboflavin actively preventing the drug from thermal degradation (Prapathanwittaya et al 2021). However, riboflavin alone may exhibit inadequate improvement of drug degradation in a saturated system, like a suspension with high drug loading. Here, a combination of stabilizers was required to limit the amount of each excipient according to FDA criteria for eye drops.

We have formulated heat-stable cediranib maleate in γ CD nanoparticle eye drops with combined stabilizers and investigated the pharmacokinetics to the posterior part of the eye following a single-dose topical application in rabbits.

2. Materials and Methods

2.1. Solubility determinations

Heating technique was used to prepare cediranib maleate/ γ CD complexes in triplicate. Excess amount of drug was saturated in 0–20% (w/v) γ CD solution. The systems were unbuffered, and the pH was between 4.5 and 5.5. The calculated pKa of cediranib is 10.1; thus, the drug can be fully ionized at such pH range. These suspensions were autoclaved at 121°C for 20 min in sealed glass vials and then allowed to cool at room temperature (22–23°C). A small amount of solid drug was added to each vial. The resealed sample was then equilibrated at room temperature under constant agitation for 7 days. The supernatant of each sample was

harvested by centrifugation at 12 000 rpm for 15 min (Heraeus Pico 17 Centrifuge, Thermo Fisher Scientific, Germany). The centrifuged samples were diluted with 50% MeOH prior to analysis of the dissolved drug amount by HPLC.

The phase solubility was determined according to the method reported by Higuchi and Connors (1965). The apparent solubility ($K_{1:1}$) of the cediranib maleate/ γ CD 1:1 (molar ratio) complex and the complexation efficiency (CE) were derived from the slope of initial linear phase-solubility diagrams (a diagram of the reciprocal of the apparent partition coefficient vs. the total CD concentration) using the following equations:

$$K_{1:1} = \text{slope}/S_0(1-\text{slope})$$

$$\text{CE} = S_0 * K_{1:1} : 1 = \text{slope}/(1-\text{slope}) \\ = [\text{CM}/\gamma\text{CD complex}]/[\gamma\text{CD}]$$

where S_0 is the intrinsic solubility of the drug, [cediranib maleate/ γ CD complex] is the concentration of dissolved complex, and $[\gamma\text{CD}]$ is the concentration of dissolved γ CD in the aqueous complexation media.

2.2. Effect of stabilizers on thermal stability of cediranib maleate

Generally, the active compound in solid form undergoes chemical degradation in the same way as drug degradation in concentrated aqueous solution (Loftsson 2013). Furthermore, drug degradation in the solid state is always significantly slower than in the solution state. Thus, this study focused on the thermal stability of drug tested in aqueous solution.

The stabilizer at concentration of 0.1% (w/v) (*i.e.* co-solvent and polymer) was included in 15% (w/v) γ CD solution as a ternary component. The complexation media were unbuffered, and pH was in the range of 5 ± 0.5 . An estimated excess amount of drug was added to the complexation media. Those samples were constantly agitated at ambient temperature overnight. One set was ready for drug analysis, while another set was further exposed to the autoclave heat as described previously. The drug concentration of each set was then determined by HPLC. Thermal stability of cediranib maleate was

presented in % drug amount that compared heated and non-heated samples. This method was applied following a previous study (Jansook et al 2020). Only dissolved drug quantities in solution form were compared.

Thermal stability of cediranib maleate in aqueous solution containing 15% (w/v) γ CD was determined at different pH. Excess amount of drug was added to the media and adjusted the desired pH (Thermo Orion 3 Star™ bench-top pH meter, Thermo Fisher Scientific, USA) by dropwise titration of the aqueous medium with concentrated sodium hydroxide or hydrochloric acid solution. The samples were incubated as mentioned earlier. The drug content of heated and non-heated sets was analysed by HPLC.

2.3. Preparation of cediranib maleate eye drop formulation

Aqueous 3% (w/v) cediranib maleate eye drops containing γ CD nanoparticles were formulated by including the selected stabilizer and other excipients, and then adjusting to a pH 5 with NaOH or HCl before heating in an autoclave (121°C for 20 min). The autoclaved solution was sonicated in an ice bath for 30 min. The sample was further incubated at room temperature under constant agitation for 3 days. The pH of the formulation was monitored throughout this process.

2.4. Solid-drug fraction

The tested formulation was centrifuged as previously described in the phase-solubility study (see Section 2.1.). The supernatant was determined by HPLC. The drug content in solid phase was calculated as follows:

$$\% \text{solid drug fraction} = \frac{\text{Total drug-dissolved drug}}{\text{Total drug content}} * 100$$

2.5. pH and osmolality

The pH values of eye drops were determined by Thermo Orion Star TM Series pH meter (Thermo Scientific, USA) at ambient temperature (22–23°C) and the osmolality with a Knauer K-7000 vapour pressure osmometer (Germany) operated at 25°C.

2.6. Dynamic light scattering (DLS)

The particle size of eye drops was determined by dynamic light scattering (DLS) using Nanotracs Wave particle size analyser (Microtrac Inc., York, PA). The diluted sample (20-folds) was illuminated by a laser beam at a wavelength of 780 nm, and its intensity fluctuation in scattered lights from Brownian motion of particles was detected at known scattering angle θ of 180° at 25 ± 0.2°C. The size population of nanoparticles was interpreted according to equation:

$$M_i = \left[\frac{(A_i/R_i^3)}{\sum(A_i/R_i^3)} \right] * 100$$

where M_i is the mass distribution percentage, A_i is the intensity area, R_i is the hydrodynamic radius of the size population i , and a is the shape parameter that equals 3, assuming spherical shaped particles (Bhattacharjee 2016; Stetefeld et al 2016).

2.7. Viscosity

A cone and plate viscometer (Brookfield model DV-II+, Brookfield Engineering Laboratories, Inc., Massachusetts, USA) was used for determining the apparent viscosity of cediranib maleate eye drops at 25°C and 37°C. The calibration check of the instrument was verified through the use of mineral oil standard with cone spindle no. CPE-40 prior to running the sample. The appropriate sample volume required for the spindle is 0.5 ml.

2.8. Morphological studies

The morphology of the eye drop was evaluated using Model JEM-1400 transmission electron microscope (JEOL, Tokyo, Japan). The negative straining technique was used. Firstly, a small amount of clear liquid (*i.e.* eye drops) was dropped on a 200-mesh coated grid and dried at 37–40°C for 1 hr. A drop of centrifuged 4%w/w uranyl acetate was then added to the loaded grid. After 6 min of straining, the sample was dried overnight at room temperature. Finally, the strained specimen was placed in a holder and inserted into the microscope.

2.9. Ethics statement

All animal procedures were performed under licence by the Icelandic Food

and Veterinary Authority (MAST) and in accordance with the ARVO Statement for the Use of Animals in Ophthalmic and Vision Research. The study was carried out according to the national regulation nr. 460/2017 on animal experiments, according to the national law on animal welfare nr. 80/2016. The Icelandic regulation on animal experiments is based on Directive 86/609/EEC of the European Parliament and of the Council on the protection of animals used for scientific purposes. Professional assistance by veterinarians at the Institute for Experimental Pathology from the University of Iceland was provided.

2.10. In vivo studies

Twenty-three French lop rabbits (*Oryctolagus cuniculus*) weighing between 3 and 6 kg were housed in individual cages with a temperature between 16 and 22°C. They had constant access to hay, pellets and fresh water during the study. They were acclimatized for a minimum of 7 days, and no treatment was administered during the acclimatization. Rabbits were awake during the eye drops administration, and no topical anaesthetic was used.

Five rabbits were used as a blank group, with no treatment administered, and 18 rabbits were tested with the eye drop micro-suspension containing cediranib maleate 3%, administered only in the left eye. Rabbits were marked with a pen in the left ear, and 50 μ l of the eye drop micro-suspension was topically administered. The eye drops were instilled with a calibrated adjustable micropipette fitted with disposable tips into the lower conjunctival sac of the eye by pulling the lower lid away from the eyeball. After instillation, the upper and the lower lids were held together for a few seconds to avoid rapid removal of the eye drop from the ocular surface. Animals were observed for overall health and local tolerance to the formulations until the end of the study.

2.11. Sample preparation

At predetermined time intervals (1, 3 and 6 hr) after administration, the animals were euthanized with pentobarbital. Just before euthanasia, tear fluid was collected from the left and the right eyes of each rabbit with surgical sponges. Blood samples were collected

by intracardiac puncture into tubes containing lithium heparin as anticoagulant and processed to obtain plasma by centrifuging at 1300 rpm.

The rabbits were euthanized immediately after blood sample extraction. Just after euthanasia, the two eyes of each animal were removed and dissected to extract surgically the different eye tissues. Samples from aqueous humour, cornea, iris, lens, vitreous humour,

retina and sclera were obtained from each eye. The ocular tissue and fluid samples were collected into labelled cryotubes and stored frozen (-80°C) until thawed for analysis.

2.12. Quantitative determinations

The concentration of cediranib maleate in each tissue was analysed in a reversed-phase high-performance liquid

chromatography (HPLC) system (Dionex, Softron GmbH Ultimate 3000 series, Germany). The analytical instrument was composed of a P680 pump with a DG-1210 degasser, an ASI-100 autosampler, VWD-3400 UV-VIS detector and a column heater, containing a C18 column ($100\text{A } 150 \times 4.6 \text{ mm}$, $5 \mu\text{m}$) from Kinetex Core-shell technology and a guard column (Phenomenex, UK). The HPLC system was operated under 30°C , isocratic condition, flow rate was 1.0 ml/min , detection wavelength was 234 nm , and injection volume was $20 \mu\text{l}$. The mobile phase consisted of acetonitrile and 0.05% (v/v) phosphoric acid (volume ratio 35:65).

Quantitative analysis of γCD was determined in a reverse-phase high-performance liquid chromatography system (Dionex, Softron GmbH Ultimate 3000 series, Germany) consisting of an LPG-3400SD pump with a built-in degasser, a WPS-3000 autosampler, a TCC-3100 column compartment and a Coronary[®] ultra-RS CAD detector. The HPLC conditions were applied from CD USP monograph 35 and previous investigators (Saokham & Loftsson 2015). The mobile phase

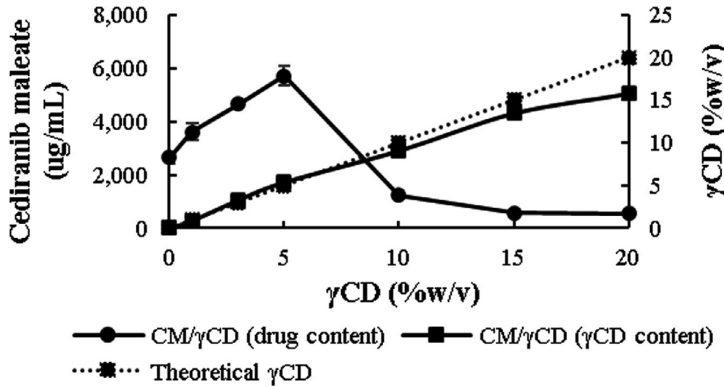


Fig. 1. Phase-solubility profile of cediranib maleate in aqueous γCD solution and concentration of dissolved γCD from such a system ($n = 3$).

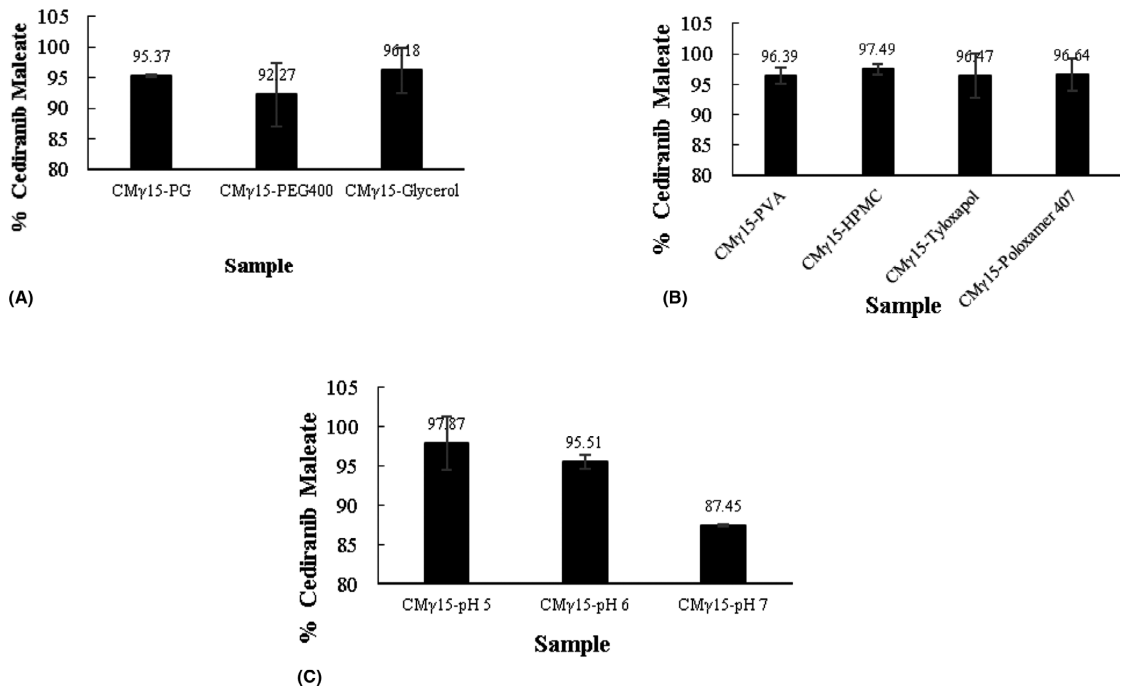


Fig. 2. Thermal stability of cediranib maleate/ γCD complex in presence of stabilizer (A) co-solvent, (B) polymer and (C) pH ($n = 3$).

consisted of acetonitrile and water (volume ratio 7:93). The temperatures of the column and sampler compartments were set at 30°C. The flow rate was 1.0 ml/min. The injection volume was 10 µl.

Drug concentration in different eye tissues after single administration for each animal was calculated using collected blood samples and harvested

tissues in order to characterize the pharmacokinetics. Drug concentrations were quantified using LC–MS/MS by Charles River Laboratories (s-Hertogenbosch, The Netherlands). All ocular tissue samples were homogenized using a Precellys Evolution bead homogenizer with an acetonitrile/methanol mixture as homogenization solvent in ratio 1:4 (4 µl solvent for

each mg ocular tissue). Homogenates were centrifugated, and the supernatant was further diluted before sample analysis. For cediranib maleate, a reversed-phase LC–MS/MS method was developed and qualified with a standard range of 1–1000 pM in a surrogate matrix.

2.13. Statistical analysis

Shapiro–Wilk and Levene tests were performed on the pharmacokinetic data obtained from the *in vivo* studies to determine whether the assumptions of normal distribution and homogeneity of variances were fulfilled. The tests indicated that our data, for the most part, did not follow a normal distribution nor showed homogeneity of variances. Therefore, to analyse whether statistically significant differences existed in drug concentration in the ocular tissues between treated and untreated eyes, a nonparametric Mann–Whitney *U*-test was carried out.

The data processing, statistical tests and analysis of the results were performed using Python 3.0 and its open-source libraries, Pandas, NumPy and SciPy.

Table 1. Cediranib maleate eye drops formula containing 15% (w/v) γCD.

No.	Ingredient	Purpose	Concentration (% w/v)
1.	Cediranib maleate	API	3
2.	γCD	Complexing agent	15
3.	Riboflavin	Main stabilizer	0.1
4.	L-arginine	Supportive stabilizer	0.1
5.	Propylene glycol	Supportive stabilizer	0.1
6.	Glycerol	Supportive stabilizer	0.1
7.	PVA (30-70 k)	Supportive stabilizer	0.2
8.	HPMC (50 cP)	Supportive stabilizer	0.1
9.	Poloxamer 407	Supportive stabilizer	0.1
10.	EDTA	Chelating agent	0.1
11.	NaCl	Isotonicity agent	0.1
12.	HCl/NaOH	pH adjustment	pH 5
13.	Purified water	Vehicle	qs 100
14.	N ₂	Oxidation inhibitor	purge
	% Drug content		102.68
	% Liquid fraction		23.46
	% Solid fraction		76.54

Table 2. Physicochemical data of eye drop formulation (*n* = 3).

No.	Physicochemical properties	Part	mean	SD	Criteria
1	Assay at initial	Suspension	30.69 mg/ml	0.10	27–33 mg/ml
		Supernatant	102.27% LA* 24.14% F [‡]	0.07	90–110% LA 10–30% Fraction (F)
		Solid	75.86% F	0.07	70–90% Fraction (F)
	Assay 3 months (ambient condition)	Suspension	30.07 mg/ml	0.05	27–33 mg/ml
		Supernatant	100.24% LA 24.19% F	0.05	90–110% LA 10–30% Fraction (F)
		Solid	75.81% F	0.05	70–90% Fraction (F)
2	pH [‡]	Suspension	5.02	0.03	min 4.0–5.0
3	Osmolality [‡]	Suspension	257	2	200–280 mOsm/kg
		Supernatant	262	2	
		Suspension	13.463	0.345	2–20 cP at 25°C
4	Viscosity at 25°C [¶]	Suspension	5.757	0.256	
		Suspension	1.06	12.20%	
5	Particle size by DLS (nm)	Suspension (dilution 1/20)	Diameter (nm)	% Vol	–
			356	85.80%	–
			1.06	12.20%	
			1689	2.00%	
6	Zeta potential	Suspension (dilution 1/20)	1.20	0.11	–

* % Label amount.

† Fraction.

‡ Refers to Ph.Eur.07/2016:20203 used as reference.

§ Refers to Ph.Eur.01/2010:20235 used as reference.

¶ Refers to Ph. Eur.01/2008:20210 used as reference.

3. Results

3.1. Solubility determinations

It has been confirmed in a previous study that γ CD can form complexes with cediranib maleate in aqueous conditions (Praphanwittaya et al 2021). The phase-solubility profile showed that cediranib maleate in aqueous γ CD solutions has limited solubility in water or classified as B_s type profiles (Fig. 1). γ CD started precipitating at a concentration of 10% (w/v) due to formation of larger aggregates and nanoparticles (Fig. 1). The optimal γ CD concentration was determined to be 15% (w/v) γ CD where the steady curve of dissolved drug concentration and obvious γ CD precipitation occurred.

3.2. Effect of stabilizers on thermal stability of cediranib maleate

Cediranib maleate is thermal labile in concentrated γ CD solution. About 15% (w/v) of the dissolved drug was lost during autoclaving (Praphanwittaya et al 2021). Although riboflavin can protect the drug from heat, other stabilizers are needed for a saturated system like eye drop suspension. Thermal stability data in (Fig. 2) showed that the presence of stabilizers such as co-solvents and polymers in cediranib maleate/ γ CD complex could protect the drug from thermal degradation. The drug in complexation media at pH 5 was more stable to heat.

Co-solvent can change the polarity of the complexation media (Loftsson et al 2005). Here, drug stability through thermal effect was dependent on the polarity of co-solvent (Fig. 2A). The dielectric constant (δ) of a compound is

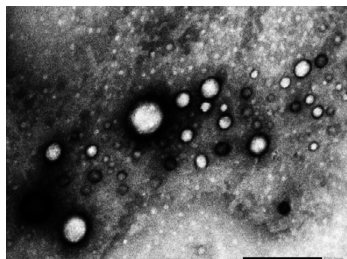


Fig. 3. Morphology of cediranib maleate in γ -CD eye drop nanosuspension by TEM at magnitude 25 000x.

Table 3. Concentration of cediranib maleate (nM, mean \pm SD; $n = 6$) in the different tissues for the study eye (left) and fellow eye (right) at different time-points after 3% eye drop formulation administration.

Tissue	Time	Study eye (nM)	Fellow eye (nM)	p-value
Aqueous humour	1	47.1 \pm 40.8	13.2 \pm 22.3	0.25
	3	90.0 \pm 63.2	0.4 \pm 1.0	0.01
	6	49.6 \pm 9.9	0.1 \pm 0.2	<0.01
Cornea	1	59391.4 \pm 10381.9	6.1 \pm 1.9	0.01
	3	35 037. \pm 7396.8	5.9 \pm 1.9	<0.01
	6	25699.8 \pm 8181.7	118.9 \pm 125.4	<0.01
Iris	1	4027.6 \pm 3274.1	383 \pm 704.3	0.05
	3	4889.4 \pm 2294.6	147.2 \pm 89.5	<0.01
	6	5421.4 \pm 4687.0	151.9 \pm 129.4	<0.01
Lens	1	38.3 \pm 27.7	6.1 \pm 13.0	0.02
	3	12.8 \pm 6.8	0.1 \pm 0.1	<0.01
	6	47.4 \pm 53.6	0.3 \pm 0.3	<0.01
Retina	1	936.6 \pm 1297.7	283.5 \pm 213.414	0.06
	3	736.9 \pm 459.4	299.5 \pm 121.5	0.01
	6	758.1 \pm 350.5	372.3 \pm 239.1	0.02
Sclera	1	10454.3 \pm 2373.7	99.8 \pm 11.4	0.01
	3	6112.5 \pm 3723.6	100.9 \pm 11.7	<0.01
	6	5057.1 \pm 4876.4	138.6 \pm 49.3	<0.01
Vitreous	1	16.4 \pm 11.3	4.9 \pm 8.3	0.06
	3	9.6 \pm 6.4	0.9 \pm 0.5	<0.01
	6	6.7 \pm 4.9	4.6 \pm 5.8	0.29

an index of its polarity, for example, glycerin (46 δ), PG (32.1 δ) and PEG400 (12.4 δ) at 20°C. Increasing polarity showed a serial decrease in drug loss. Glycerin and PG are relatively higher polar than PEG400. The drug was the most thermally stabilized in presence of glycerin followed by PG and PEG400.

3.3. Cediranib maleate eye drop formulation

Main formulation vehicle consisted of 15% (w/v) γ CD, EDTA and sodium chloride (NaCl). Riboflavin and other stabilizers were introduced to protect the drug from thermal degradation. L-arginine was also used as supportive stabilizer due to its ability to decrease drug loss during the heating process in a preliminary study (data not shown). After mixing those substances, nitrogen (N_2) was used for removal of oxygen from the finished products. The compositions of eye drops are summarized in Table 1.

3.4. Physicochemical characterizations

The eye drops had a yellow colour due to the presence of riboflavin. The formulation was thick and homogeneous. The suspended particles settled out of the fluid after storage overnight

at room temperature, and that sediment was easily resuspended by shaking. Table 2 shows that drug assay, pH, osmolality and viscosity are within the acceptable range. The drug content of eye drop was equal to the theoretical value. The main particle diameter is 340 nm, only about 2% of particles have a diameter of 1.6 μ m, and thus, these eye drops are a micro-suspension.

3.5. Morphology

Transmission electron microscopy (TEM) images demonstrate that the eye drop micro-suspension obtained spherical particles with an average size between 100 and 300 nm in diameter (Fig. 3). The morphology study confirmed the presence of nanoparticles in cediranib maleate eye drops.

Table 4. Concentration of cediranib maleate (nM, mean \pm SD; $n = 6$) in blood samples at different time-points after 3% eye drop formulation administration.

Blood	
Time (h)	nM
1	9.0 \pm 3.7
3	14.4 \pm 7.6
6	6.9 \pm 1.3

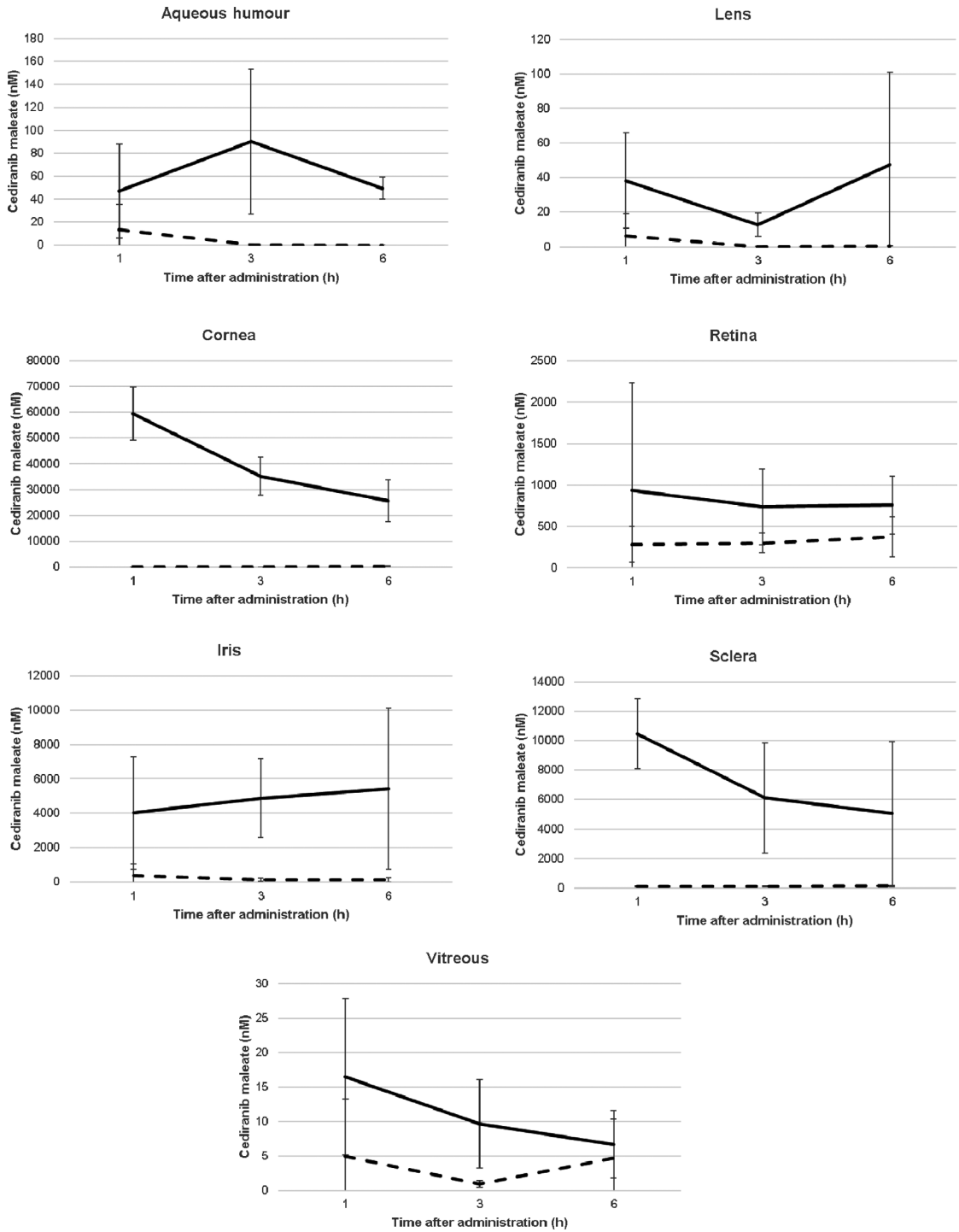


Fig. 4. Concentration of cediranib maleate (mean \pm SD; nM, $n = 6$) in the different eye tissues of the study eye (solid line) and the untreated fellow eye (dotted line) at different time-points after administration of 3% eye drop formulation.

3.6. *In vivo* studies

The pharmacokinetic data regarding rabbit eye tissue distribution of γ -cyclodextrin 3% (w/v) cediranib maleate in both anterior and posterior segment of the eye, as well as the concentration in blood samples, at different time-points after administration (1, 3 and 6 hr) are shown in the tables and figures below (Tables 3 and 4) (Figs. 4 and 5):

4. Discussion

4.1. Effect of stabilizers on thermal stability of cediranib maleate

In the case of polymers, the drug survived from heat due to different types of polymeric stabilizers similarly. Cellulose derivatives and other polymers also have been shown to have a stabilizing effect on CD aggregates (Loftsson et al 1994; Ryzhakov et al 2016). In aqueous solutions, it is believed that polymers reduce CD mobility by changing the hydration properties of CD molecules (Loftsson et al 2005; Veiga 2006). The steric inclusion–dissociation behaviours between host and guest molecules response to temperature change (Amiri & Amiri 2017). Thus, the elevated temperature due to autoclaving process may change the rotation of tested polymers to γ CD and cediranib maleate/ γ CD complexes that caused a steric barrier against thermal degradation of the drug.

The stabilizers with at least 95% of drug content according to European Pharmacopeia general text (Ph. Eur. 2.9.40) specification such as PG, glycerol, PVA, HPMC and poloxamer 407 were also selected to further formulate the aqueous eye drops. Tyloxapol was also a good choice, but, because this

polymer can generate bubbles as well as the drug itself, it was excluded from the study.

The formulation remained stable with acceptable values of 102% drug content, 23% liquid fraction and 74% solid fraction. Other studies have been proved that about 70–75% or two-thirds of the total drug in solid part provided high sustained concentrations of dissolved drug over time and helped deliver the drug to the back of the eye (Jansook et al 2010; Jóhannesson et al 2014; Loftsson & Stefánsson 2017; Johannsdottir et al 2018). The eye drops with this fraction ratio had shown a significant clinical effect in patients with diabetic macular oedema (DME) or with non-infectious uveitic macular oedema and vitritis (Ohira et al 2015; Shulman et al 2015).

The pH of the binary complex apparently affected the thermal stability of cediranib maleate (Fig. 2B). The drug had lower thermal degradation at acidic environment. pH 5 was the optimal point to be used in further study.

4.2. *In vivo* studies

Cediranib maleate was detected in all studied tissues after topical administration in γ -cyclodextrin eye drop nanosuspension. Moreover, the drug concentration levels are significantly higher in the treated eye compared with the untreated eye. Regarding the blood samples, the peak concentration of cediranib maleate, 14.4 ± 7.6 (nM, mean \pm SD, $n = 6$), was detected 3 hr after the administration. The drug levels in the blood samples are substantially lower than the concentrations in the ocular tissues, especially compared with the retina, which is the target site of the drug. This suggests that little systemic absorption is present after the administration and that the eye drop suspension delivers cediranib maleate locally in the ocular tissues, which would contribute to minimizing systemic side effects.

As recently reported by Lucy et al. cediranib has been shown to inhibit VEGF-stimulated proliferation and VEGFR-2 phosphorylation in human umbilical vein endothelial cells, with IC_{50} values of 0.4 and 0.5 nM respectively (Lucy et al 2017). According to these data, our results show drug concentrations 10 times higher than the

reported IC_{50} in the vitreous and more than 100 times higher in the retina, suggesting that the drug is delivered in therapeutically active concentrations to the posterior segment of the eye.

Several studies have been performed to determine the pharmacokinetic properties of γ -cyclodextrin/drug complexes after topical administration to the eye. Johannsdóttir et al. recently investigated whether topically applied dexamethasone/ γ CD micro-suspension could deliver dexamethasone to various tissues of the eye in therapeutic concentrations in rabbits. Maximum drug concentrations were reached after 2 hr of the administration in all tissues. Regarding the delivery to the anterior segment, the highest concentrations of 7600, 2300, 430 and 130 nM were found in the cornea, iris, aqueous humour and lens respectively. For the sclera, retina and vitreous humour, the highest concentrations were 1530, 510 and 150 nM respectively (Johannsdottir et al 2018). These results are in agreement with those obtained in our study, where the highest concentrations were found in the cornea, iris, sclera and retina. This supports that γ -cyclodextrins represents an effective drug delivery system from the surface of the eye to the posterior segment in rabbits.

5. Conclusions

The formulated eye drops with aqueous 3% (w/v) cediranib maleate micro-suspension containing γ CD nanoparticles successfully delivered the drug to both anterior and posterior segments of the eye after topical application. Cediranib maleate was detected in all treated eye tissues tested in this study, with relatively high concentrations, suggesting that the drug can penetrate the eye *via* both corneal and conjunctiva–sclera routes. Moreover, compared with the reported IC_{50} value for the VEGF type-II receptor (Lacy et al 2017), the drug is delivered in concentrations above its therapeutic level into the rabbit retina.

Therefore, our results suggest that cediranib maleate in γ CD micro-suspension eye drops could provide a new treatment as an anti-VEGF therapy to the back of the eye, potentially replacing the need for invasive intraocular drug delivery such as repeated intravitreal injections.

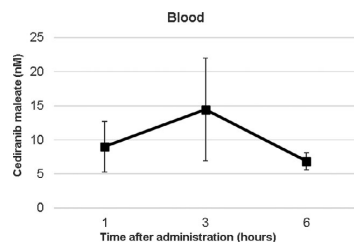


Fig. 5. Concentration of cediranib maleate (mean \pm SD; nM, $n = 6$) in blood samples at different time-points after administration of 3% eye drop formulation.

References

- Amadio M, Govoni S & Pascale A (2016): Targeting VEGF in eye neovascularization: What's new?: A comprehensive review on current therapies and oligonucleotide-based interventions under development. *Pharmacol Res* **103**: 253–269.
- Amiri S & Amiri S (2017): *Cyclodextrins: Properties and Industrial Applications*.
- Bhattacharjee S (2016): DLS and zeta potential - What they are and what they are not? *J Control Release* **235**: 337–351.
- Cheung N, Mitchell P & Wong TY (2010): Diabetic retinopathy. *Lancet* **376**: 124–136.
- Cook HL, Patel PJ & Tufail A (2008): Age-related macular degeneration: Diagnosis and management. *Br Med Bull* **85**: 127–149.
- Dietrich J, Wang D & Batchelor TT (2009): Cediranib - Profile of a novel anti-angiogenic agent in patients with glioblastoma. *Expert Opin Investig Drugs* **18**: 1549–1557.
- Falavarjani KG & Nguyen QD (2013): Adverse events and complications associated with intravitreal injection of anti-VEGF agents: A review of literature. *Eye* **27**: 787–794.
- Göktürk S, Çalişkan E, Talman RY & Var U (2012): A study on solubilization of poorly soluble drugs by cyclodextrins and micelles: Complexation and binding characteristics of sulfamethoxazole and trimethoprim. *Sci World J* **2012**: 718791.
- Higuchi T & Connors KA (1965): Phase solubility techniques. *Adv Anal Chem Instrum* **4**: 4117–4212.
- Jansook P, Praphanwittaya P, Sripecth S & Loftsson T (2020): Solubilization and in vitro permeation of dovitinib/cyclodextrin complexes and their aggregates. *J Incl Phenom Macrocycl Chem* **97**: 195–203.
- Jansook P, Stefánsson E, Thorsteinsdóttir M, Sigurdsson BB, Kristjánsdóttir SS, Bas JF, Sigurdsson HH & Loftsson T (2010): Cyclodextrin solubilization of carbonic anhydrase inhibitor drugs: Formulation of dorzolamide eye drop microparticle suspension. *Eur J Pharm Biopharm* **76**: 208–214.
- Jóhannesson G, Moya-Ortega MD, Ásgrímsdóttir GM, Lund SH, Thorsteinsdóttir M, Loftsson T & Stefánsson E (2014): Kinetics of γ -cyclodextrin nanoparticle suspension eye drops in tear fluid. *Acta Ophthalmol* **92**: 550–556.
- Johannsdottir S, Jansook P, Stefánsson E et al. (2018): Topical drug delivery to the posterior segment of the eye: Dexamethasone concentrations in various eye tissues after topical administration for up to 15 days to rabbits. *J Drug Deliv Sci Technol* **45**: 449–454.
- Lacy SA, Miles DR & Nguyen LT (2017): Clinical Pharmacokinetics and Pharmacodynamics of Cabozantinib. *Clin Pharmacokinet* **56**: 477–491.
- Loftsson T (2013): *Drug Stability for Pharmaceutical Scientists*. London: Academic Press.
- Loftsson T, Frikdriksdóttir H, Sigurkdardóttir AM & Ueda H (1994): The effect of water-soluble polymers on drug-cyclodextrin complexation. *Int J Pharm* **110**: 169–177.
- Loftsson T, Hreinsdóttir D & Stefánsson E (2007): Cyclodextrin microparticles for drug delivery to the posterior segment of the eye: Aqueous dexamethasone eye drops. *J Pharm Pharmacol* **59**: 629–635.
- Loftsson T, Jarho P, Másson M & Järvinen T (2005): Cyclodextrins in drug delivery. *Expert Opin Drug Deliv* **2**(2), 335–351.
- Loftsson T & Stefánsson E (2017): Cyclodextrins and topical drug delivery to the anterior and posterior segments of the eye. *Int J Pharm* **531**: 413–423.
- Moisseiev E & Loewenstein A (2017): Drug delivery to the posterior segment of the eye. *Dev Ophthalmol* **58**: 87–101.
- Ohira A, Hara K, Jóhannesson G, Tanito M, Ásgrímsdóttir GM, Lund SH, Loftsson T & Stefánsson E (2015): Topical dexamethasone γ -cyclodextrin nanoparticle eye drops increase visual acuity and decrease macular thickness in diabetic macular oedema. *Acta Ophthalmol* **93**: 610–615.
- Patel A, Cholkar K, Agrahari V & Mitra AK (2013): Ocular drug delivery systems: An overview. *World J Pharmacol* **2**: 47–64.
- Phillip Lee YH, Sathigari S, Jean Lin YJ et al. (2009): Gefitinib/cyclodextrin inclusion complexes: physico-chemical characterization and dissolution studies Gefitinib/cyclodextrin inclusion complexes. *Drug Dev Ind Pharm* **35**: 1113–1120.
- Praphanwittaya P, Saokham P, Jansook P & Loftsson T (2020): Aqueous solubility of kinase inhibitors: I the effect of hydrophilic polymers on their γ -cyclodextrin solubilization. *J Drug Deliv Sci Technol* **55**: 101462.
- Praphanwittaya P, Saokham P, Jansook P & Loftsson T (2021): Solubility and stability of cediranib maleate. *J Drug Deliv Sci Technol* **62**: 102359.
- Radu CD, Parteni O & Ochiuz L (2016): Applications of cyclodextrins in medical textiles — review. *J Control Release* **224**: 146–157.
- Ryzhakov A, Do Thi T, Stappaerts J et al. (2016): Self-Assembly of Cyclodextrins and Their Complexes in Aqueous Solutions. *J Pharm Sci* **105**: 2556–2569.
- Saokham P & Loftsson T (2015): A New Approach for Quantitative Determination of γ -Cyclodextrin in Aqueous Solutions: Application in Aggregate Determinations and Solubility in Hydrocortisone/ γ -Cyclodextrin Inclusion Complex. *J Pharm Sci* **104**(11): 3925–3933.
- Shi S, Peng F, Zheng Q, Zeng L, Chen H, Li X & Huang J (2019): Micelle-solubilized axitinib for ocular administration in anti-neovascularization. *Int J Pharm* **560**: 19–26.
- Shibuya M (2011): Vascular endothelial growth factor (VEGF) and its receptor (VEGFR) signaling in angiogenesis: A crucial target for anti- and pro-angiogenic therapies. *Genes Cancer* **2**: 1097–1105.
- Shulman S, Jóhannesson G, Stefánsson E, Loewenstein A, Rosenblatt A & Habet-Wilner Z (2015): Topical dexamethasone-cyclodextrin nanoparticle eye drops for non-infectious Uveitic macular oedema and vitritis - A pilot study. *Acta Ophthalmol* **93**: 411–415.
- Stetefeld J, McKenna SA & Patel TR (2016): Dynamic light scattering: a practical guide and applications in biomedical sciences. *Biophys Rev* **8**: 409–427.
- Tóth Gergő Jánoska Á, Völgyi G, Szabó ZI, Orgován G, Mirzahosseini A & Noszáli B (2017): Physicochemical characterization and cyclodextrin complexation of the anticancer drug lapatinib. *J Chem* **2017**: 1–9.
- Tóth Gergő Jánoska Á, Szabó ZI, Völgyi G, Orgován G, Szenté L & Noszáli B (2016): Physicochemical characterisation and cyclodextrin complexation of erlotinib. *Supramol Chem* **28**: 656–664.
- Veiga F (2006): As ciclodextrinas em tecnologia farmaceutica. Coimbra: Minerva Coimbra.

The p-value indicates the difference ($p < 0.05$) in concentration levels of cediranib maleate between the study eye and the untreated fellow eye at each time-point after administration.

Received on November 26th, 2021.
Accepted on January 4th, 2022.

Correspondence: Laura Lorenzo-Soler, MSc
Faculty of Medicine
University of Iceland
Reykjavík, Iceland
Tel: +354 767 7313

Email: lauralrnzs@gmail.com

Paper III

Corneal and conjunctival-scleral routes for topical ocular drug delivery.

Laura Lorenzo-Soler, MSc*

Olof B. Olafsdottir, PhD

Einar Stefánsson, MD, PhD

Faculty of Medicine, University of Iceland, Reykjavík, Iceland.

*Corresponding author:

Mailing address: Faculty of Medicine, University of Iceland, Vatnsmyrarvegur 16, 101 Reykjavík

Phone: +354 7677313

E-mail: lls10@hi.is

DRAFT

Abstract

Purpose: Eye drops deliver drugs through the cornea into the aqueous humour and anterior segment. We propose that topical drug delivery to the posterior segment predominantly traverses the conjunctiva-sclera-choroid on its way to the retina. The exposed surface of the conjunctiva-sclera is twice the area of the cornea and the location is closer to the retina and posterior segment.

In this study, we measure the *ex-vivo* permeability of different compounds across full-thickness cornea and conjunctiva-sclera-choroid-retina to test the hypothesis that conjunctiva-sclera rather than the cornea is the major pathway for drugs to the posterior segment.

Materials and methods: We measured the permeability of 27 different molecular compounds using Franz-diffusion cells across porcine eye tissues, including full-thickness cornea and conjunctiva-sclera-choroid-retina, for their structural resemblance with the human eye.

Results: 22 out of the 27 compounds (81%) showed a higher permeability across conjunctiva-sclera-choroid-retina than full-thickness cornea. The mean permeability across conjunctiva-sclera was 3 times higher than the corneal.

Discussion: Our data indicate that the conjunctiva-sclera is about 3 times more permeable for most compounds than the cornea. The conjunctiva-sclera has a closer location to the retina than the cornea, where aqueous humour currents and crystalline lens present additional barriers to drug delivery, and presents about double the exposed surface. These findings suggest that the conjunctiva-sclera-choroid-retina is a more important route for drug delivery to the posterior segment than the cornea.

1 Introduction

To date, topical drug delivery to the eye has been limited to treatment of diseases in the ocular surface and anterior segment, and it has been generally assumed that the way through which drugs penetrate the eye after topical administration is the corneal route (Agarwal & Rupenthal, 2016; Barar et al., 2008). This route, however, presents different anatomical barriers that act as rate-limiting steps for drugs, including the epithelium, which hinders the permeation of hydrophilic substances, and the corneal stroma, which, in contrast, limits the penetration of lipophilic compounds (Gaudana et al., 2010). Moreover, blindness leading disorders generally take place in the back of the eye, where topical drug delivery through the corneal route is inefficient due to the distance to target tissues (Maurice, 2002).

The current standard treatment for posterior segment disorders is intravitreal injection (Moisseiev & Loewenstein, 2017). This procedure allows high levels of drugs to be delivered in the vitreous, however, it is associated with the risk of complications due to the invasiveness of the procedure and the need for long treatments with repeated injections (Edelhauser et al., 2010; Falavarjani & Nguyen, 2013).

The conjunctival-scleral route has gained increasing interest as an alternative pathway of drug delivery to the posterior segment. Some of its advantages over the corneal route include a higher relative permeability to potential drug compounds, fewer structural barriers to drug diffusion (i.e., lens, aqueous humour, vitreous) and a closer location to the back of the eye compared with the cornea, which has been estimated to be between 1.7-2.2 cm (Ranta & Urtti, 2006; Serway & Beichner, 2000; Yves Le Grand, 1968).

Moreover, the conjunctiva-sclera has a mean total surface area of 16-17 cm², which is relatively large compared with a corneal surface area of approximately 1 cm² (Olsen et al., 1995). Although a clear measurement of the area of exposed sclera has not been found in the literature, several studies have calculated the index of the size of visible sclera, which has been reported to be twice that of the cornea, suggesting a significantly larger avenue for drug diffusion to the inside of the eye (Caspar et al., 2021; Danel et al., 2018; Kobayashi & Kohshima, 1997, 2001). These facts suggest that the conjunctival-sclera

route could represent a more important and efficient way of topical drug delivery to the back of the eye (Ahmed & Patton, 1985; Hämäläinen et al., 1997; Lee et al., 2004).

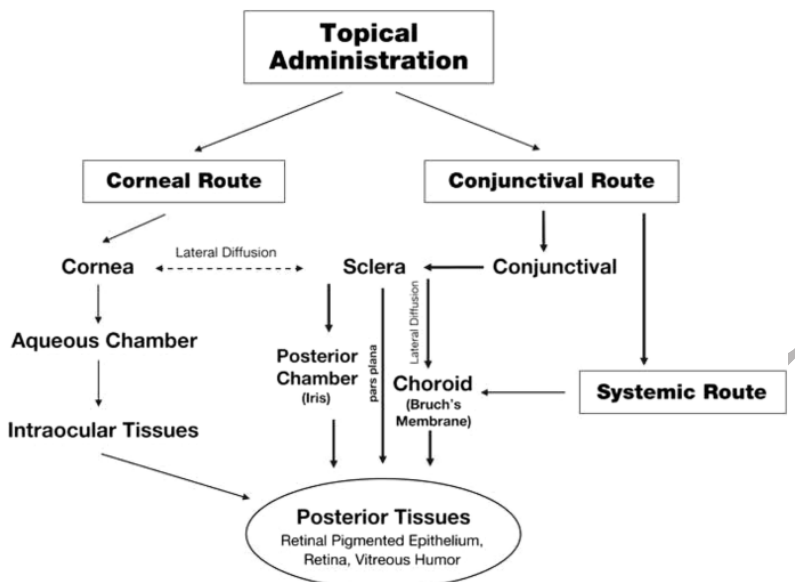


Figure 1. Drug distribution pathways through the corneal and conjunctival/scleral routes following topical administration (Rodrigues et al., 2018).

To test this hypothesis, we compared the *ex vivo* permeability of 27 molecular compounds with different physicochemical properties. We used porcine ocular tissues, for their resemblance with the human eye regarding anatomy, size and structure, mounted on Franz-diffusion cells (Nicoli et al., 2009; Olsen et al., 2002; Sanchez et al., 2011). In addition, the *ex vivo* permeability data were correlated with different properties for our compounds to find the most relevant characteristics affecting permeability across full-thickness cornea and conjunctiva-sclera.

2 Materials and methods

2.1 Test compounds

27 drug-like compounds with different physicochemical properties were used for the permeability experiments using Franz-diffusion cells and porcine ocular tissues, including full-thickness cornea and conjunctiva-sclera-choroid-retina. The compounds were dissolved in ultrapure water at concentrations according to their water solubilities. The compounds used were: acetazolamide, ampicillin sodium, atenolol, brimonidine tartrate, bromfenac sodium, caffeine, candesartan, chlorpheniramine maleate, ciprofloxacin hydrochloride, dexamethasone, fluconazole, fluorescein, flurbiprofen, hesperetin, hesperidin, hydroquinone, imidazole, labetalol hydrochloride, lincomycin hydrochloride, metoprolol tartrate, nadolol, pilocarpine hydrochloride, prednisolone, propranolol hydrochloride, riboflavin, timolol maleate, xylometazoline hydrochloride.

2.2 Tissue preparation

Fresh porcine eyes were obtained from a local slaughterhouse. The eyes were transported in PBS and refrigeration and stored at -80°C within one hour of collection and until use.

Before proceeding with dissection, the eyes were taken from storage and submerged in cold PBS for around 15 minutes, until completely thawed. To separate the corneas from the rest of the eyeball, a small cut was made at the limbus and the cornea was excised leaving approximately 1 cm of sclera around, to easily fix the tissue between the donor and receptor compartments of the Franz-diffusion cells. The conjunctiva-sclera-choroid-retina were placed in a different Franz-cell and the lens, aqueous humour and vitreous were discarded.

To ensure that the freezing-thawing procedure did not affect the integrity of the tissues, we performed preliminary experiments comparing the permeability of irbesartan across fresh and frozen full-thickness corneas and conjunctiva-sclera-choroid-retina. Irbesartan was chosen as the test compound based on the amount of substance available. The permeability values across frozen tissues were not statistically different from the ones obtained with fresh tissues.

2.3 Permeation experiments

Custom-made jacketed glass Franz-type diffusion cells with a diffusion area of 2.54 cm² were ordered from PermeGear, Inc (Hellertown, PA USA). The receptor chamber was filled with 5 ml of fresh PBS buffer, and magnetic stirring was used to avoid any boundary layer effect. The circulating water around the jacketed cells was always kept at 37 ± 0.2 °C, using a heating system connected to the cells. The tissues were placed between the receiver and the donor compartments, endothelial side down. The donor compartment was filled with 1 ml of the test solution and covered with Parafilm to avoid evaporation of the donor solution. For up to 6 hours and at established timepoints (0, 30, 60, 90, 120, 180, 240, 300 and 360 minutes) 200 µl of the receiving solution were extracted and stored at 4°C until analysis. The sampled volume in the receiving chamber was immediately replaced with fresh PBS. The experiments were carried out in triplicate for each of the compounds, using ocular bulbs from different animals.

2.4 Analytic methods

The samples extracted from the receiving phase were placed in 96-wells microplates, using a different well for each sample, and the microplates were kept at 4°C until analyzed. The analysis was carried out by fluorescence, without preliminary separation, placing the microplates in a reader equipped with a UV-Vis spectrophotometric detector (SpectraMax, Molecular Devices, San Jose, CA).

To quantify the drug concentration in the samples, two replicas of a calibration curve were prepared for each compound, with concentrations ranging from 5 to 1000 µl. We ensured that the coefficient of determination (r^2) for each of the curves was equal to or above 0.9. The drug quantification procedure was carried out at room temperature.

2.5 Permeability calculations

The individual permeability profiles for each compound and tissue were plotted as the cumulative amount of drug permeated per area (µg/cm²) as a function of time.

For those compounds that maintained sink conditions, where the drug concentration in the receiving chamber was <10% of the donor at all timepoints, the flux was calculated as the amount of drug permeated

during the steady-state period, whereas the apparent permeability coefficient (P_{app} , cm/s) was calculated as:

$$P_{app} \text{ (cm/s)} = J_{ss} / (C_d * A)$$

where J_{ss} is the flux during the steady-state period, C_d is the drug concentration in the donor compartment and A is the diffusion area of the tissue.

The steady-state of a permeation experiment is usually determined by visual inspection of the permeation profile or by approximation to the maximum observed absorption rate, which can lead to subjective and/or inaccurate results. To avoid biased estimations of the fluxes, we applied the calculations described by Niedorf et al. in their algorithm for the determination of steady-states for percutaneous permeability experiments (Niedorf et al., 2008).

On the other hand, for those compounds that did not maintain sink conditions throughout the whole experiment, the following equation, which accounts for continuous changes in both donor and receiving compartments, was used (Hubatsch et al., 2007; Kratz et al., 2011; Mangas-Sanjuan et al., 2014; Teixeira et al., 2020):

$$C_{receiver,t} = \frac{Q_{total}}{V_{receiver} + V_{donor}} + \left((C_{receiver,t-1} \cdot f) - \frac{Q_{total}}{V_{receiver} + V_{donor}} \right) \cdot e^{-P_{eff} \cdot S \cdot \left(\frac{1}{V_{receiver}} + \frac{1}{V_{donor}} \right) \cdot \Delta t}$$

where $C_{receiver,t}$ is the concentration of drug in the receptor at time t , Q_{total} is the amount of total drug in receiver and donor compartments, $V_{receiver}$ and V_{donor} are the volumes of each chamber, $C_{receiver,t-1}$ is the concentration of drug in the receptor at the previous time, f is the sample replacement dilution factor, S is the diffusion area of the tissue, Δt is the time interval and P_{eff} is the permeability coefficient (Teixeira et al., 2020).

An independent t-test was performed to compare the permeability of each compound between full-thickness cornea and conjunctiva-sclera-choroid-retina. The permeability values were considered to be statistically different with p -value < 0.05 .

2.6 Correlation between permeability and physicochemical properties

Various molecular descriptors, potentially related to drug permeability and based on previous publications were selected from different databases (Mordred, PubChem, DrugBank) using the structure of each compound (Edwards & Prausnitz, 2001; Kidron et al., 2010; Prausnitz, 1998; Ramsay et al., 2018).

We analyzed the correlations between the permeability coefficients for each tissue and the physicochemical properties of the compounds tested using Pearson's correlation coefficient (r^2). An independent t-test was used to determine the statistical significance of the obtained correlations, where p-values < 0.05 indicated that significant correlation existed between variables.

2.7 Data analysis

All calculations obtained from the permeation experiments, the analysis of data, correlation analysis and statistical tests were carried out using Python 3.0 and its open-source libraries and packages Pandas, NumPy, Scikit-learn and Seaborn.

3 Results

3.1 Corneal and conjunctival-scleral permeability

22 out of the 27 compounds tested (81%) showed a higher permeability across conjunctiva-sclera-choroid-retina than full-thickness cornea. For some compounds, the permeability across conjunctiva-sclera-choroid-retina ranged from 2 to 30-fold their permeability through full-thickness cornea. This resulted in a mean conjunctival-scleral permeability 3 times higher than the corneal. The individual permeability values, as well as the mean permeability across both tissues, are shown in the tables and figures below.

Table 1. Individual permeability values (mean \pm SD, n = 3) for each compound across full-thickness cornea and conjunctiva-sclera-choroid-retina. p-values less than 0.05 indicate that the difference in permeability between cornea and sclera is statistically significant.

Compound	Cornea	Sclera	p-value
Acetazolamide	11.9 \pm 4.8	68.5 \pm 42.5	0.00
Ampicillin sodium	2.3 \pm 0.6	14.4 \pm 8.3	0.00
Atenolol	4.4 \pm 1.2	33.1 \pm 8.5	0.00

Brimonidine tartrate	1.8 ± 0.5	5.8 ± 1.3	0.00
Bromfenac sodium	2.6 ± 0.8	8.0 ± 1.7	0.00
Caffeine	3.0 ± 1.1	4.1 ± 1.7	0.00
Candesartan	0.09 ± 0.04	0.07 ± 0.001	0.00
Chlorpheniramine maleate	5.5 ± 2.3	11.1 ± 4.0	0.00
Ciprofloxacin hydrochloride	5.2 ± 0.6	7.8 ± 3.3	0.00
Dexamethasone	3.4 ± 1.5	8.1 ± 4.7	0.00
Fluconazole	1.0 ± 0.5	15.1 ± 4.1	0.00
Fluorescein	0.2 ± 0.05	3.1 ± 0.2	0.00
Flurbiprofen	13.4 ± 1.2	2.6 ± 0.5	0.00
Hesperetin	0.7 ± 0.2	0.6 ± 0.3	0.68
Hesperidin	3.1 ± 2.1	6.4 ± 9.3	0.06
Hydroquinone	0.8 ± 0.4	0.7 ± 0.3	0.33
Imidazole	47.0 ± 22.1	66.0 ± 11.3	0.00
Labetalol hydrochloride	17.0 ± 5.7	34.1 ± 25.4	0.00
Lincomycin hydrochloride	0.8 ± 0.2	10.8 ± 8.5	0.00
Metoprolol tartrate	0.5 ± 0.2	16.1 ± 3.5	0.00
Nadolol	2.4 ± 1.1	29.2 ± 23.7	0.00
Pilocarpine hydrochloride	0.7 ± 0.03	7.3 ± 2.3	0.00
Prednisolone	4.1 ± 0.8	3.3 ± 0.4	0.00
Propranolol hydrochloride	6.6 ± 2.9	7.0 ± 2.5	0.54
Riboflavin	8.4 ± 2.8	19.3 ± 11.7	0.00
Timolol maleate	0.4 ± 0.1	1.5 ± 0.5	0.00
Xylometazoline hydrochloride	3.2 ± 1.2	65.4 ± 43.2	0.00

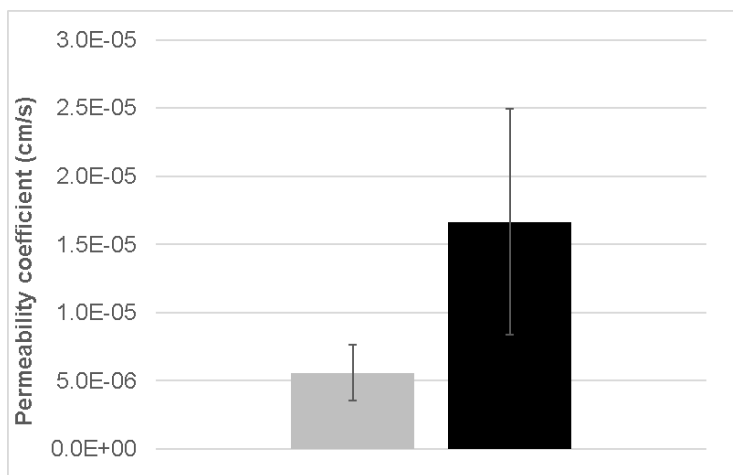


Figure 2. Mean permeability values (mean \pm SD, n = 27, bottom) for full-thickness cornea (grey) and conjunctiva-sclera-choroid-retina (black).

3.2 Comparison between fresh and frozen tissues

Regarding the use of fresh and frozen tissues, the permeability coefficient values for irbesartan across full-thickness cornea were $2.7 \pm 0.4 \times 10^{-6}$ cm/s for fresh tissues and $3.4 \pm 0.3 \times 10^{-6}$ cm/s for frozen tissues (mean \pm SD, n = 3). A p-value of 0.7 was obtained from an independent t-test, indicating that the differences in the permeability values between fresh and frozen tissues are not statistically significant. Similarly, for conjunctiva-sclera-choroid-retina we obtained permeability coefficients of $0.6 \pm 0.5 \times 10^{-6}$ cm/s for fresh tissue and $0.8 \pm 0.4 \times 10^{-6}$ cm/s for frozen tissue, with a p-value of 0.5.

3.3 Correlation between permeability and molecular properties

The permeability of our compounds across both tissues was positively affected by solubility, while it decreased with increasing number of rings and lipophilicity, measured as logP. The permeability across conjunctiva-sclera showed significant correlations with two additional properties that were not observed for full-thickness cornea: molecular weight and lipophilicity, measured as logD. The results of the correlation analysis are shown in the table below:

Table 2. Correlation results between permeability coefficient across full-thickness cornea/conjunctiva-sclera and physicochemical properties. Data is shown as Pearson's coefficient (r^2) and p-value.

Descriptor	Full-thickness cornea	Conjunctiva-sclera-choroid-retina
Solubility (logS)	0.42 (p = 0.003)	0.32 (p < 0.001)
Number of rings	-0.50 (p < 0.001)	-0.58 (p < 0.001)
LogP	-0.65 (p < 0.001)	-0.54 (p < 0.001)
LogD	-	-0.52 (p < 0.001)
Molecular weight	-	-0.42 (p < 0.001)

4 Discussion

4.1 Corneal and conjunctival-scleral permeability

Based on our results, most compounds show higher permeation rates across conjunctiva-sclera-choroid-retina when compared to full-thickness cornea. The mean permeability across conjunctiva-sclera for our molecules was 3 times higher than that of the cornea. This, added to an area of exposed tissue approximately twice larger, results in a permeability 6 times higher than the permeability across the corneal route.

Some of the compounds used in our study have been tested before using the same methodology and model and, our results are in general agreement with those reported previously by other authors. For example, our permeability value obtained for dexamethasone, $3.4 \pm 1.5 \times 10^{-6}$ cm/s, is within the range of values obtained previously across porcine corneas by other authors: $1.5 \pm 0.1 \times 10^{-6}$ cm/s (Hahne et al., 2012), $7.6 \pm 1.2 \times 10^{-6}$ cm/s (Loch et al., 2012), $0.9 \pm 0.3 \times 10^{-6}$ cm/s (Juretić et al., 2018) and $0.2 \pm 0.07 \times 10^{-6}$ cm/s (Ramsay et al., 2018).

Pescina et al. compared the permeability of propranolol hydrochloride across full-thickness cornea and conjunctiva-sclera-choroid-retina. In our case, the permeability rate across full-thickness cornea for propranolol was $6.6 \pm 2.9 \times 10^{-6}$ cm/s, which is within the range of values reported by Pescina et al., $14.6 \pm$

0.5 x 10⁻⁶ cm/s, and Ramsay et al., 1.5 ± 1.4 x 10⁻⁶ cm/s (Pescina et al., 2015; Ramsay et al., 2018). For conjunctiva-sclera-choroid-retina, on the other hand, our permeability coefficient, 7.0 ± 2.5 x 10⁻⁶ cm/s, is very similar to the one obtained by Pescina et al., 5.9 ± 2.1 x 10⁻⁶ cm/s (Pescina et al., 2012).

Noticeable variability exists between the permeability results of compounds obtained by different groups. Hahne et al. reported a permeability coefficient for fluorescein across full-thickness cornea of 0.18 ± 0.15 x 10⁻⁶ cm/s, very similar to the one obtained in our study, 0.2 ± 0.05 x 10⁻⁶ cm/s (Hahne & Reichl, 2011). Pescina et al., however, obtained a permeability value for the same compound, 0.6 ± 0.2 x 10⁻⁶ cm/s, four times higher than that reported by Hahne et al. (Pescina et al., 2015).

Loch et al. obtained a permeability value for timolol across full-thickness cornea of 5.1 ± 0.6 x 10⁻⁶ cm/s, similar to the one reported by Hahne et al., 7.1 ± 1.8 x 10⁻⁶ cm/s, but 2 times lower than the one obtained by Juretic et al., 10.7 ± 2.1 x 10⁻⁶ cm/s (Hahne et al., 2012; Juretić et al., 2018; Loch et al., 2012). These results are between 12 and 25 times higher than the result obtained in our experiments across full-thickness cornea, 0.4 ± 0.1 x 10⁻⁶ cm/s, which is more similar to the values obtained by Taka et al., 0.8 ± 0.1 x 10⁻⁶ cm/s, and Arnold et al., 0.9 ± 0.1 x 10⁻⁶ cm/s (Arnold et al., 2013; Taka et al., 2020). On the other hand, our permeability value for timolol across conjunctiva-sclera-choroid-retina, 1.5 ± 0.5 x 10⁻⁶ cm/s, is almost the same as the one reported by Loch et al., 1.3 ± 0.4 x 10⁻⁶ cm/s (Loch et al., 2012).

4.2 Correlation between permeability and molecular properties

4.2.1 Lipophilicity

Permeation through cornea has been shown to follow a parabolic relationship with an optimal logP of 2–3 and that, at high lipophilicity values (logP > 4), the corneal permeability decreases, presumably due to the poor desorption from the lipoidal epithelium to the hydrophilic stroma (Rimpelä et al., 2018; Schoenwald & Ward, 1978). The sclera shows a structure comparable to the corneal stroma, with a high degree of water content that renders it conducive to hydrophilic molecules (Miao et al., 2013; Pitkänen et al., 2005). Kadam et al. studied the influence of permeant lipophilicity on the permeability across conjunctiva- sclera-choroid-retina, showing higher permeability for hydrophilic molecules when compared to lipophilic ones (Kadam et al., 2011). Similarly, Cheruvu and Kompella found that the solute permeability coefficients measured in

both bovine and porcine sclera exhibited a negative correlation with the logarithm of distribution coefficients (Cheruvu & Kompella, 2006).

Regarding the cornea, Balla et al obtained in their study that lipophilicity shows a positive relationship with the permeability across the epithelium but inversely correlates with the permeability across the stroma, indicating that this layer is the rate-limiting step for lipophilic compounds (Balla et al., 2021). Sieg et al. reported the behaviour of fluorometholone and pilocarpine across cornea, concluding that these lipophilic compounds readily penetrate the intact corneal epithelium and accumulate in the hydrophilic stroma! layers of the cornea (Sieg & Robinson, 1981).

4.2.2 *Solubility*

Low aqueous solubility of drugs is one of the main challenges in drug development. Hydrophobicity of poorly soluble compounds causes a limited capacity to combine with the surrounding water phase and partition into the tissues, causing low bioavailabilities after administration (Bergström & Larsson, 2018; Praphanwittaya et al., 2020). Higher lipophilicity correlates with lower water solubility, which explains the opposite correlation between these descriptors and the permeability across both cornea and conjunctiva-sclera. Thakur et al. studied the permeability of different corticosteroids related to their lipophilicity and solubility. They concluded that higher transscleral diffusion correlated with higher aqueous solubilities and decreased with increasing lipophilicity (Thakur et al., 2011).

4.2.3 *Molecular weight*

The inverse relationship between the molecular weight and the permeation of compounds through ocular tissues has been reported previously. Miao et al. studied the permeability of macromolecules through the noncorneal route and concluded that larger molecules are more likely to accumulate in the outer surface, hampering their permeability across the tissue. They suggested that differences in thickness between topographical locations of the sclera may have pharmacokinetic implications when considering transscleral diffusion of macromolecules (Miao et al., 2013).

4.2.4 Number of rings

The number of rings counts the number of cyclic structures present in a compound, where one or more series of atoms are connected forming a ring. This descriptor shows a high positive correlation with the molecular weight of the compound ($r^2 = 0.64$), indicating that a greater number of rings lead to an increase in the mass and size of a compound. This association explains the negative effect of the number of rings on permeability through both corneal and conjunctival-sclera routes.

This is, to the best of our knowledge, the first study to systematically compare the permeability of multiple compounds, with differing physicochemical properties, across the corneal and scleral-conjunctival routes. The permeability of drugs across the ocular tissues has been extensively studied, however, most studies have focused on limited groups of compounds with similar properties (i.e., macromolecules, lipophilic compounds...) or using isolated layers to understand the mechanisms independently.

Our results are in general agreement with the literature, indicating that *ex vivo* permeability studies using Franz-diffusion cells represent a good resource for the preliminary testing of compounds as an alternative to *in vivo* studies. Although this methodology often suffers from poor reproducibility, validation of the protocol and refinement of the technique can greatly reduce variability in the resulting data and increase the reproducibility (Ng et al., 2010).

We were able to obtain significant correlations for both full-thickness cornea and conjunctiva-sclera-choroid-retina with a limited number of compounds, representing a narrow chemical space. Performing these experiments with a high number of molecules will provide more relevant information on the matter, but it will require a considerable amount of time and resources. Understanding which descriptors affect the permeability of compounds across biological membranes could represent a fast and easy-to-use method for preliminary screening and selection of molecules (Kidron et al., 2010; Ramsay et al., 2018). Especially in the early stages of drug development, where no experimental data is available, the rapid evaluation of drug candidates could minimize major failures in later steps of the process and offer an alternative to the use of animal studies (del Amo, 2015; Deng et al., 2016; Moiseev et al., 2019).

5 Conclusions

Our data indicate that the conjunctival-scleral permeability for most drug-like compounds is much higher than the corneal. In addition, the area of exposed conjunctiva-sclera has been reported to be twice that of the cornea, providing a larger avenue for drug diffusion to the intraocular tissues (Caspar et al., 2021; Danel et al., 2018; Kobayashi & Kohshima, 1997, 2001). Another advantage of this route regarding drug delivery to the posterior segment is its close location to the retina, which significantly shortens the distance molecules need to diffuse across compared with the cornea. This suggests that the conjunctiva-sclera might be an important alternative to topically deliver drugs to the posterior segment.

6 Funding

This study has received funding from the European Union's Horizon 2020; research and innovation program, under the Marie Skłodowska-Curie ITN grant agreement No 765441.

7 References

- Agarwal, P., & Rupenthal, I. D. (2016). In vitro and ex vivo corneal penetration and absorption models. *Drug Delivery and Translational Research*, 6(6), 634–647. <http://dx.doi.org/10.1007/s13346-015-0275-6>
- Ahmed, I., & Patton, T. F. (1985). Importance of the noncorneal absorption route in topical ophthalmic drug delivery. *Investigative Ophthalmology and Visual Science*, 26(4), 584–587.
- Arnold, J. J., Hansen, M. S., Gorman, G. S., Inoue, T., Rao, V., Spellens, S., Hunsinger, R. N., Chapleau, C. A., Pozzo-Miller, L., Daniel Stamer, W., & Challa, P. (2013). The effect of Rho-associated kinase inhibition on the ocular penetration of timolol maleate. *Investigative Ophthalmology and Visual Science*, 54(2), 1118–1126.
- Balla, A., Auriola, S., Grey, A. C., Demarais, N. J., Valtari, A., Heikkinen, E. M., Toropainen, E., Urtti, A., Vellonen, K. S., & Ruponen, M. (2021). Partitioning and spatial distribution of drugs in ocular surface tissues. *Pharmaceutics*, 13(5), 1–15.
- Barar, J., Javadzadeh, A. R., & Omid, Y. (2008). Ocular novel drug delivery: Impacts of membranes and

- barriers. *Expert Opinion on Drug Delivery*, 5(5), 567–581.
- Bergström, C. A. S., & Larsson, P. (2018). Computational prediction of drug solubility in water-based systems: Qualitative and quantitative approaches used in the current drug discovery and development setting. *International Journal of Pharmaceutics*, 540(1–2), 185–193.
<https://doi.org/10.1016/j.ijpharm.2018.01.044>
- Caspar, K. R., Biggemann, M., Geissmann, T., & Begall, S. (2021). Ocular pigmentation in humans, great apes, and gibbons is not suggestive of communicative functions. *Scientific Reports*, 11(1).
- Cheruvu, N. P. S., & Kompella, U. B. (2006). Bovine and Porcine Transscleral Solute Transport. *Investigative Ophthalmology & Visual Science*, 47(10), 1–7.
- Danel, D. P., Waciewicz, S., Lewandowski, Z., Żywiczyński, P., & Perea-Garcia, J. O. (2018). Humans do not perceive conspecifics with a greater exposed sclera as more trustworthy: a preliminary cross-ethnic study of the function of the overexposed human sclera. *Acta Ethologica*, 21(3), 203–208.
- del Amo, E. M. (2015). *Ocular and systemic pharmacokinetic models for drug discovery and development* [University of Helsinki]. <https://helda.helsinki.fi/handle/10138/156330>
- Deng, F., Ranta, V. P., Kidron, H., & Urtili, A. (2016). General Pharmacokinetic Model for Topically Administered Ocular Drug Dosage Forms. *Pharmaceutical Research*, 33(11), 2680–2690.
<http://dx.doi.org/10.1007/s11095-016-1993-2>
- Edelhauser, H. F., Rowe-Rendleman, C. L., Robinson, M. R., Dawson, D. G., Chader, G. J., Grossniklaus, H. E., Rittenhouse, K. D., Wilson, C. G., Weber, D. A., Kuppermann, B. D., Csaky, K. G., Olsen, T. W., Kompella, U. B., Holers, V. M., Hageman, G. S., Gilger, B. C., Campochiaro, P. A., Whitcup, S. M., & Wong, W. T. (2010). Ophthalmic Drug Delivery Systems for the Treatment of Retinal Diseases: Basic Research to Clinical Applications. *Investigative Ophthalmology & Visual Science*, 51(11), 5403. <http://iovs.arvojournals.org/article.aspx?doi=10.1167/iovs.10-5392>
- Edwards, A., & Prausnitz, M. R. (2001). Predicted permeability of the cornea to topical drugs. *Pharmaceutical Research*, 18(11), 1497–1508.
- Falavarjani, K. G., & Nguyen, Q. D. (2013). Adverse events and complications associated with

- intravitreal injection of anti-VEGF agents: A review of literature. *Eye (Basingstoke)*, 27(7), 787–794. <http://dx.doi.org/10.1038/eye.2013.107>
- Gaudana, R., Ananthula, H. K., Parenky, A., & Mitra, A. K. (2010). Ocular drug delivery. *The AAPS Journal*, 12(3), 348–360.
- Hahne, M., & Reichl, S. (2011). Development of a serum-free human cornea construct for in vitro drug absorption studies: The influence of varying cultivation parameters on barrier characteristics. *International Journal of Pharmaceutics*, 416(1), 268–279. <http://dx.doi.org/10.1016/j.ijpharm.2011.07.004>
- Hahne, M., Zorn-Kruppa, Mi., Guzman, G., Brandner, J. M., Haltner-Ukomado, E., Wätzig, H., & Reichl, S. (2012). Prevalidation of a Human Cornea Construct as an Alternative to Animal Corneas for In Vitro Drug Absorption Studies. *Journal of Pharmaceutical Sciences*, 101(8), 2976–2988. <http://onlinelibrary.wiley.com/doi/10.1002/jps.22007/full%5Cnhttp://www.ncbi.nlm.nih.gov/pubmed/19967780>
- Hämäläinen, K. M., Kananen, K., Auriola, S., Kontturi, K., & Urtti, A. (1997). Characterization of paracellular and aqueous penetration routes in cornea, conjunctiva, and sclera. *Investigative Ophthalmology and Visual Science*, 38(3), 627–634.
- Hubatsch, L., Ragnarsson, E. G. E., & Artursson, P. (2007). Determination of drug permeability and prediction of drug absorption in Caco-2 monolayers. *Nature Protocols*, 2(9), 2111–2119.
- Juretić, M., Cetina-Čižmek, B., Filipović-Grčić, J., Hafner, A., Lovrić, J., & Pepić, I. (2018). Biopharmaceutical evaluation of surface active ophthalmic excipients using in vitro and ex vivo corneal models. *European Journal of Pharmaceutical Sciences*, 120(November 2017), 133–141.
- Kadam, R. S., Cheruvu, N. P. S., Edelhauser, H. F., & Kompella, U. B. (2011). Sclera-choroid-RPE transport of eight β -blockers in human, bovine, porcine, rabbit, and rat models. *Investigative Ophthalmology and Visual Science*, 52(8), 5387–5399.
- Kidron, H., Vellonen, K. S., Del Amo, E. M., Tissari, A., & Urtti, A. (2010). Prediction of the corneal permeability of drug-like compounds. *Pharmaceutical Research*, 27(7), 1398–1407.

- Kobayashi, H., & Kohshima, S. (1997). Unique morphology of the human eye. *Nature*, 387(1992), 766–767.
- Kobayashi, H., & Kohshima, S. (2001). Unique morphology of the human eye and its adaptive meaning: Comparative studies on external morphology of the primate eye. *Journal of Human Evolution*, 40(5), 419–435.
- Kratz, J. M., Teixeira, M. R., Koester, L. S., & Simões, C. M. O. (2011). An HPLC-UV method for the measurement of permeability of marker drugs in the Caco-2 cell assay. *Brazilian Journal of Medical and Biological Research*, 44(6), 531–537.
- Lee, S. B., Geroski, D. H., Prausnitz, M. R., & Edelhauser, H. F. (2004). Drug delivery through the sclera: Effects of thickness, hydration, and sustained release systems. *Experimental Eye Research*, 78(3), 599–607.
- Loch, C., Zakelj, S., Kristl, A., Nagel, S., Guthoff, R., Weitschies, W., & Seidlitz, A. (2012). Determination of permeability coefficients of ophthalmic drugs through different layers of porcine, rabbit and bovine eyes. *European Journal of Pharmaceutical Sciences*, 47(1), 131–138.
<http://dx.doi.org/10.1016/j.ejps.2012.05.007>
- Mangas-Sanjuan, V., González-Álvarez, I., González-Álvarez, M., Casabó, V. G., & Bermejo, M. (2014). Modified nonsink equation for permeability estimation in cell monolayers: Comparison with standard methods. *Molecular Pharmaceutics*, 11(5), 1403–1414.
- Maurice, D. M. (2002). Drug delivery to the posterior segment from drops. *Survey of Ophthalmology*, 47 Suppl 1(August), S41-52. <http://www.ncbi.nlm.nih.gov/pubmed/12204700>
- Miao, H., Wu, B. D., Tao, Y., & Li, X. X. (2013). Diffusion of macromolecules through sclera. *Acta Ophthalmologica*, 91(1), 1–6.
- Moiseev, R. V., Morrison, P. W. J., Steele, F., & Khutoryanskiy, V. V. (2019). Penetration enhancers in ocular drug delivery. *Pharmaceutics*, 11(7).
- Moisseiev, E., & Loewenstein, A. (2017). Drug delivery to the posterior segment of the eye. *Developments in Ophthalmology*, 58, 87–101.

- Ng, S. F., Rouse, J. J., Sanderson, F. D., Meidan, V., & Eccleston, G. M. (2010). Validation of a static Franz diffusion cell system. *AAPS PharmSciTech*, 11(3), 1432–1441. <https://doi.org/10.1007/s11997-010-9141-1>.
- Nicoli, S., Ferrari, G., Quarta, M., Macaluso, C., Govoni, P., Dallatana, D., & Santi, P. (2009). Porcine sclera as a model of human sclera for in vitro transport experiments: histology, SEM, and comparative permeability. *Molecular Vision*, 15(November 2008), 259–266. <http://www.ncbi.nlm.nih.gov/pubmed/19190734> <http://www.pubmedcentral.nih.gov/articlerender.fcgi?artid=PMC2633461>
- Niedorf, F., Schmidt, E., & Kietzmann, M. (2008). The automated, accurate and reproducible determination of steady-state permeation parameters from percutaneous permeation data. *ATLA Alternatives to Laboratory Animals*, 36(2), 201–213.
- Olsen, T. W., Edelhauser, H. F., Lim, J. I., & Geroski, D. H. (1995). Human scleral permeability: Effects of age, cryotherapy, transscleral diode laser, and surgical thinning. *Investigative Ophthalmology and Visual Science*, 36(9), 1893–1903.
- Olsen, T. W., Sanderson, S., Feng, X., & Hubbard, W. C. (2002). Porcine sclera: Thickness and surface area. *Investigative Ophthalmology and Visual Science*, 43(8), 2529–2532.
- Pescina, S., Govoni, P., Potenza, A., Padula, C., Santi, P., & Nicoli, S. (2015). Development of a convenient ex vivo model for the study of the transcorneal permeation of drugs: Histological and permeability evaluation. *Journal of Pharmaceutical Sciences*, 104(1), 63–71.
- Pescina, S., Santi, P., Ferrari, G., Padula, C., Cavallini, P., Govoni, P., & Nicoli, S. (2012). Ex vivo models to evaluate the role of ocular melanin in trans-scleral drug delivery. *European Journal of Pharmaceutical Sciences*, 46(5), 475–483. <http://dx.doi.org/10.1016/j.ejps.2012.03.013>
- Pitkänen, L., Ranta, V. P., Moilanen, H., & Urtti, A. (2005). Permeability of retinal pigment epithelium: Effects of permeant molecular weight and lipophilicity. *Investigative Ophthalmology and Visual Science*, 46(2), 641–646.

- Praphanwittaya, P., Saokham, P., Jansook, P., & Loftsson, T. (2020). Aqueous solubility of kinase inhibitors: I the effect of hydrophilic polymers on their γ -cyclodextrin solubilization. *Journal of Drug Delivery Science and Technology*, 55(December 2019).
- Prausnitz, M. R. (1998). Permeability of cornea, sclera, and conjunctiva: A literature analysis for drug delivery to the eye. *Journal of Pharmaceutical Sciences*, 87(12), 1479–1488.
- Ramsay, E., del Amo, E. M., Toropainen, E., Tengvall-Unadike, U., Ranta, V. P., Urtti, A., & Ruponen, M. (2018). Corneal and conjunctival drug permeability: Systematic comparison and pharmacokinetic impact in the eye. *European Journal of Pharmaceutical Sciences*, 119(April), 83–89. <https://doi.org/10.1016/j.ejps.2018.03.034>
- Ranta, V. P., & Urtti, A. (2006). Transscleral drug delivery to the posterior eye: Prospects of pharmacokinetic modeling. *Advanced Drug Delivery Reviews*, 58(11), 1164–1181.
- Rimpelä, A. K., Reunanen, S., Hagström, M., Kidron, H., & Urtti, A. (2018). Binding of Small Molecule Drugs to Porcine Vitreous Humor. *Molecular Pharmaceutics*, 15(6), 2174–2179.
- Rodrigues, G. A., Lutz, D., Shen, J., Yuan, X., Shen, H., Cunningham, J., & Rivers, H. M. (2018). Topical Drug Delivery to the Posterior Segment of the Eye: Addressing the Challenge of Preclinical to Clinical Translation. *Pharmaceutical Research*, 35(12).
- Sanchez, I., Martin, R., Ussa, F., & Fernandez-Bueno, I. (2011). The parameters of the porcine eyeball. *Graefe's Archive for Clinical and Experimental Ophthalmology*, 249(4), 475–482.
- Schoenwald, R. D., & Ward, R. L. (1978). Relationship between steroid permeability across excised rabbit cornea and octanol-water partition coefficients. *Journal of Pharmaceutical Sciences*, 67(6), 786–788.
- Sellick, J. (2011). Enhancing the protection of animals used for scientific purposes. In *Environmental Law and Management* (Vol. 23, Issue 2).
- Serway, R., & Beichner, R. (2000). *Physics for Scientists and Engineers with Modern Physics* (5th ed.). Saunders College Publishing.
- Sieg, J. W., & Robinson, J. R. (1981). Mechanistic Studies on Transcorneal Permeation of

Fluorometholone. *Journal of Pharmaceutical Sciences*, 70(9), 1026–1029.

- Taka, E., Karavasili, C., Bouropoulos, N., Moschakis, T., Andreadis, D. D., Zacharis, C. K., & Fatouros, D. G. (2020). Ocular co-delivery of timolol and brimonidine from a self-assembling peptide hydrogel for the treatment of glaucoma: In vitro and ex vivo evaluation. *Pharmaceutics*, 13(6), 1–13.
- Teixeira, L. de S., Chagas, T. V., Alonso, A., Gonzalez-alvarez, I., Bermejo, M., Polli, J., & Rezende, K. R. (2020). Biomimetic artificial membrane permeability assay over franz cell apparatus using bcs model drugs. *Pharmaceutics*, 12(10), 1–16.
- Thakur, A., Kadam, R. S., & Kompella, U. B. (2011). Influence of drug solubility and lipophilicity on transscleral retinal delivery of six corticosteroids. *Drug Metabolism and Disposition*, 39(5), 771–781.
- Yves Le Grand. (1968). Light, Colour and Vision. In *Physiological Optics* (p. 566). Chapman and Hall.

Appendix I

Example of calculation of the permeability coefficient for compounds under non-sink conditions.

1. Determine the volume of sample in the receiver and donor chambers, the area of the membrane, the sample volume and the initial concentration.

Donor compartment (ml)	1
Receiver compartment (ml)	5
Area of membrane (cm²)	2.54
Sample volume (ml)	0.1
Initial concentration donor (µg/ml)	250

2. Determine the experimental receiver concentrations for the compound as indicated in sections 3.3.3 and 3.3.4.

Time (sec)	Concentration receiver (experimental, µg/ml)
0	0.0
1800	1.9
3600	9.3
7200	14.7
10800	22.7
14400	28.9

3. Calculate the total amount of substance in the system from the experimentally determined receiver concentration as follows:
 - a) At the beginning of the first time interval:

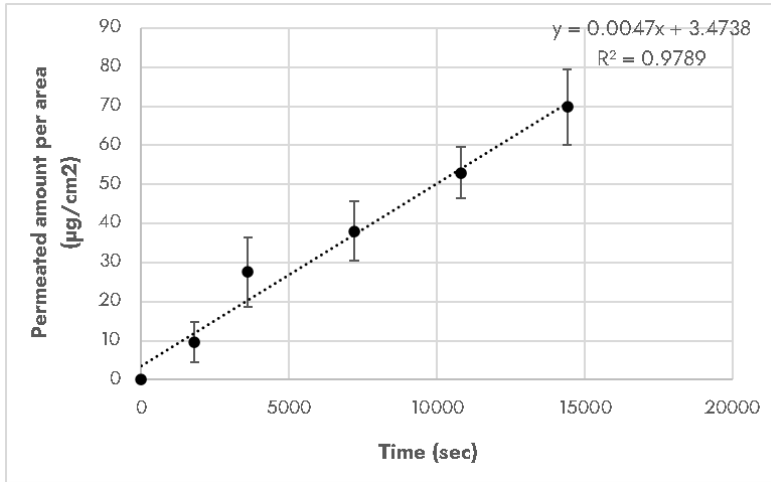
$$M_{tot}(1) = Cr_0 * V_r + Cd_0 * V_d$$

where Cr_0 is the experimentally determined concentration in the receiver at time 0, which is usually 0.

b) At subsequent time intervals

$$M_{tot}(t) = M_{tot}(t - 1) - V_s * C_r, \exp(t - 1)$$

4. Make an intermediate sink condition determination for the permeability coefficient for the studied drug as described in section 3.3.5.



$$P = \frac{J_{ss}}{C_d - C_r} = \frac{0.0047}{167.7} = 0.000028$$

5. Calculate the theoretical receiver concentration for each sampling interval by applying the following formula (Equation 10):

$$C_r(t) = \left(\frac{M_{tot}}{V_d + V_r} \right) + \left(C_{r0} - \frac{M_{tot}}{V_d + V_r} \right) * e^{-P_{app} * A \left(\frac{1}{V_r} + \frac{1}{V_d} \right) * t}$$

P_{app} is the initial guess of the permeability coefficient calculated for sink conditions.

Time (sec)	Concentration receiver (theoretical, µg/ml)
0	0
1800	5.11
3600	9.50
7200	16.77
10800	22.27
14400	26.43

6. Calculate the squared difference between experimentally and theoretically determined receiver concentration at each time interval as:

$$(C_{r, \text{exp}} - C_{r, \text{theor}})^2$$

Time (sec)	$(C_{r, \text{exp}} - C_{r, \text{theor}})^2$
0	0.0
1800	16.8
3600	2.9
7200	18.5
10800	4.6
14400	0.0

7. Calculate the Sum of Squared Error by:

$$\text{SSE} = \sum [(C_{r, \text{exp}} - C_{r, \text{theor}})^2] = 42.8$$

8. Use Solver tool in Excel or a similar software to apply non-linear curve fitting and obtain the non-sink permeability coefficient. The theoretical final concentration values of the intervals are used to generate a nonlinear curve-fit to the experimental concentrations. This curve-fit will change the initial permeability coefficient in order to minimize the sum squared error between theoretical and experimental concentration values.

Initial permeability coefficient = 28×10^{-6} cm/s

Final permeability coefficient = 24×10^{-6} cm/s

Examples before and after curve fitting between experimental and theoretical concentration data for Atenolol through conjunctiva-sclera-choroid-retina is shown below.

